CHAPTER 3

MAJOR AND TRACE ELEMENT GEOCHEMISTRY AND MINERAL CHEMISTRY

Volcanic Rock Alteration

General Characteristics

MAJOR ELEMENT GEOCHEMISTRY

Volcanic Rocks

Intrusive Rocks

TRACE ELEMENT GEOCHEMISTRY

(a) Dundee Rhyodacite Suite

(b) Andesite to Basic Rhyodacite Suite

(c) Related Series - Acid Emmaville Volcanics and Granitoids of the Major Intrusive Lineage

(d) Mineralized Granitoids

(e) Porphyries Group

RARE EARTH ELEMENTS

MINERAL CHEMISTRY

(A) MAJOR ELEMENT CHEMISTRY

(i) General Characteristics
Biotites
Amphiboles
K-Feldspar
Iron and Titanium Oxides

(ii) Dundee Rhyodacite Suite
Pyroxene Thermometry

(iii) Granitoids and Emmaville Volcanics

(B) TRACE ELEMENT CHEMISTRY

Adamellites

Mole River Diorite

Dundee Rhyodacite

MAFIC XENOLITHS

(A) Xenoliths in the Dundee Rhyodacite

(B) Mafic Xenoliths in Adamellites

CHAPTER 3

MAJOR AND TRACE ELEMENT GEOCHEMISTRY AND MINERAL CHEMISTRY

The Late Permian volcanic and intrusive rocks of the Emmaville-Tenterfield region have the mineral and whole-rock geochemical characteristics of typical continental calc-alkaline series. The data collectively indicate that 3 volcanic and at least 2 intrusive suites or groups are represented in the region, and these provide a basis for discussions of genesis and evolution of the magmas presented in Chapter 6.

Volcanic Rock Alteration

One of the major problems encountered in studies of old volcanic terrains concerns the choice of samples that are suitable for chemical analysis. The effects of surficial weathering, hydrothermal alteration and low-grade thermal metamorphism are all evident in the more silicic members of the Emmaville Volcanics, and the rejection of these rocks on petrographic grounds has produced an unavoidable bias towards the number of intermediate and basic members analysed for this study. Equally important are the chemical changes which may accompany high-temperature deuteric (Scott, 1966; Zielinski *et al.*, 1977) and low-temperature processes such as ion exchange (Jezek and Noble, 1978) and differential leaching (*e.g.* Aramaki and Lipman, 1965; Lipman, 1965, 1967; Kochhar, 1977).

High- to moderate-temperature deuteric alteration of rhyolitic volcanics is generally associated with textural modification such as the development of microgranular or spherulitic devitrification textures (Noble, 1965; Ewart, 1971; Lofgren, 1971), but there is often no record of low-temperature processes. As many of the rhyolites and rhyodacites analysed for this study display varying degrees of devitrification (*not* spherulitic devitrification) and intensity of welding of the groundmass, it was necessary to (a) establish whether significant compositional changes had occurred, and (b) to monitor any deviation in abundances of specific elements from the assumed magmatic compositions.

Zielinski *et al.* (1977) have summarized the chemical changes accompanying crystallization and hydration of acid volcanic glass. Hydration results in oxidation of iron, loss of Si and Na (up to 3% Na_2O - Noble, 1965; Lipman, 1965), possibly an increase in K, and initiates exchanges of the type H^+, K^+, Ba^{2+}, $Sr^{2+} \rightleftarrows Na^+$, Li^+.

The loss of halogens is more equivocal (cf. Noble et al. 1967) but F and Mo may be depleted in hydrated glasses. Zielinski et al. (1977) report crystallized calc-alkaline rhyolites that are enriched in Ba, Sr and Eu and are depleted in Li, Cs, Mo and U, relative to corresponding obsidians. They attribute loss of Mo and U to groundwater leaching, and loss of Li and Cs to leaching and/or mobilization as high-temperature volatile halides (also see Sheridan and Burt, 1979; Smith and Zielinski, 1979).

However Lipman et al. (1969) argued that alkali modification involving Na and K does not accompany crystallization of calc-alkaline rhyolite lavas and that the devitrified volcanics are not susceptible to leaching and ion exchange by groundwater (cf. Kochhar, 1977; Noble, 1965). Kochhar (1977) concedes that ". . . more slowly cooled rocks such as quartz porphyry have primary quartz in their groundmass and are not susceptible to the leaching of sodium", implying that the susceptibility of rocks to low-temperature alteration processes is a function of mineral stabilities as well as porosity. Strongly welded ignimbritic rhyolites with low porosities are similarly resistant to leaching, and ion mobility in the rocks is largely related to early high-temperature deuteric alteration (Scott, 1966), dependent on the composition and abundance of the primary aqueous phase (Lofgren, 1970). The high temperatures and volatile contents required to produce welding in ignimbritic rhyolites (Sparks, 1978) also favour devitrification (Smith, 1960) and the compositional changes which accompany the deuteric alteration (Scott 1966). That ion mobility during devitrification is largely dependent on the initial volatile content of the cooling volcanic glass is also consistent with the observations of Lipman et al. (1969), who studied rhyolite lavas with initially low volatile contents (see above).

Analyses of the Emmaville and Tent Hill Volcanics were examined for evidence of the alkali modification and hydration which might indicate post-eruptive alteration processes. No abnormalities in Na_2O, K_2O or H_2O^{total} were detected in rocks assumed to be fresh (refer Figures 3.1 and 3.3) and MgO is not dependent on the degree of welding (cf. Scott, 1966). Chemical trends are regular and compositional variation in petrographically equivalent rocks appears related only to the abundance and composition of the phenocryst phases. Of the five samples of Tent Hill Volcanics with textural and mineral modification caused by biotite-grade contact metamorphism, only two showed an increase of $\sim$0.8% K_2O (Figure 3.1A). Metamorphism was essentially iso-chemical for the bulk of samples analysed, as there is petrographic evidence to suggest that the high-K_2O samples have suffered minor late-stage hydrothermal alteration (e.g. sericitized plagioclase, quartz-sericite veinlets and very minor calcite).

Published data on the mobility of trace metals in retextured volcanic rocks are considered to be equivocal. The effects of low-temperature hydration and hydrothermal leaching are well documented, but the behaviour of incompatible alkali metals sensitive to early high-temperature deuteric processes is less well understood because of the possible overprinting of subsequent lower temperature alteration processes. Furthermore, Zielinski et al. (1977) suggest that felsites may represent magma compositions which differ from those represented by closely associated obsidians used as standards for studies of rock alteration. Recent studies of zoned ash-flow sheets (e.g. Lipman, 1967; Lipman and Friedman, 1975; Hildreth, 1979) have shown that individual flows of a comagmatic series may display remarkable primary variations in alkali and alkaline-earth trace metal concentrations. Sheridan and Moore (1981) analysed fresh, glassy pumice and devitrified, welded samples from the Bishop Tuff using the presumably mobile elements C, N and S and confirmed the geochemical integrity of such rocks. There is also evidence to suggest that even extensively altered (zeolitized) tuffs may preserve primary trace element concentrations in some surface environments (Zielinski et al., 1980).

The volcanics analysed for this study generate coherent trends on major element variation diagrams (Figure 3.3) which suggests they may closely approximate the compositions of the original magmas. The volcanics are also considered to provide an indication of the trace element composition of the original magmas. Certain aspects of this assumption are discussed in Chapter 6.

General Characteristics

Volcanics and granitoids display the regular major element abundance variations with silica content of typical continental calc-alkaline series (Figure 3.2). They delineate a typical calc-alkaline trend of uniform alkali enrichment on an AFM diagram (Figure 3.8) and, on the Ab-An-Or ternary diagram (Figure 3.7C) plot towards the high K-side of the field of "average" rocks defined by Irvine and Baragar (1971). Oxygen and hydrogen isotopic data on several leucogranitoids, the Bungulla Porphyritic Adamellite and the Dundee Rhyodacite, indicate the calc-alkaline magmas were derived from an igneous source (O'Neil et al., 1977). This conclusion is consistent with the mineralogical and chemical criteria for the recognition of I-type granitoids proposed by Chappell and White (1974). The intrusive rocks have Na_2O >3.2 wt %, generally <1% mesonormative corundum, display regular inter-element variations within plutons, and the adamellites are typically hornblende-bearing.

The intermediate intrusives are chemically similar to the Moonbi and Uralla Plutonic Suite rocks in the southwestern portion of the Tablelands Complex (O'Neil

et al., 1977; Chappell, 1978; Flood, 1971) and, with the Dundee Rhyodacite, they are isotopically indistinguishable from intrusives of the Moonbi Suite (O'Neil et al., loc.cit.; Flood et al., 1977). The leucogranitoids form a distinctly high-K series and are related to the more leucocratic adamellites. Comparable epizonal high-K suites occur in volcanic terrains such as the Georgetown Inlier in northeast Queensland (Bailey, 1977; Branch, 1966), and high K_2O tends to be characteristic of granitoids with a high Sn (and Mo) ore potential (Hesp, 1971; Flinter, 1971). The leucogranitoids are slightly more potassic, for example, than members of the Sierra Nevada Batholith with equivalent silica contents (Bateman and Dodge, 1972; cf. the White Mountains granites - Crowder and Ross, 1973).

The Emmaville Volcanics define a high-K series which overlaps the leucogranitoid field on a K_2O vs. SiO_2 plot (Figure 3.1C). The Tent Hill Volcanics and Dundee Rhyodacite form a distinct series with more normal K_2O. On a (Na_2O + K_2O) vs. SiO_2 diagram (not shown), the volcanics plot within the sub-alkaline field proposed by MacDonald (1968).

The average K/Rb ratio for volcanics and granitoids of 200 is similar to the value obtained by Flood (1971) for intrusives of the Uralla district, but is distinctly lower than 230 proposed for "normal" igneous rocks (Shaw, 1968; Dodge et al., 1970). Moderate Rb enrichment in the barren leucogranitoids (cf. Kolbe and Taylor, 1966) is reflected by the decrease in K/Rb from >200 in the adamellites to 128 (av.) in the Bolivia Range Leuco-adamellite. This contrasts with the extreme Rb enrichment in the mineralized Mole Granite (K/Rb = 71) and Ruby Creek Adamellite (K/Rb = 117) shown in Figure 3.12.

MAJOR ELEMENT GEOCHEMISTRY

Although the SiO_2 contents of the volcanic and intrusive rocks in the area span a similar range, many of the intrusives apparently lack an extrusive equivalent. Two volcanic suites and a single, major granitoid suite are now recognized. Associated with these suites are rocks which may be categorized into groups on the basis of one or more geochemical parameters. Further subdivision of these groups is possible using trace element and mineral chemical data.

Volcanic Rocks

Rocks of the first and second extrusive episodes comprise two distinct

volcanic suites. The Dundee Rhyodacite and Tent Hill Volcanics have higher FeO^*, MgO, CaO and P_2O_5 than Emmaville Volcanics with similar silica contents (see Figure 3.3). The comparatively low K_2O of the Rhyodacite Suite (Figure 3.1C) is particularly characteristic. In even the most siliceous members of this suite K-feldspar remains a very minor phenocryst component and the rocks have correspondingly low differentiation indices (Figure 3.4A). Three of the "Emmaville Volcanics" which plot within the well defined Rhyodacite field in Figure 3.1A, have the same mineralogy as the Dundee Rhyodacite (refer Table 2.4). Their compositions also closely approximate the average chemical composition of the Dundee Rhyodacite, which strongly suggests they were comagmatic. These volcanics exhibit pronounced eutaxitic textures and resemble the Tent Hill Volcanics, but are considered to represent remnants of the outflow facies of the Dundee Caldera, produced during the second episode of volcanism. They are associated with apparently unrelated clinopyroxene-bearing ignimbritic Emmaville Volcanics south and southeast of Rangers Valley, but on most diagrams have been grouped with the Emmaville Volcanics to distinguish them from other members of the Dundee Rhyodacite Suite.

The acid rhyodacites and rhyolites (i.e. Emmaville Volcanics with > 67% SiO_2) constitute the other volcanic lineage. Rocks of this suite have relatively low FeO^*, MgO, CaO and P_2O_5. They can be compared directly with granitoids containing equivalent amounts of silica (Figure 3.3). The major element data therefore provide a preliminary indication of related intrusive and extrusive activity during the Late Permian in the Emmaville-Tenterfield region.

Andesites, which occur in the vicinity of the Dundee Caldera, are a very minor component of the Emmaville Volcanics. These volcanics contain more K_2O than comparable rocks from western U.S.A., which belong to the most potassic regional group of the continental high-K series quoted by Ewart (1979). The possible causes of the high-K content of the andesites will be discussed in a later section in conjunction with trace element data.

The andesites (< 61% SiO_2) are distinguished by relatively high FeO^*, MgO and P_2O_5 contents and reference to Figure 3.3 shows that, except for MnO, they do not plot on the linear trends defined by the Dundee Rhyodacite Suite. Similarly the andesites diverge from an extrapolation of the trends delineating the acid

---

FeO^* = total Fe as FeO

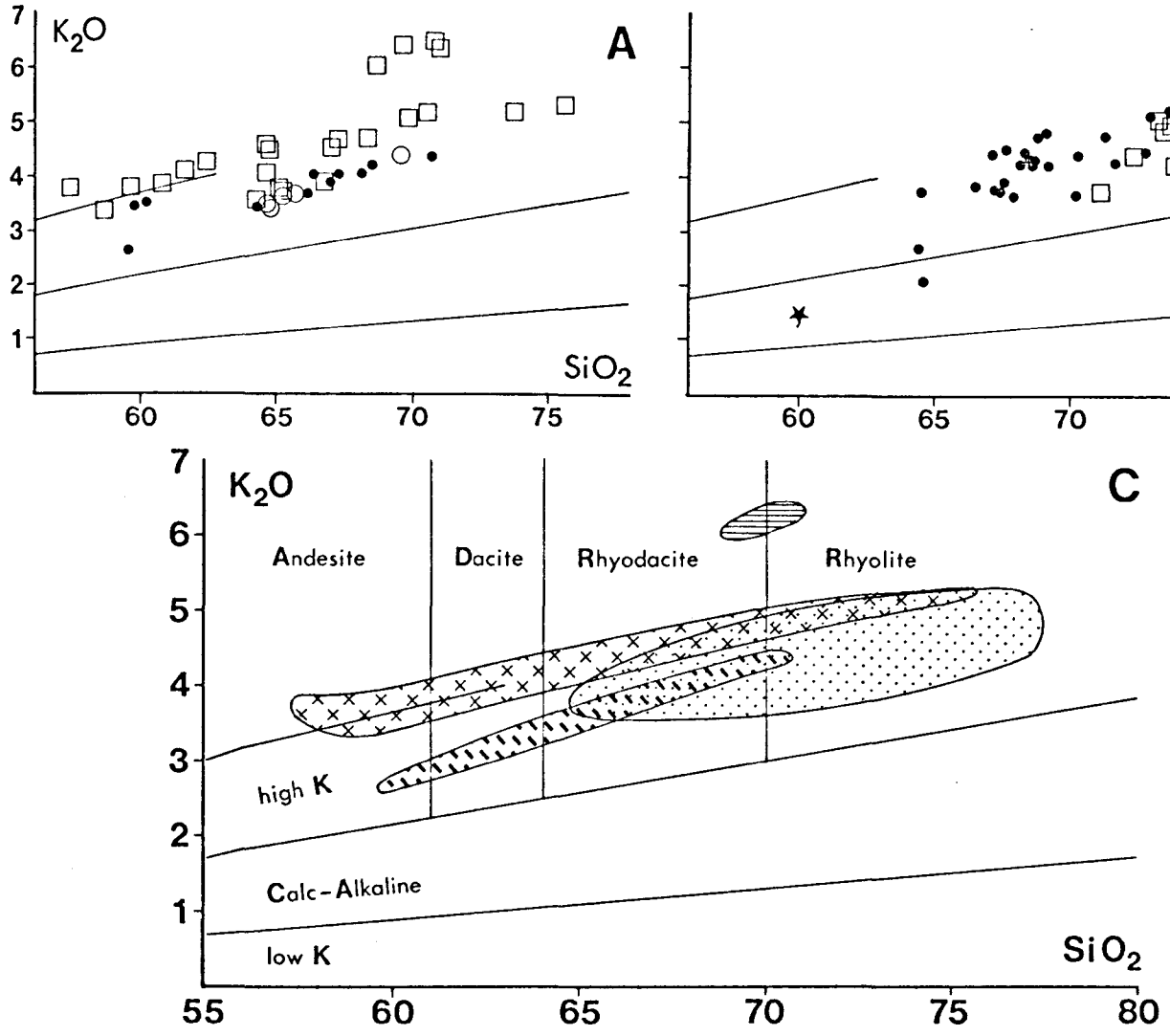

Figure 3.1. Plot showing the relationship between SiO_2 and K_2O (wt.%) for intrusive and extrusive rocks in the Tenterfield region.

A Volcanic Rocks

dot - Tent Hill Volcanics
open circle - Dundee Rhyodacite
open square - Emmaville Volcanics

B Intrusive Rocks

dot - Adamellite and Granodiorites
open square - Leucogranitoids
star - quartz diorite

C Summary of data from diagrams A and B

The boundaries defining the low K, Calc-Alkaline and high K series for volcanic rocks are from Peccerillo and Taylor (1976) with a minor modification (Ewart, 1979). The rock nomenclature is that adopted for this thesis. The high K character of the Emmaville Volcanics is evident but all the rocks plotted have calc-alkaline affinities.

stippled - intrusive rocks
crosses and lined - Emmaville Volcanics
dashed - Dundee Rhyodacite and Tent Hill Volcanics

Figure 3.2 Combined major element variation diagrams for volcanic and intrusive rocks in the Tenterfield region. Mole Granite and Stanthorpe and Ruby Creek Adamellites not included. Total iron as FeO.

large dot - xenoliths in undifferentiated adamellites
star - Mole River Diorite
asterisk - xenolith in Bungulla Porphyritic Adamellite
open square - xenoliths in Dundee Rhyodacite

Solid regression lines relate all data.
Solid line on the Al_2O_3 plot is a quadratic curve of best fit for all data excluding xenoliths. Best fit regression lines for the Dundee Rhyodacite and Tent Hill Volcanics are shown as broken lines.

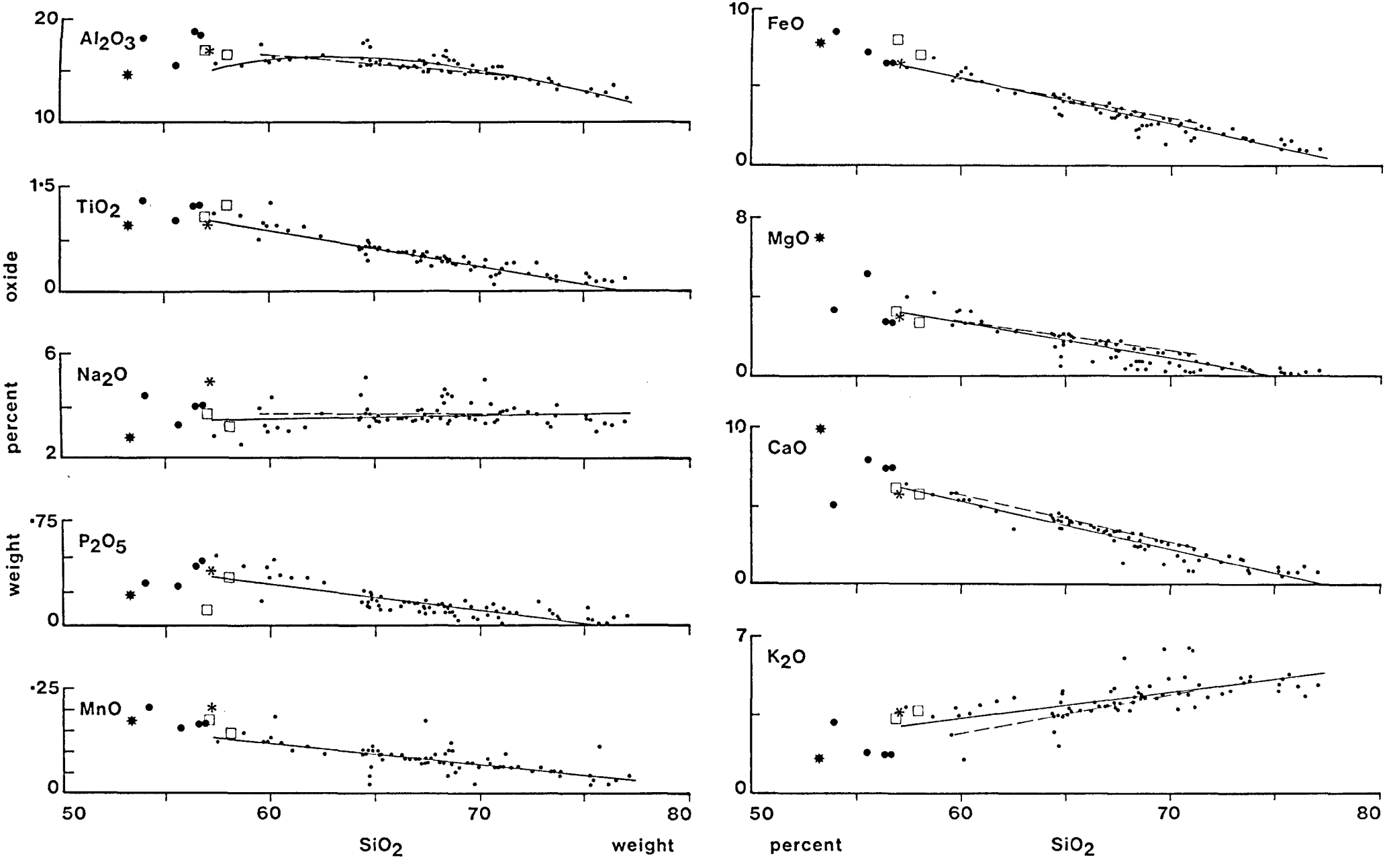
Al_2O_3
20
10
TiO_2
1·5
0
Na_2O
6
2
P_2O_5
·75
0
MnO
·25
0
oxide
percent
weight
50
60
70
80
SiO_2
weight
FeO
10
0
MgO
8
0
CaO
10
0
K_2O
7
0
50
60
70
80
percent
SiO_2

Figure 3.3 Volcanic and Intrusive Rocks - Comparative major element variation diagrams.

Total iron as FeO*. Mole River Diorite, Mole Granite, Ruby Creek and Stanthorpe Adamellites not included.

Solid regression lines relate all data.
Best fit regression lines for the Dundee Rhyodacite and related volcanics are shown as broken lines.

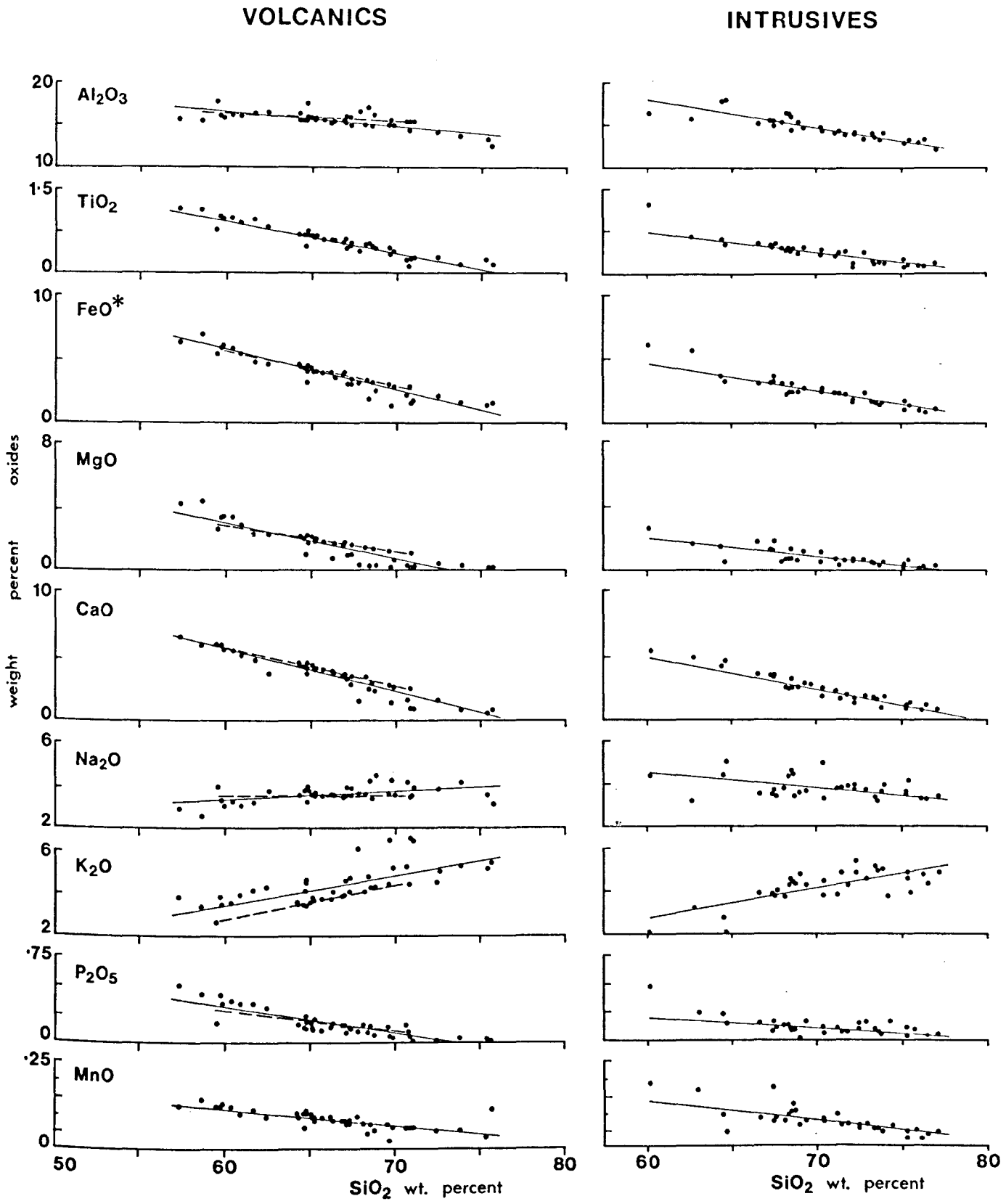
VOLCANICS
INTRUSIVES
20
10
Al2O3
1·5
0
TiO2
10
0
FeO*
8
0
MgO
10
0
CaO
6
2
Na2O
6
2
K2O
·75
0
P2O5
·25
0
MnO
weight percent oxides
50
60
70
80
SiO2 wt. percent
60
70
80
SiO2 wt. percent

Figure 3.4 SiO_2 (weight percent) plotted against differentiation index for volcanics (A) and intrusive rocks (B). The trend line is the same for both diagrams and represents the line of best fit for analyses of the Dundee Rhyodacite and Tent Hill Volcanics.

Explanation for Keys

(A) Volcanics

- Xenoliths in Dundee Rhyodacite
- Emmaville Volcanics
- Tent Hill Volcanics and Dundee Rhyodacite

(B) Intrusive Rocks

- Diorite and quartz diorite
- Xenoliths in Dundee Rhyodacite
- Xenoliths in named granitoids and undifferentiated granitoids
- Undifferentiated granitoids
- named granitoids

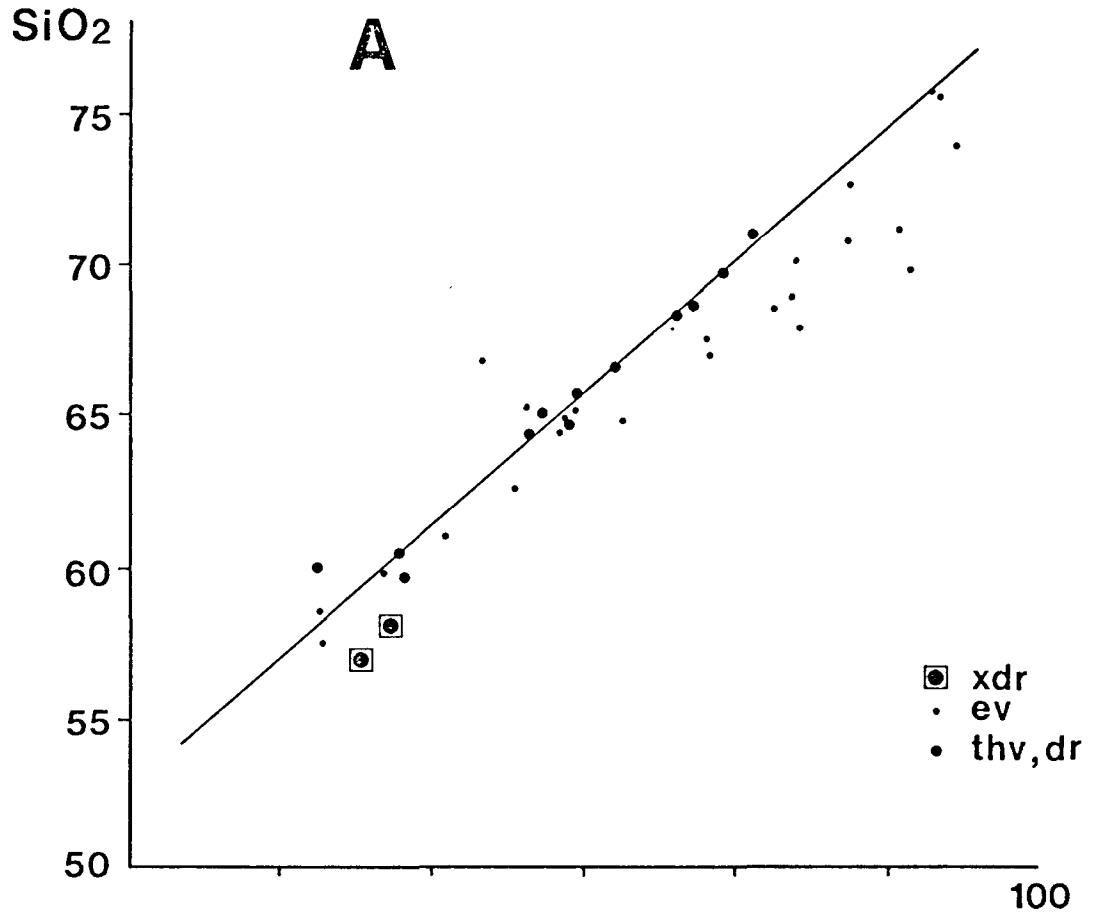
SiO2
A
75
70
65
60
55
50
100
xdr
ev
thv,dr

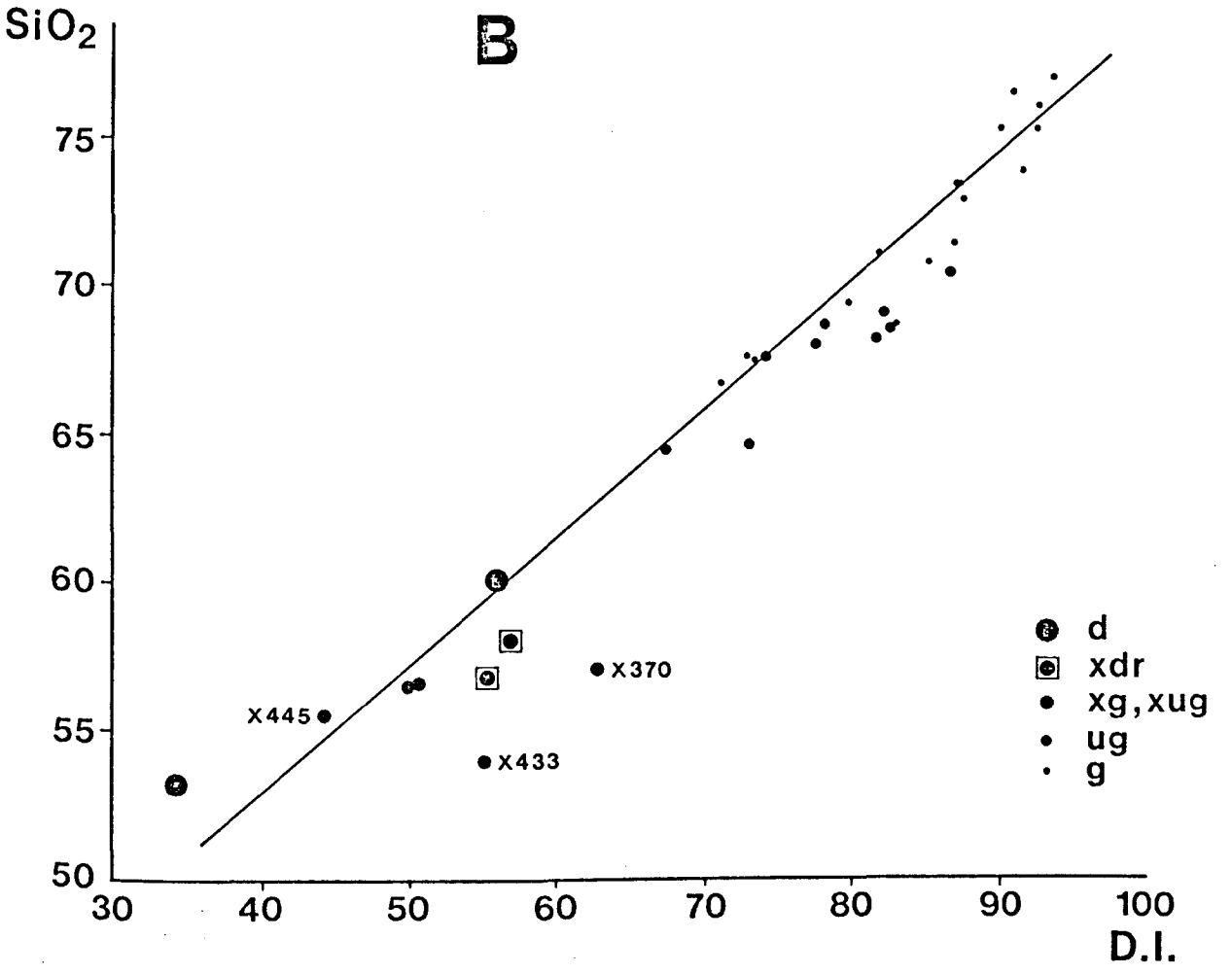
SiO2
B
75
70
65
60
55
50
30
40
50
60
70
80
90
100
D.I.
X445
X433
X370
d
xdr
xg,xug
ug
g

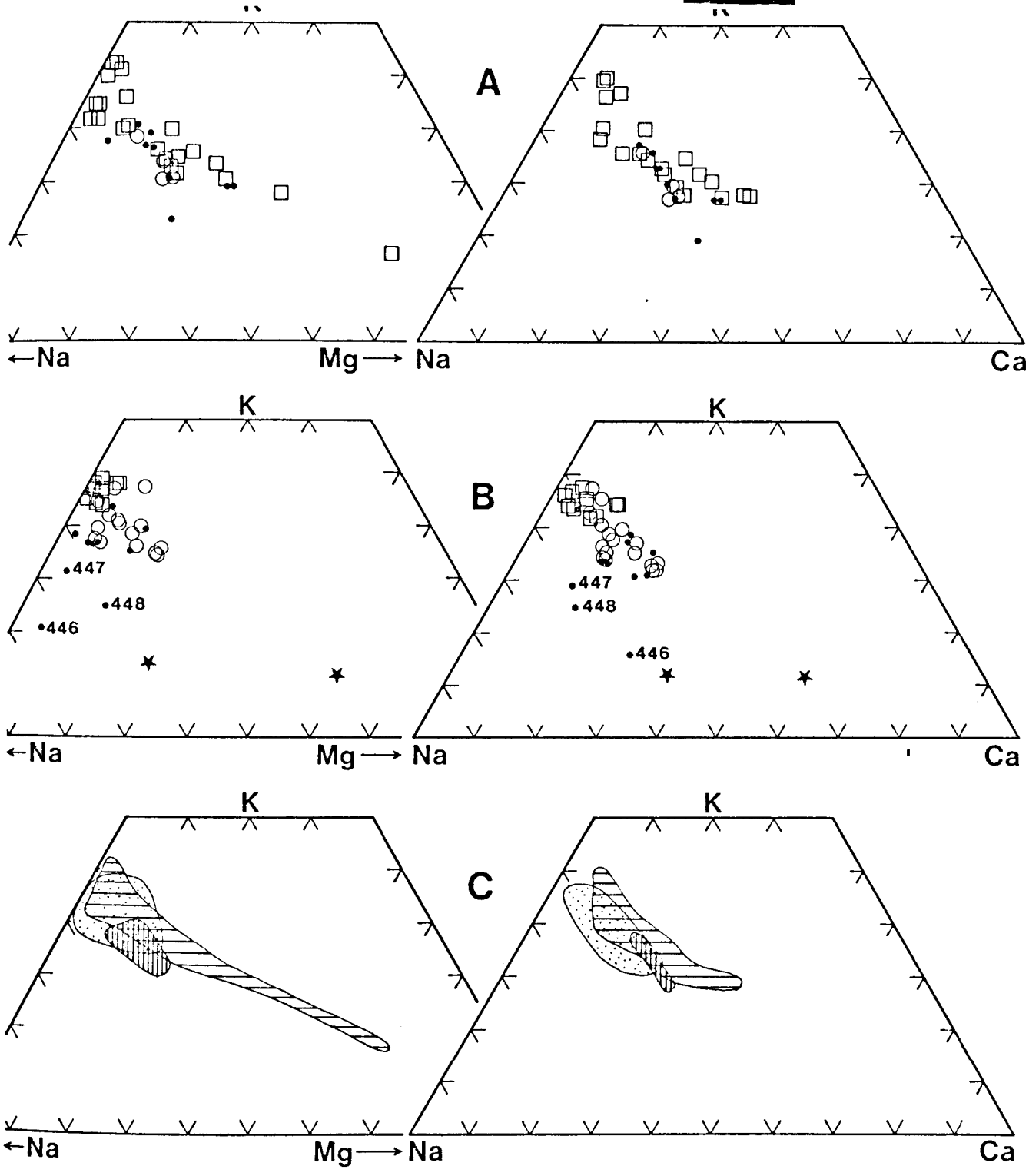

Intrusive and extrusive rocks of the Tenterfield region, plotted in terms of Na, K, Ca and Na, K, Mg (atomic %)

A Volcanic Rocks

dot - Tent Hill Volcanics
open circle - Dundee Rhyodacite
open square - Emmaville Volcanics

B Intrusives

dot - Undifferentiated Granitoids
open circle - Adamellites
open square - Leucogranitoids
star - Diorites

C Summary of data from diagrams A and B

Fields are Intrusives, Emmaville Volcanics, Dundee Rhyodacite and Tent Hill Volcanics.

FIG 3·5

Figure 3.6 Mole Granite, Ruby Creek Adamellite and Stanthorpe Adamellite major element variation diagrams. All oxides in wt. %.

open circle - Mole Granite, silexite, aplite, adamellite (approx. 65% SiO_2).

star - Ruby Creek Adamellite and more leucocratic variants.

dot - Stanthorpe Adamellite.

Solid lines define the trends for unmineralized intrusives analysed for this study.

Data Sources:
Kleeman (unpubl.), Flinter *et al.* (1972), Butler (1974), Thomson (1976), Juniper (1974).

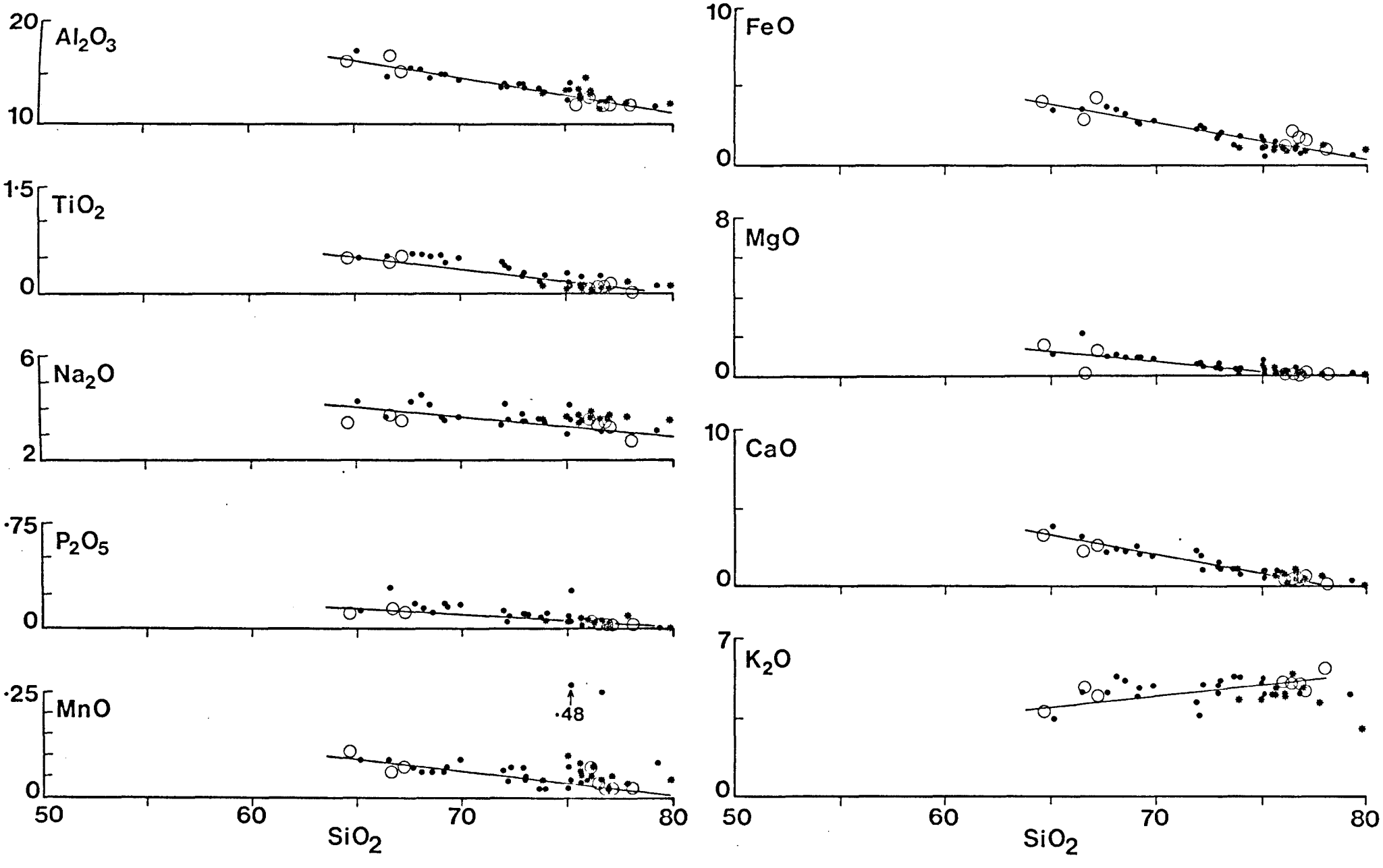
20
Al_2O_3
10
1·5
TiO_2
0
6
Na_2O
2
·75
P_2O_5
0
·25
MnO
·48
0
50
60
70
80
SiO_2
10
FeO
0
8
MgO
0
10
CaO
0
7
K_2O
0
50
60
70
80
SiO_2

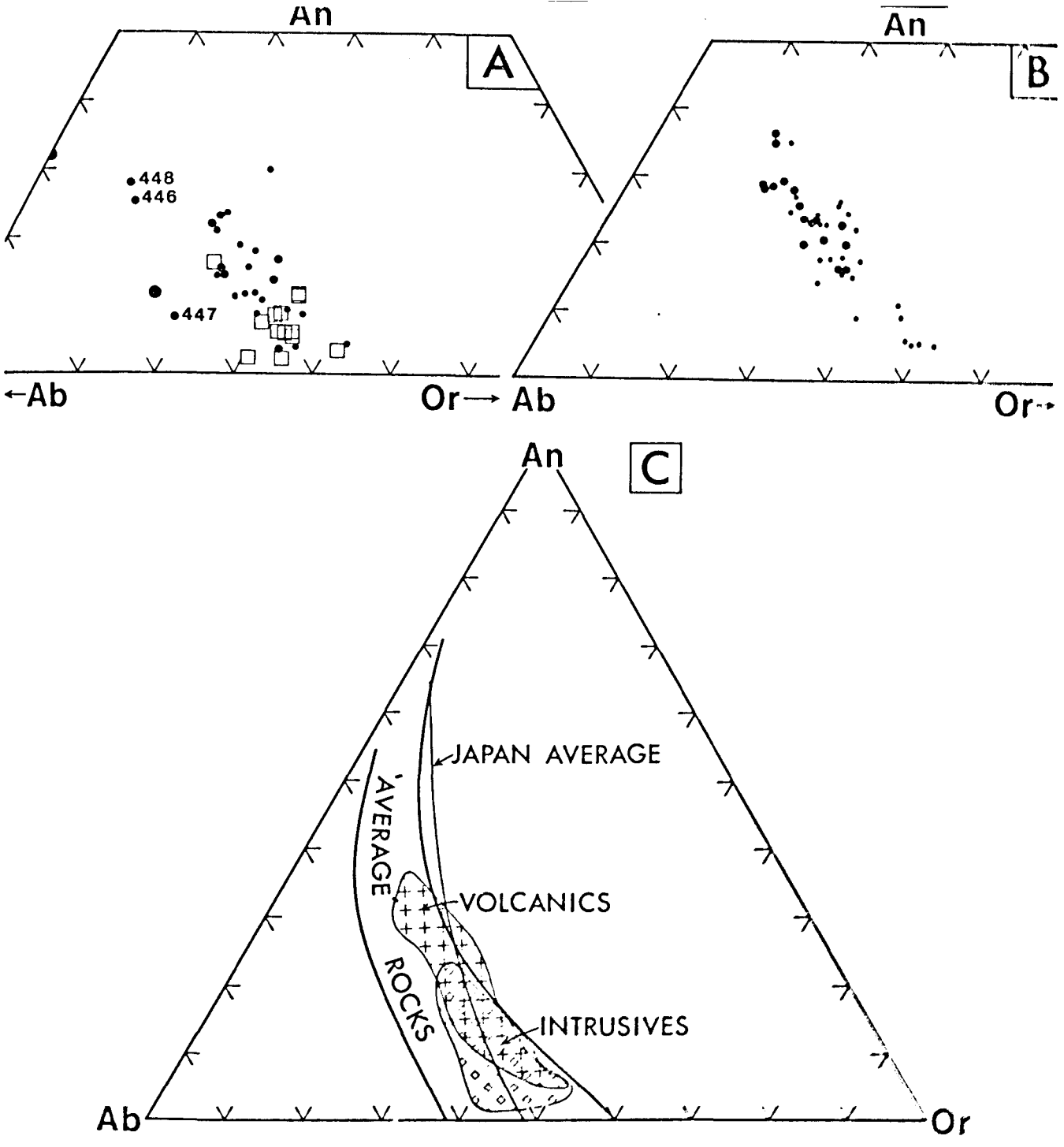

Fig. 3.7. Calc-alkaline intrusive and volcanic rocks plotted in terms of mesonormative An, Ab and Or components.

A Intrusive Rocks

- ● Diorites
- • Undifferentiated granitoids
- • Adamellites and granodiorites
- □ Leucogranitoids

B Volcanic Rocks

- • Tent Hill Volcanics and Dundee Rhyodacite
- • Emmaville Volcanics

C Summary of data from diagrams A and B

Shown are the general fields for volcanics and intrusive rocks, the average trend for granitoids and related rocks from Japan (Aramaki, *et al.*, 1972) and the field of "average" rocks from Irvine and Baragar (1971).

rhyodacites and rhyolites. These data suggest the andesites are not related to members of either the Dundee Rhyodacite Suite or the acid Emmaville Volcanic lineage. The available chemical data are insufficient to establish a possible relationship between the andesites and the other minor group of Emmaville Volcanics, the dacites and basic rhyodacites. However the observed mineralogical variation from andesite through to basic rhyodacite appears compatible with established trends of fractional crystallization of andesite magmas. These volcanics apparently have no intrusive equivalents.

Intrusive Rocks

As shown in Figure 3.3, the granitoids (> 61% SiO_2) constitute a geochemically more coherent series than the volcanic rocks. The regular geochemical trends suggest the majority of plutons belong to a single lineage. However, associated with these plutons are two apparently unrelated diorites and a small number of adamellites with distinctive textural and chemical characteristics.

The quartz diorite (60.4% SiO_2, see Figure 3.3) and the Mole River Diorite (see Figure 3.2) are apparently not related to the more felsic granitoids. The Harker diagrams show that for most oxides the diorites diverge from the trends delineating the major plutons. The diagrams also reveal that the two diorites share very few common chemical characteristics. Contrasting mineralogical and textural features (see Chapter 2) also suggest the diorites bear no relation to each other.

The adamellites can be divided into two series or groups, the main series being dominated by adamellites with seriate hypidiomorphic to equigranular textures. With the leucogranitoids and granodiorites, adamellites of the main series produce a continuum of rock compositions ranging from 65 to > 76% SiO_2. Major element trends for the Mole Granite, Ruby Creek and Stanthorpe Adamellites are illustrated in Figure 3.6. There is an obvious close relationship between these plutons and the main series unmineralized granitoids of the first intrusive episode, and justifies the allocation of all the silicic granitoids in the region to a single suite (e.g. O'Neil et al., 1977).

Adamellites which outcrop near the Mole River Valley north of the Clive Adamellite (samples 446, 447 and 448) and north of Wallangarra (samples 399, 391 and 387) comprise the minor adamellite group. These rocks are readily distinguished from adamellites belonging to the main series by Na_2O/K_2O ratios greater than unity, which results in high mesonormative plagioclase contents and relatively high D.I. On a SiO_2 vs. D.I. diagram (Figure 3.4), adamellites of the main series plot on or

near the trend delineating the Dundee Rhyodacite Suite whereas those of the minor group, with similar silica contents, are comparatively enriched in the low-temperature melting components (i.e. mesonormative Q, Ab and Or). However, there is little to suggest that adamellites of the minor group shared a common cooling history. The Mole River adamellites have seriate textures whereas those from the Wallangarra region are strongly porphyritic. Adamellites from the Mole River Valley also have much higher Na_2O/K_2O ratios.

TRACE ELEMENT GEOCHEMISTRY

The volcanics and granitoids were analysed for a number of trace elements primarily to confirm, if possible, the allocation of rocks to specific suites and minor groups recognized on the basis of major element characteristics. The trace element data may also provide some evidence for open-system magma fractionation processes which at present are poorly documented and little understood. In this section, discussion is restricted to the trace element characteristics of each lineage and rock group. The theoretical aspects of magma evolution will be discussed in Chapter 6.

Variations in whole rock trace element abundance are shown diagramatically in Figures 3.8 and 3.16. For these diagrams parameters were chosen to accentuate essential features which best discriminate the individual suites and illustrate the coherence of trace element trends within each suite or group.

(a) Dundee Rhyodacite Suite

For all elements analysed, there is a high degree of correlation between members of the Dundee Rhyodacite Suite. Variation trends are linear and usually very well defined. Elements such as Sr, Rb and Ba usually produce curved trends in series composed of members which represent individual systems of crystal-liquid equilibrium (e.g. Bowen, 1928). However, in the Dundee Rhyodacite Suite, trace element variation is largely determined by the modal phenocryst content, as the composition of the groundmass (representing the liquid) is very similar for all members of the suite. The trace element geochemistry of the suite is therefore not determined by the composition of successive (derivative) liquids which would be the case if fractional crystallization was the major process controlling evolution of the magma. The linear nature of the major and trace element trends suggest that the Dundee Rhyodacite Suite is a crystal-melt mixing series.

(b) Andesite to Basic Rhyodacite Group

Trace element abundances in the andesites, dacites and basic rhyodacites are similar to those in the Dundee Rhyodacite Suite. The exception is Ba which is consistently higher in the Emmaville Volcanics (see Figures 3.11, 3.14A and 3.16D). Elements such as Ni, V and Sr, which occupy lattice sites in early-formed minerals such as pyroxene and hornblende (Ni, V) and plagioclase (Sr), show moderately regular variation with variable SiO_2. However the relatively incompatible elements Li, Pb, Zn, Cu and Nb produce no regular trends (Figure 3.9) and there is no obvious relationship in these elements between members of the group. This may be due to a number of factors such as differential loss of trace elements during extrusion, depending on the style of eruption (i.e. lava flow or ash flow (see Hildreth, 1979)); sorting of intratelluric biotite, K-feldspar and accessory phases rich in incompatible elements, or derivation of the magmas from different source rocks. Mobilization of various elements during low-grade contact metamorphism, leaching associated with hydration, and other post-eruptive processes are not considered responsible for the observed trace element distribution in members of the andesite to basic rhyodacite group.

The andesites contain relatively high abundances of the trace alkali metals, consistant with their high K_2O contents. This is considered to be largely a reflection of the composition of the parent rocks.

(c) Related Series - Acid Emmaville Volcanics and Granitoids of the Major Intrusive Lineage

The proposed relationship between siliceous Emmaville Volcanics and rocks of the major intrusive series, is confirmed by the trace element data. Within the limits of analytical error, the trends for Cu, Ni, V, Cr, Sr, Nb, Nd and Ce and the abundances of these elements are very similar for both suites (compare Figures 3.9 and 3.10). It is important to note that the volcanics appear to contain more Pb, Ba, Zr, Zn and slightly less Li and Rb than comparable granitoids (Figures 3.9 to 3.12). Zr and Zn abundances are highly variable and may be attributed to the sporadic distribution of zircon and sulfide inclusions in biotite and other phases in the volcanics. The high-K rhyolites (see Figure 3.1A) are especially enriched in Zr (Figure 3.11) which suggests Zr may also be concentrated in the groundmass of these volcanics (cf. Watson, 1979). Both Ba and Pb are considered to be concentrated in the K-feldspar phenocrysts (Taylor, 1966; Oftedahl, 1967; Dostal et al., 1979) and in

the groundmass. The Li and Rb data are more equivocal and the behaviour of these and other incompatible elements will be discussed in detail in Chapter 6.

"Intrusive rhyolites", which occur as pipe-like bodies intimately associated with rhyolitic Emmaville Volcanics at Webbs Consols Mine and east of Deepwater (see Chapter 2), are most appropriately grouped with the analysed high-K rhyolites. They have relatively high Y, Nd and Ce (Figure 3.9) and are considered to be the intrusive equivalents of the allanite-bearing high-K rhyolites sampled from nearby areas. The "intrusive rhyolites" have textures similar to the porphyries in the Wallangarra region, but are more highly evolved and therefore relatively depleted in Sr (Figure 3.14B). Significantly they have Na_2O/K_2O ratios < 1. Like the high-K rhyolites, these siliceous porphyries are richer in Ba than equigranular leucogranitoids with similar major element chemistries (Figures 3.14A and B).

(d) Mineralized Granitoids

In Figure 3.13, the trace element chemistry of the cassiterite-bearing Mole Granite and Ruby Creek Adamellite is compared with other granitoids in the region. The Stanthorpe Adamellite plots within the general field for unmineralized granitoids of the first intrusive episode, although there is considerable variation in the relative abundances of Zr, Li and Rb. Nevertheless these data suggest that magmas which crystallized to form the barren plutons were derived from the same source rock. This conclusion also applies to those adamellites west of Mount Mackenzie which, although not occurring as sizeable bodies, are probably related to nearby plutons of the major intrusive lineage.

The Mole Granite and Ruby Creek Adamellite have very low concentrations of Ba, Zr and Sr and for these relatively magmaphile elements, the rocks plot on the high-silica extension of the trend for unmineralized granitoids. Such predictable behaviour is not shared by the more mobile incompatible elements. Anomalously high Rb and Li are particularly characteristic and these elements are potential indicators of leucogranitoids with associated Sn-W mineralization. The data of Shaw (1964), Thomson (1976), Flinter et al. (1972) and Kleeman (unpubl.) suggest that F, Cs and U may also serve as geochemical indicators, as all are significantly enriched in the mineralized plutons. A table comparing the average concentrations of these elements in mineralized and barren leucogranitoids, is presented below. In all cases the more strongly mineralized Mole Granite has the highest trace element abundances.

(μg/g)	Mole Granite	Ruby Creek Adamellite Leucogranitoids	Unmineralized
U	18	11	5 *
Th	51	27	18 *
Cs	26	13	7
Rb	575	304	207
Li	206	101	32
Ce	112	53	55
Y	93 #	55	38
F	2790 **	1065 **	

* Stanthorpe Adamellite only

\# Mole Granite proper; microgranite types excluded

** Average in fluorite-bearing samples

The Mole Granite and Ruby Creek Adamellite show a greater range of Ce and Y than comparable barren leucogranitoids. The utilization of Ce and Y as indicator elements is, however, limited because their abundance in the mineralized plutons may be influenced by the sporadic distribution of minor accessory phases such as allanite, zircon and apatite.

In an earlier section of this chapter it was shown that the major element data do not discriminate between the cassiterite-bearing and barren leucogranitoids. The logical interpretation that all leucogranitoids may be related to the same parent rock is supported by the Ba, Sr and Zr data. However in apparent contradiction of this conclusion, the mineralized leucogranitoids have anomalous concentrations of trace alkali metals, F, U and possibly other mobile, incompatible trace elements (e.g. Th). This presents a problem similar to that outlined by the Pb, Ba, Li and Rb data for the proposed comagmatic acid intrusive and volcanic rocks of the region. A possible solution to these problems requires a thorough investigation of the likely behaviour of these incompatible elements at all stages of formation and evolution of the magmas (see Chapter 6).

(e) Porphyries Group

The Wallangarra porphyries and seriate-textured adamellites from the Mole River Valley have distinctive trace element chemistries. On a Rb vs. Sr diagram (Figure 3.16A), the Mole River adamellites plot well away from the major intrusive lineage. Figure 3.16A also illustrates the wide range of Rb and Sr in these adamellites.

The two low-silica adamellites (samples 446 and 448), with the highest Al_2O_3 and Na_2O/K_2O ratios ($Na_2O/K_2O > 1.6$), are readily segregated from the more acid members of the group. They have high Sr and Zr, and average Ba contents (Figures 3.10, 3.16A and C) which may be correlated with the observed abundances of plagioclase, K-feldspar and zircon in the rocks (see Chapter 2). The more siliceous members of the group are low in Sr and V and have above average concentrations of Ba relative to both the low-silica adamellites of the group and the granitoids of the major lineage (Figures 3.10, 3.12 and 3.14). The majority of members in the porphyry group plot on the high-Sr side of the average on a Sr vs. CaO diagram (Figure 3.12).

RARE EARTH ELEMENTS

Very few rare earth element (REE) data are presently available for the igneous rocks in the Tenterfield region, which limits the scope for a comparative study. The unmineralized leucogranitoids have not been analysed for REE.

Chondrite normalized REE trends for the mineralized Ruby Creek Adamellite, Mole Granite and associated aplite and silexite are shown in Figure 3.15. The trends for the mineralized leucogranitoids are very similar, and feature a very pronounced negative Eu anomaly and very mild light REE enrichment. The REE patterns of other tin granitoids in the New England region (e.g. the Gilgai Granite and Round Mountain Adamellite) are very similar with only a slight variation in the size of the Eu anomaly (Kleeman, unpubl.). The silexite or topazite of the Mole Granite pluton is relatively depleted in REE and this is partly a function of a mode devoid of REE-rich accessory minerals.

The REE patterns for two samples of the Moonbi Adamellite are also shown in Figure 3.15. An almost identical pattern of mild light REE enrichment and uniform middle and heavy REE abundance with no Eu anomaly, also characterizes a small body of adamellite within the Mole Granite pluton (Kleeman, pers. comm.). The REE data are consistent with the recently proposed origin for the Moonbi Suite magmas (Chappell, 1978). Chappell considered the magmas formed by moderate degrees of partial melting of an igneous parent and incorporated a considerable amount of refractory residua. The absence of an Eu anomaly indicates that the magmas probably carried a considerable amount of plagioclase from the zone of melting, and that gravity settling of this restite plagioclase prior to crystallization was minimal. Large degrees of partial melting, which substantially deplete the parent in plagioclase, may also produce magmas with no Eu anomaly, but Chappell (1978) has argued that the bulk of the plagioclase in rocks on Moonbi Suite is restite and was not derived from the melts.

Figure 3.8 AFM and modified AFM diagrams for analysed volcanic and intrusive rocks in the Tenterfield region.

Oxides are in weight percent, F = FeO = total iron as FeO, A = $Na_2O + K_2O$, M = MgO.

Trace elements in ug/g are multiplied by a factor chosen to centre the data on the ternary diagram.

Only in diagrams involving Sr and CaO has M been replaced by MgO + FeO + MnO.

small dot - Volcanic and intrusive rocks
large dot - Xenoliths in adamellites
open square - Xenoliths in Dundee Rhyodacite
asterisk - Xenolith in Bungulla Porphyritic Adamellite
star - Mole River Diorite

The diagrams show that the calc-alkaline trend generated on a standard AFM plot is also well defined for a number of minor and trace elements of vastly differing geochemical characteristics.

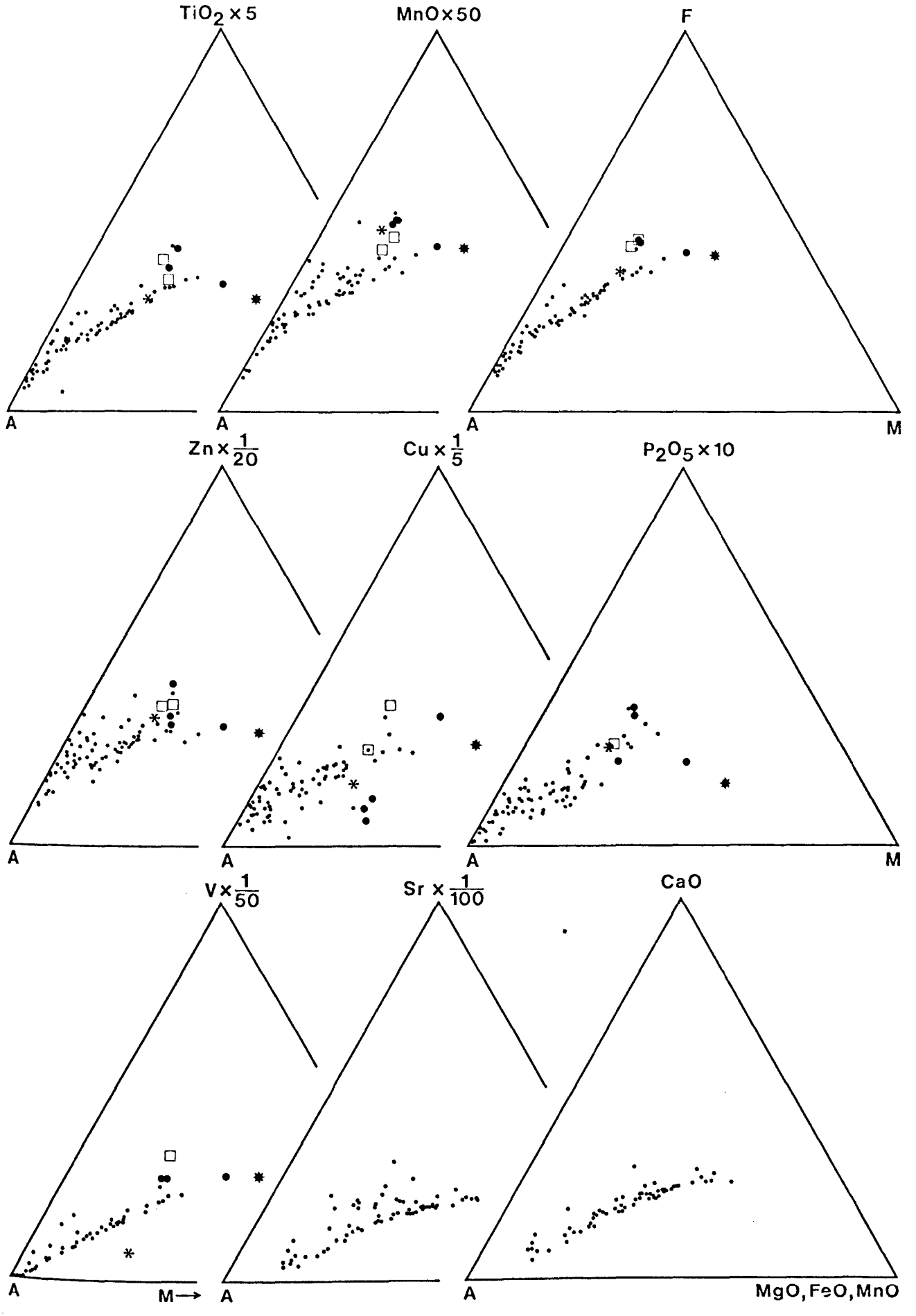
$TiO_2 \times 5$
MnO×50
F
A
A
A
M
Zn × 1/20
Cu × 1/5
$P_2O_5 \times 10$
A
A
A
M
V × 1/50
Sr × 1/100
CaO
A
M→
A
A
MgO, FeO, MnO

Figure 3.9 Trace element Harker diagrams for volcanic rocks.

Large dot = xenoliths in the Dundee Rhyodacite.

Solid regression line applies to all data.
Line of best fit for the Dundee Rhyodacite and related volcanics is shown by a broken line for Zn, V and Rb.
Samples W305 and 250, with high Y, Nd and Ce, are allanite-bearing "intrusive rhyolites".

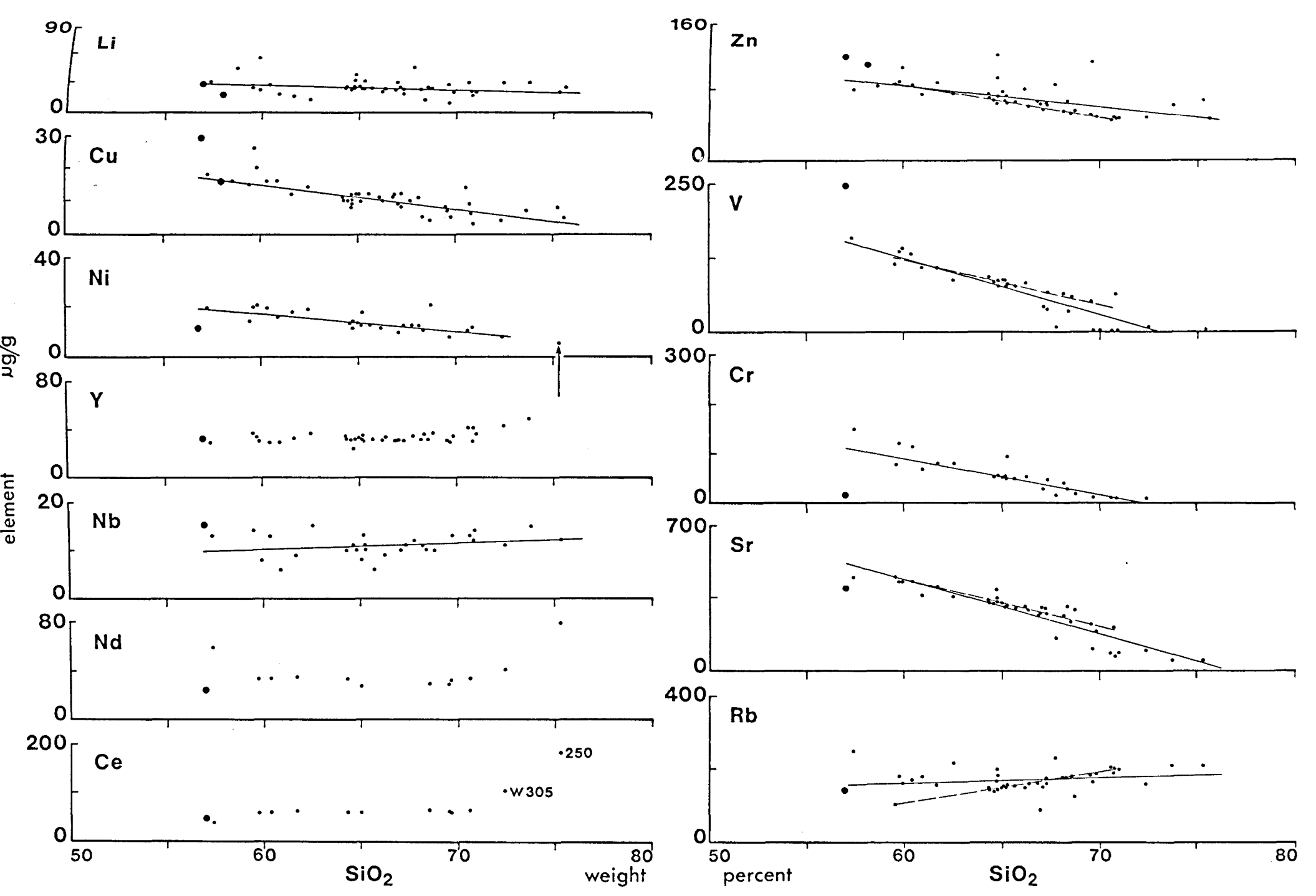
Li
90
0
Cu
30
0
Ni
40
0
Y
80
0
Nb
20
0
Nd
80
0
Ce
200
0
•250
•W305
50
60
70
80
SiO2
weight
percent
element
µg/g
Zn
160
0
V
250
0
Cr
300
0
Sr
700
0
Rb
400
0
50
60
70
80
SiO2

Figure 3.10 Trace element Harker diagrams for intrusive rocks.

small dot - granitoids

large dot - xenoliths in the granitoids

star - Mole River Diorite

asterisk - xenolith in Bungulla Porphyritic Adamellite

square and dot - quartz diorite

Mole Granite, Ruby Creek and Stanthorpe Adamellites not included.

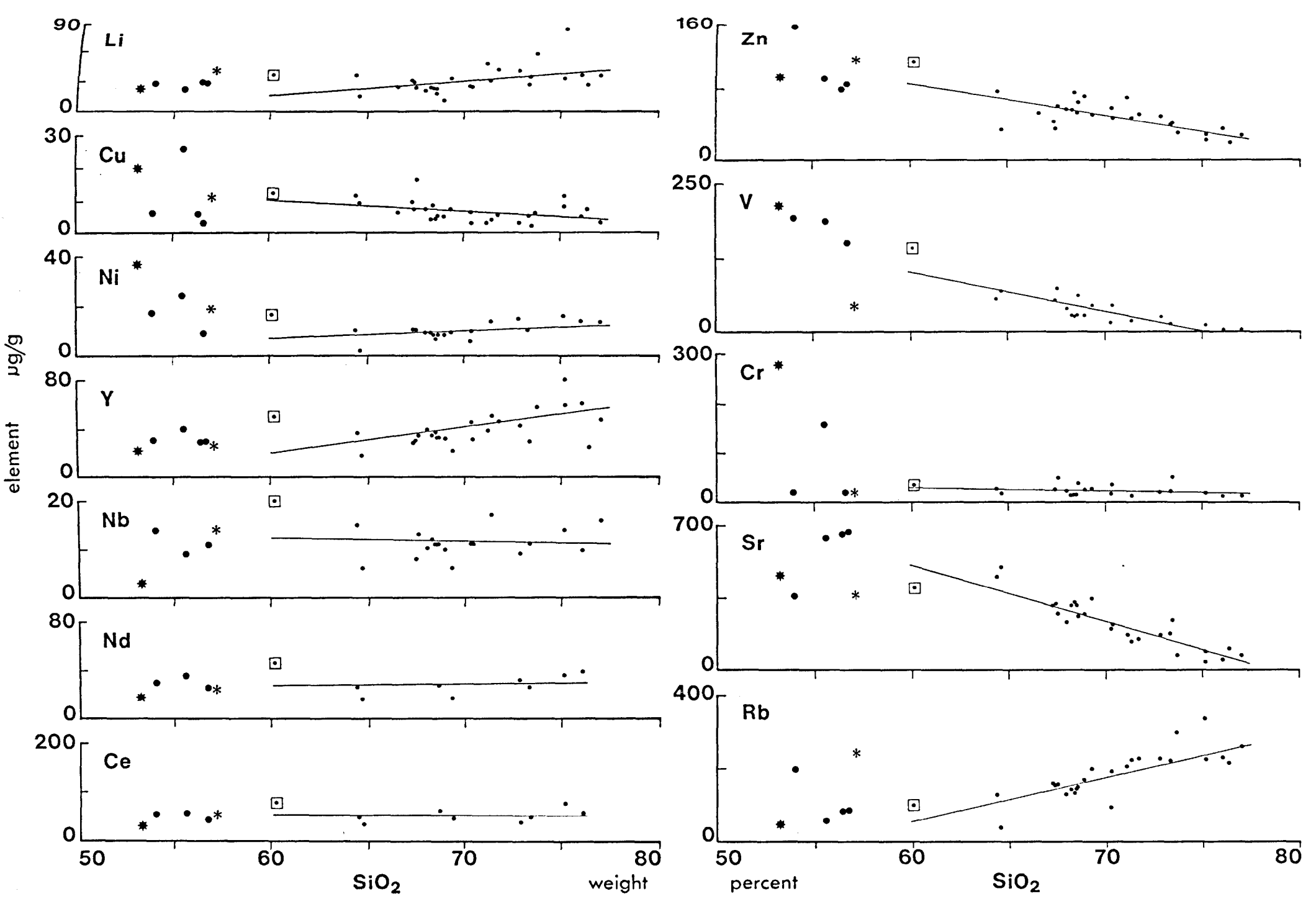
Li
Cu
Ni
Y
Nb
Nd
Ce
Zn
V
Cr
Sr
Rb
element µg/g
SiO_2 weight percent
SiO_2

Figure 3.11 Selected trace element variation diagrams for volcanic rocks.

Oxides in wt. %, trace elements in ug/g.

log K_2O vs. log Rb

dot - Emmaville Volcanics

open square - Dundee Rhyodacite and Tent Hill Volcanics

Leucogranitoids and most adamellites plot within the stippled field.

Pb, Ba and Zn vs. SiO_2

Solid line represents the line of best fit for members of the Dundee Rhyodacite Suite.

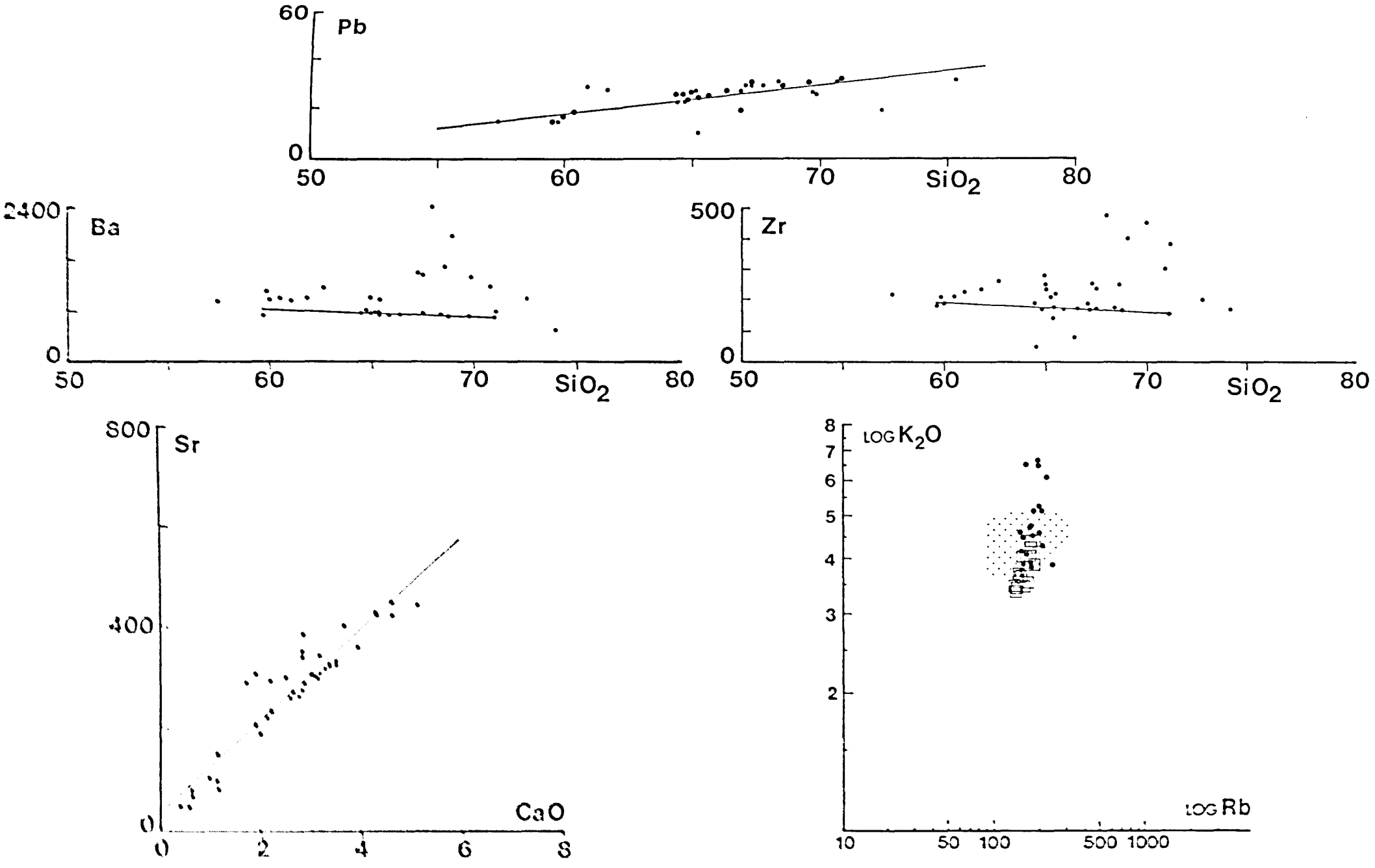
60
Pb
0
50
60
70
SiO2
80
2400
Ba
0
50
60
70
SiO2
80
500
Zr
0
50
60
70
SiO2
80
800
Sr
400
0
0
2
4
6
8
CaO
8
7
6
5
4
3
2
LOG K2O
10
50
100
500
1000
LOG Rb

Figure 3.12 Selected trace element variation diagrams for intrusive rocks.

Oxides in wt. %, trace elements in ug/g.

Numbers denote adamellites from the Mole River Valley.

log K_2O vs. log Rb

dot	-	unmineralized granitoids
open square	-	Ruby Creek Adamellite
open circle	-	Mole Granite
star	-	Mole River Diorite
circled dot	-	quartz diorite

The majority of Emmaville Volcanics plot within the field marked by crosses.

Pb vs SiO_2

large dot	-	mafic xenoliths
star	-	Mole River Diorite
circled dot	-	quartz diorite

Solid line represents the line of best fit for the Dundee Rhyodacite Suite from Fig. 3.11.

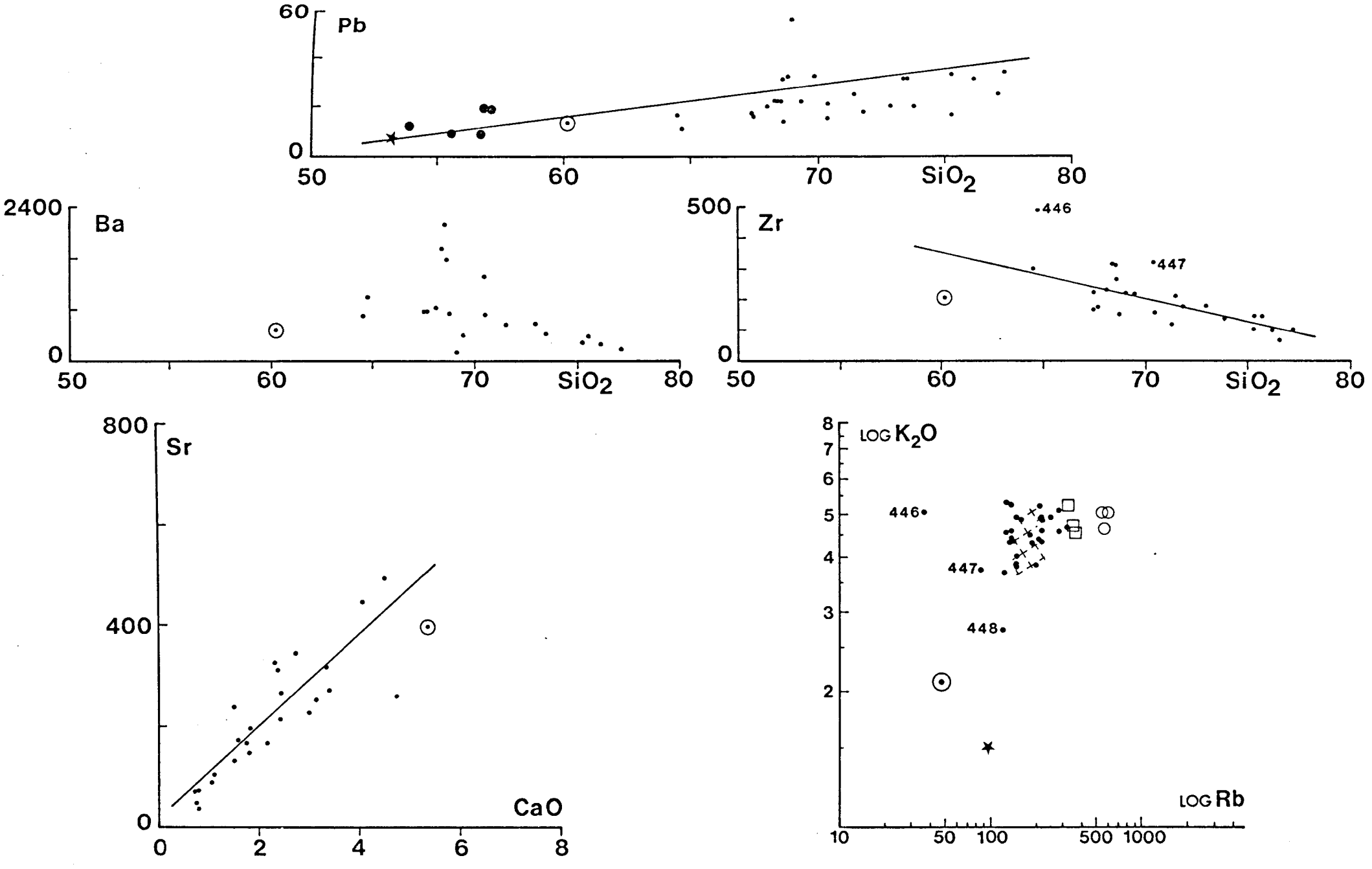
Pb
60
0
50
60
70
SiO_2
80
Ba
2400
0
50
60
70
SiO_2
80
Zr
500
0
50
60
70
SiO_2
80
446
447
Sr
800
400
0
0
2
4
6
8
CaO
LOG K_2O
8
7
6
5
4
3
2
446
447
448
LOG Rb
10
50
100
500
1000

Figure 3.13 Compilation of selected trace element data for granitoids in the Tenterfield region. Harker diagrams for trace elements Sr, Ce, Ba, Y, Zr, Rb and Li. Trace element values in µg/g.

filled star - Ruby Creek Adamellite and more siliceous variants

open star - Mole Granite, silexite, aplite, adamellite (approx. 65% SiO_2)

large dot - Stanthorpe Adamellite

small dot - granitoids analysed for this study

Compared to the unmineralized granitoids, the tin-bearing Mole Granite and Ruby Creek Adamellite are anomalously rich in Rb and Li, and generally have higher abundances of Ce and Y.

Data Sources:
Kleeman (unpubl.), Flinter *et al.* (1972), Butler (1974), Thomson (1976), Juniper (1974).

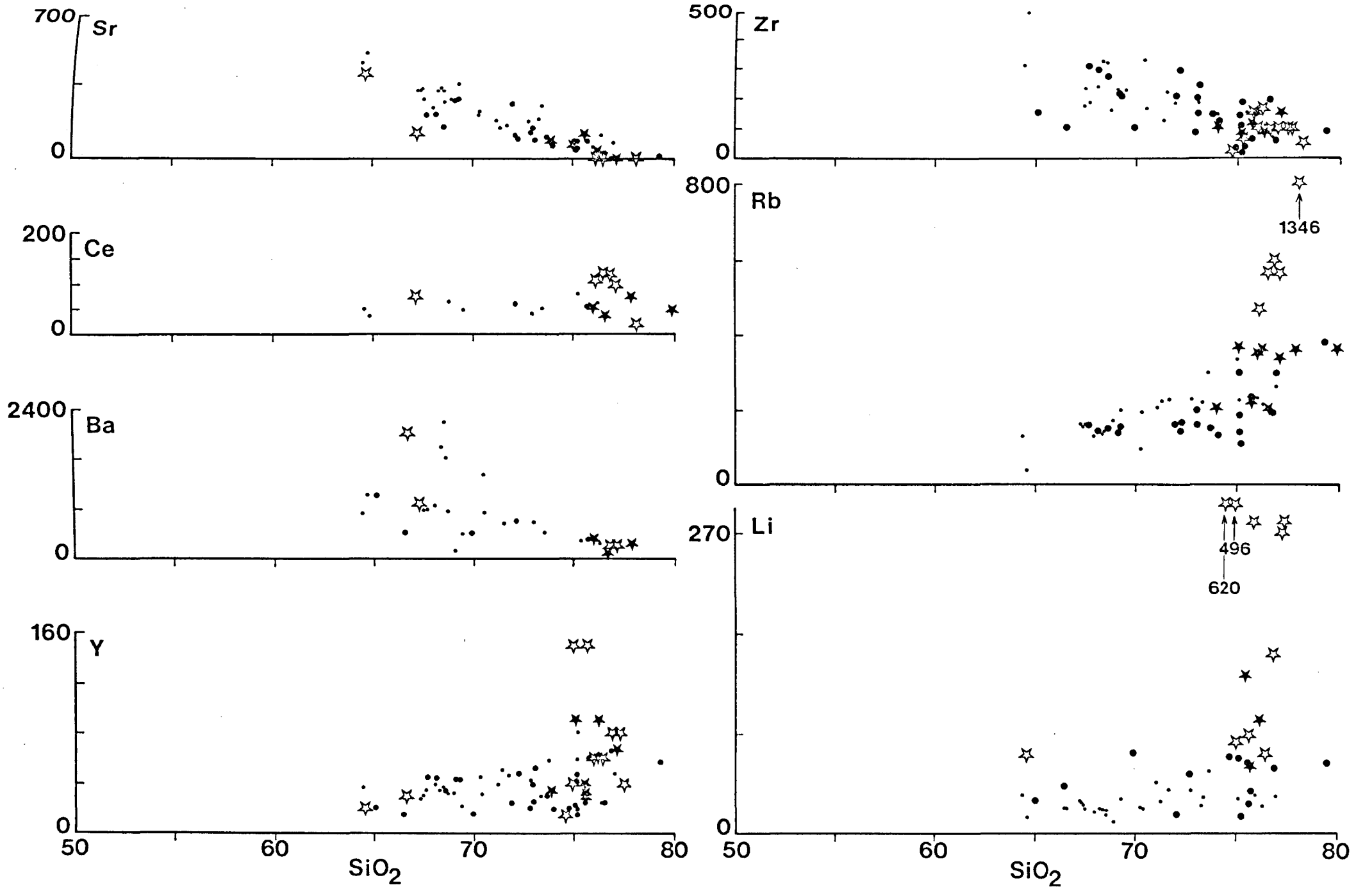
700
Sr
0
500
Zr
0
200
Ce
0
800
Rb
1346
0
2400
Ba
0
270
Li
496
620
0
160
Y
0
50
60
70
80
SiO2
50
60
70
80
SiO2

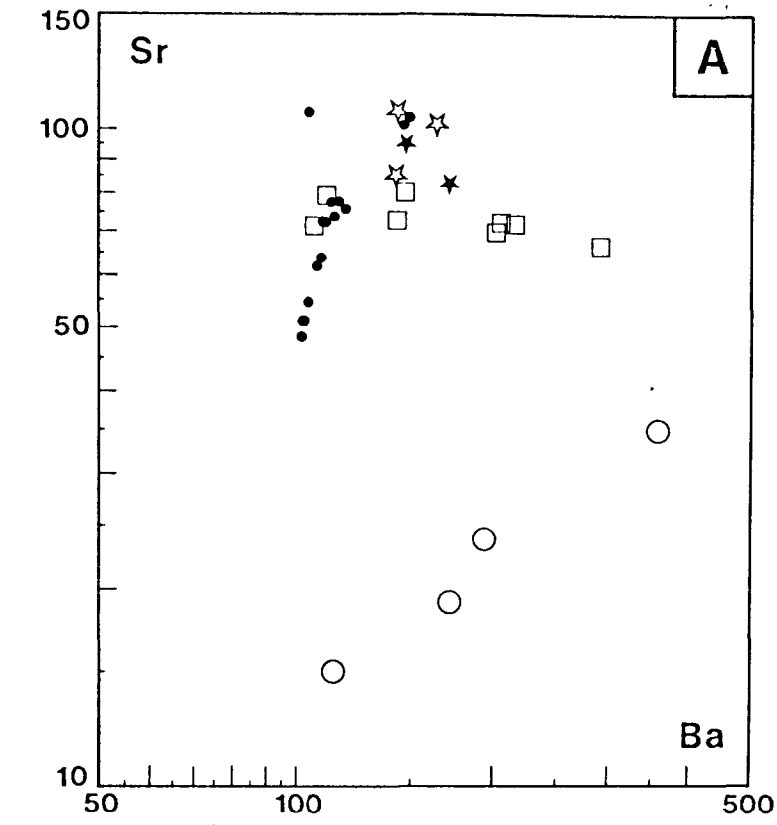

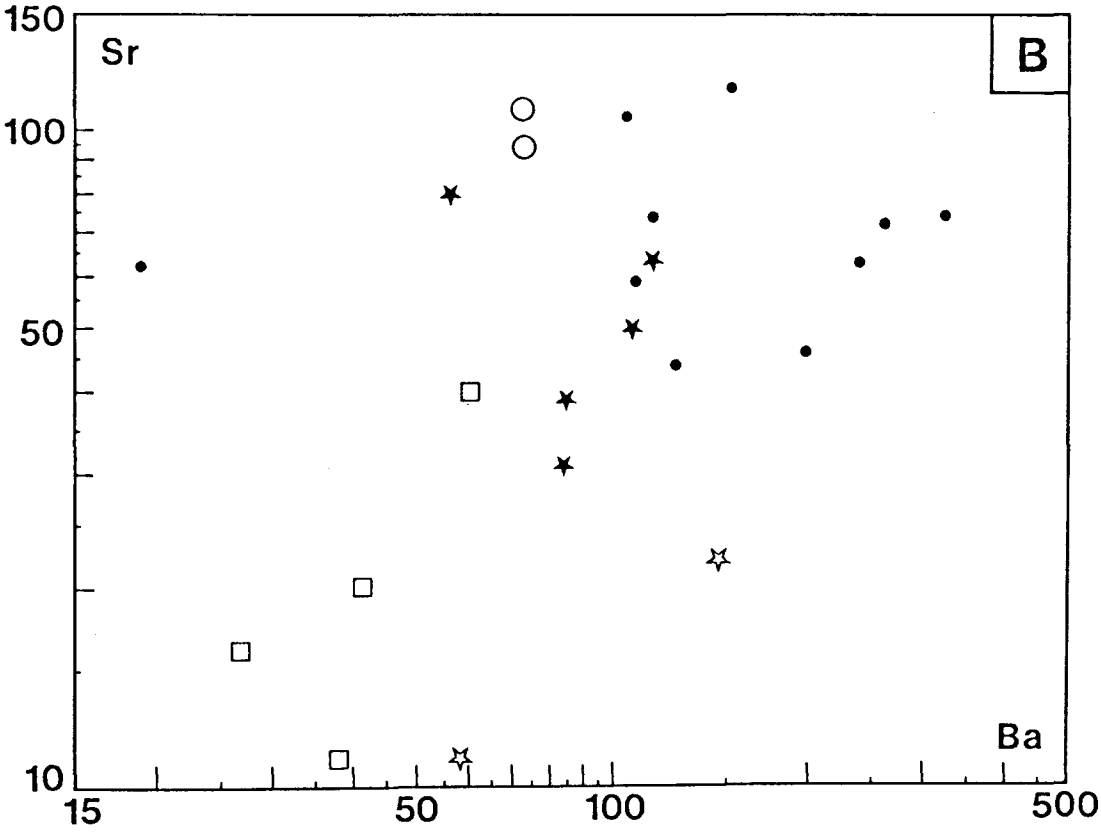

Fig. 3.14. Plots of Sr vs. Ba for volcanic, and unmineralized calc-alkaline intrusive rocks. Mole Granite, Stanthorpe and Ruby Creek Adamellites not included. Sr and Ba as atoms per million.

A Volcanic Rocks

dot	-	Dundee Rhyodacite and Tent Hill Volcanics
open star	-	Andesites
filled star	-	Dacites
open square	-	Rhyodacites
open circle	-	Rhyolites

(Andesites, Dacites, Rhyodacites, Rhyolites: Emmaville Volcanics)

B Intrusives

dot	-	Undifferentiated granitoids and porphyries
closed star	-	Adamellites and granodiorites
open star	-	"Intrusive rhyolites"
open circle	-	Diorites
open square	-	Leucocratic granitoids

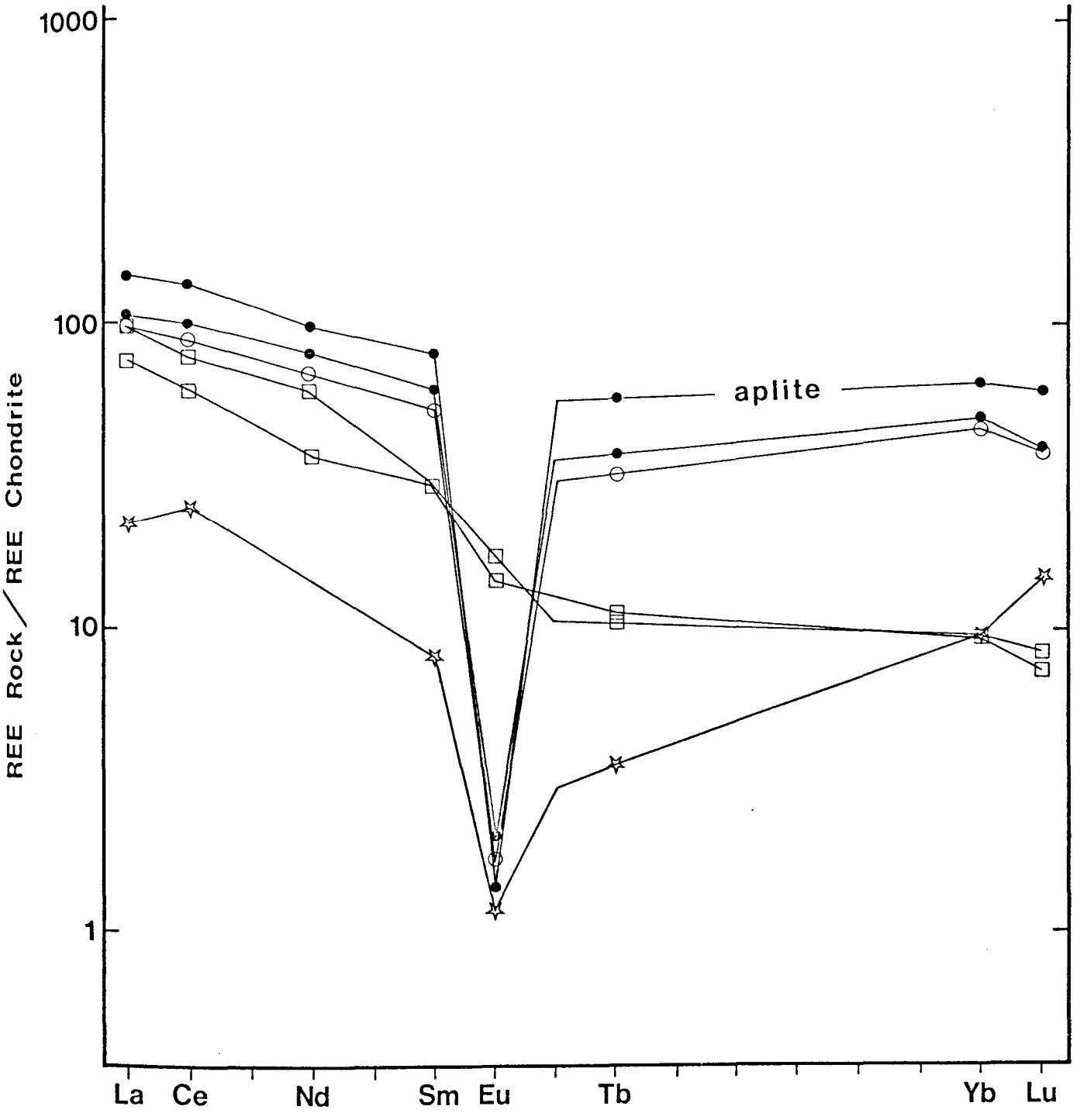

Fig. 3.15 (Leedey) Chondrite normalized rare earth element (REE) abundances vs. REE atomic number for selected intrusive rocks.

- ● Mole Granite
- ☆ Silexite (Mole mass)
- □ Moonbi Plutonic Suite
- ○ Ruby Creek Adamellite

Data provided by J.D. Kleeman (unpubl.)

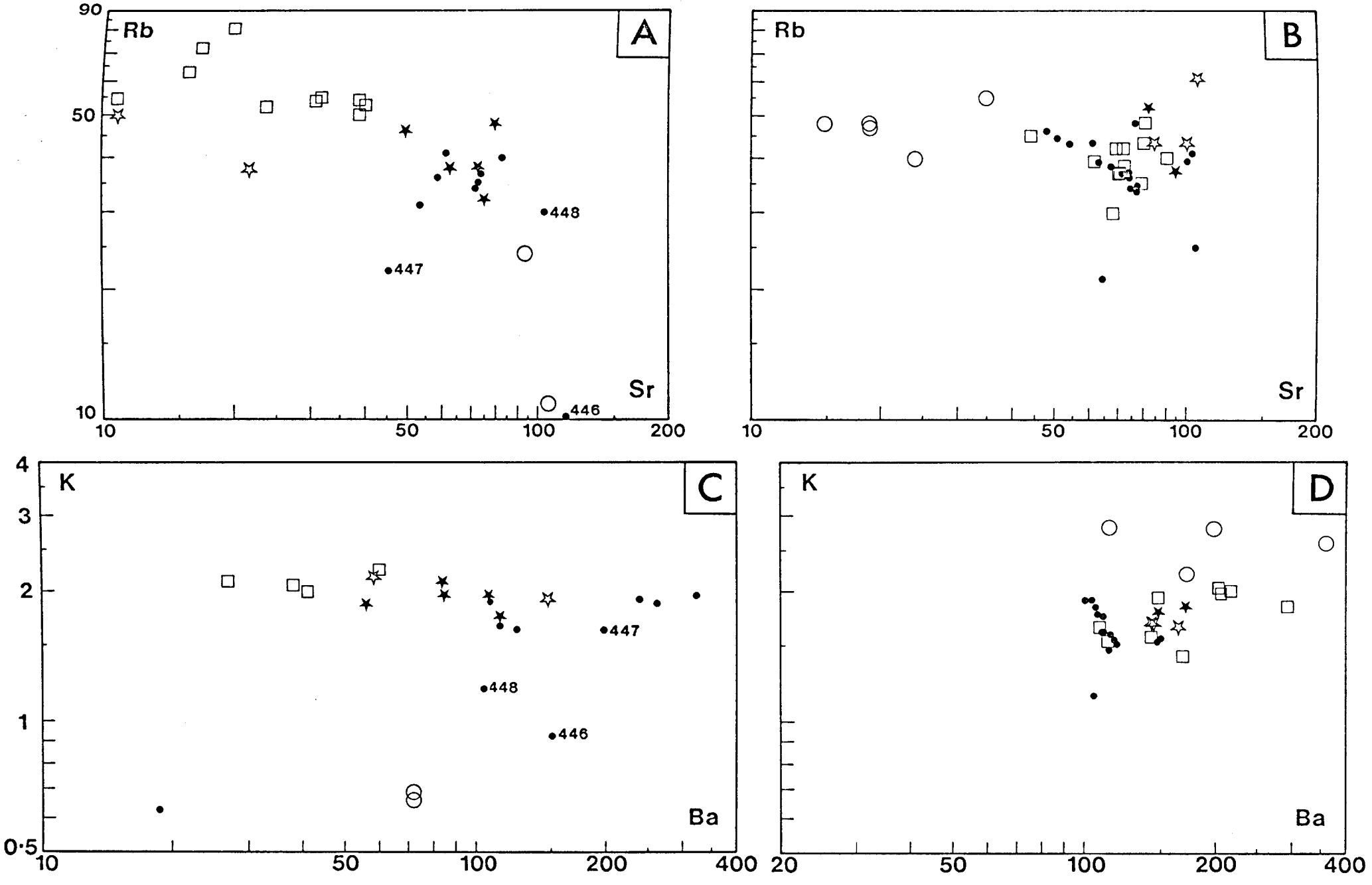
A
Rb
Sr
90
50
10
10
50
100
200
447
448
446
B
Rb
Sr
10
50
100
200
C
K
Ba
4
3
2
1
0·5
10
50
100
200
400
447
448
446
D
K
Ba
20
50
100
200
400

The distinctive REE patterns for the mineralized leucogranitoids may also be interpreted in terms of a partial melting model. The large negative Eu anomalies suggest the magmas were able to separate from the source region after only a small amount of melting had occurred, leaving a considerable quantity of plagioclase residuum in the slightly depleted parent. The regular, high concentrations of light and heavy REE in the leucogranitoids is consistent with the conclusions of Koljonen and Rosenberg (1974) and Price and Taylor (1974) that all rare earths except Eu may partition strongly into the liquid phase at the onset of melting. This implies that all the REE are transported to the site of crystallization as components of the melt where they may be concentrated in accessory phases such as apatite, zircon and allanite (Buma et al., 1971; Condie and Lo, 1971; Yeliseyeva, 1978). In this case accessory minerals have only a minor influence on the REE content of the leucogranitoids. The uniform, high abundances of light and heavy REE do not correlate with the irregular distribution of apatite, zircon and allanite in the mineralized leucogranitoids. Although some of the REE-rich accessory minerals may be refractory residuals of partial melting that were transported in the magmas, the regularity of the REE trends again implies that the contribution of such restite to the magmas was insignificant.

It is considered highly improbable that the observed negative Eu anomalies were produced by gravitational settling of Eu-rich plagioclase.

MINERAL CHEMISTRY

(A) MAJOR ELEMENT CHEMISTRY

(i) General Characteristics

The compositions of minerals in volcanic and intrusive rocks of the Emmaville-Tenterfield region are typical of calc-alkaline rocks in continental regions. The range of biotite and amphibole compositions is shown in Figures 3.17 and 3.18 respectively. Biotites and hornblendes in the granitoids are similar to those in the other calc-alkaline intrusives of the New England Batholith s.l. (e.g. Flood, 1971; Neilson, 1971; O'Neil et al., 1977). In general, granitoids of intermediate composition have co-existing magnesio-hornblende and Mg biotite, and more iron-rich ferromagnesians occur in the leucocratic adamellites and leucogranitoids.

Biotite and hornblende compositions in the volcanic and intrusive rocks are compared in Figures 3.22, 3.23 and 3.24. Ferromagnesians in the granitoids span the widest range in composition.

Examples of overlap of mg for co-existing hornblende and biotite were noted in the siliceous granitoids and rhyodacitic Emmaville Volcanics (see Figure 3.20). The overlap is partly due to the late-stage crystallization of a more iron-rich hornblende and deuteric alteration of hornblende to biotite with a relatively high mg. However mg of the ferromagnesians generally decrease in the order pyroxene-hornblende-biotite (see Figure 3.20; Jakes and White, 1972; Piwinskii, 1975).

The field of clinopyroxene compositions (Figure 3.19) closely resembles the fields for a number of continental calc-alkaline provinces (see Ewart, 1979). Clinopyroxenes in the volcanics have low Al^{iv} and Al^{vi} consistent with the findings of Kushiro (1960) for silica-saturated sub-alkaline magmas. Jakes and White (1972) noted the common association of clino and orthopyroxene in calc-alkaline volcanic rocks, and, in members of the Dundee Rhyodacite Suite, clinopyroxene co-exists with colourless hypersthene (av. $Ca_3\ Mg_{58}\ Fe_{39}$).

Plotted on a Fe^{3+}, Fe^{2+}, Mg ternary diagram used by Dodge et al. (1969) and Dodge and Ross (1971) (not figured), biotite analyses scatter about the experimental compositions determined using a Ni-NiO buffer by Wones and Eugster (1965). Although the compositions of the experimental systems may not be suitable for comparison with real systems, the diagram indicates that biotites from rocks with the same mineral assemblage probably crystallized under conditions of similar fO_2. Hornblendes co-existing with biotite generally have higher Fe^{3+}/Fe^{2+} and MgO/FeO ratios which, according to Dodge and Ross (1971), also indicates crystallization of these ferromagnesians under conditions of buffered oxygen fugacity. Hornblendes typically have low Al, and the data of Jakes and White (1972) based on Al^{iv}, Al^{vi}, Na + K and $(Fe^{2+} + Fe^{3+})/Mg$ suggest the hornblendes are those typically found in continental calc-alkaline rocks.*

Biotites: Nockolds (1947), De Alberquerque (1973) and De Pieri et al. (1978) have shown that variations in biotite composition defined in terms of Al_2O_3, FeO* and MgO, are related to the paragenesis of the biotites. In granitoids of the Uralla District, Flood (1971) noted that biotites co-existing with ilmenite contain less Fe^{3+} than biotites associated with magnetite (cf. Carmichael, 1967). Titanomagnetites in the Tenterfield granitoids and Emmaville Volcanics

---

* Using the fully analysed hornblendes of this study and the data of Shaw (1964), a reasonable estimate of Fe^{3+} was made to determine the distribution of Al^{iv} and Al^{vi} in hornblendes analysed by electron microprobe. The technique advocated by Papike et al. (1974) to determine Fe^{3+} in hornblendes yielded widely variable results.

originally had a significant Fe_2TiO_4 component and co-existing biotites contain correspondingly low Fe^{3+}.

As Al is almost invariant in biotites from the Tenterfield region (see Figure 3.22C), MgO/FeO* or simply the Fe/Mg ratio can be used in place of the Al_2O_3, FeO*, MgO ternary plot to investigate the relationship between biotite compositions and paragenesis. As expected, biotites co-existing with hornblende are generally more magnesian than those in rocks lacking hornblende. This is shown in Figure 3.20 where mg of the ferromagnesian minerals is used as the discriminating parameter. The curved line in Figure 3.20B broadly delineating a field dominated by leucoadamellites (biotite only), therefore also distinguishes all rocks which lack, or contain only minor amounts of, hornblende. For example, the biotite in sample 448 from the Mole River area is much less magnesian than biotite in the hornblende-bearing equivalent, sample 446. The Emmaville Volcanics (Figure 3.20A) similarly may be divided on the basis of biotite compositions, but in this case more exceptions exist and several rhyodacites contain low-magnesium hornblendes which plot in the "biotite only" field. However all volcanics containing pyroxene and hornblende have relatively magnesian biotites.

Consistent with the findings of De Pieri et al. (1978), biotites in rocks from the Tenterfield region show a moderate negative correlation between Mn and Mg, but correlations of other major elements (excluding Fe), are generally very poor. Good inter-element correlation is restricted to biotites in the leucoadamellites (Shaw, 1964). Ti in biotites from the Dundee Rhyodacite Suite is generally higher than in all other biotites analysed. The foxy red-brown absorption colour of these biotites may be related to the high Ti content and low Fe^{3+}/Fe^{2+} ratio (De Pieri et al., 1978).

Amphiboles: Hornblendes in granitoids of the major intrusive lineage have slightly higher Mg/Mn + Fe ratios (Figure 3.24C) than proposed related volcanic rocks. Hornblendes with <30 atom % Mg (in terms of the Ca, Mg, Fe + Mn triangle) are from members of the porphyries group. Similarly in Figure 3.24B four scattered analyses denote hornblendes from the minor andesite-rhyodacite group.

The field for granitoid hornblendes (Figure 3.23C) is similar to the field for hornblendes in intrusives of the Uralla district (Flood, 1971), but extends to higher alkali values (shown on the diagram as Σ Na + Ca + K > 2.5). Ca in the hornblendes is relatively constant (Figure 3.24C) and the high values are due to increased Na in the unit cell. The four rocks with relatively sodic amphibole have $Na_2O/K_2O \geq 1$ which conforms to the suggestion of Jakes and White (1972) that Na and K in hornblende reflect host rock composition.

The Bungulla Porphyritic Adamellite is the only granitoid which contains euhedral actinolitic hornblende, and this amphibole co-exists with abundant magmatic sphene. Studies of granitic (Verhoogen, 1962) and alkaline volcanic rocks (Carmichael and Nicholls, 1967) have shown that sphene is a stable liquidus phase under conditions of fO_2 at least as high as the FMQ buffer, and De Alberquerque (1974) concluded that at low P and T, actinolitic hornblende is stable at this oxygen fugacity. This suggests the actinolitic hornblende in the Bungulla Porphyritic Adamellite is a primary phase and the low value of the distribution coefficient $(Fe/Mg)^{hornblende}_{biotite}$ also indicates that it crystallized at relatively low P and T (De Alberquerque, loc.cit.).

The partial pressure of CO_2 may also affect the stability of sphene in evolved liquids, and if the conclusions of Hunt and Kerrick (1977) are in any way applicable to magmas, the paragenesis of sphene in the Bungulla Porphyritic Adamellite indicates that it crystallized at low P_{fluid} and T.

Many of the undifferentiated hornblende-bearing adamellites and their xenoliths contain accessory sphene, where it forms coronas around iron-titanium oxides and biotite. This sphene formed by subsolidus oxidation and reaction (Charmichael and Nicholls, 1967) during low-grade thermal metamorphism, under conditions of elevated fO_2. Significantly, it is these rocks which contain deuteric actinolitic hornblende.

Some andesites and rhyodacites of the Emmaville Volcanics also contain actinolitic amphibole. Leake (1971) has suggested that magmatic and post-magmatic amphibole compositions do not exceed half-unit cell Si values of 7.30 and 7.50 respectively. However, magmatic crystallization of actinolitic amphibole under high-fO_2 conditions has been proposed by Haslam (1968) and Czamanske and Wones (1973). Highly oxidizing conditions may prevail during eruption and flow of magmas (e.g. Ewart, 1971), but there is no evidence of significant oxidation of any volcanics in the region, regardless of the style of eruption (i.e. ash flow or lava flow). On a Fe^{3+}, Fe^{2+}, Mg diagram, biotites in the volcanics appear to have crystallized under the same fO_2 conditions as the biotites in the granitoids. The actinolitic amphiboles are therefore likely to be post-eruptive alteration products whereas the iron-rich hornblendes mantling clinopyroxene probably crystallized from the melt.

K-Feldspar: Although no detailed analysis of K-feldspar composition and morphology was undertaken in this study, the orthoclase mega crysts which characterize the Bungulla Porphyritic Adamellite merit some comment. Shaw (1964) considered the megacrysts to be magmatic (see Hibbard,

1965; Mehnert, 1978; Kerrick, 1969; Kawachi and Sato, 1968; Bateman and Chappell, 1979). However the temperatures of crystallization (after Barth, 1956) and trace element compositions of the K-feldspars determined by Shaw (loc.cit.) are in error and conflict with the determinations made in this study. Shaw (1964) overestimated Sr by ∿700 µg/g and underestimated Rb by ∿300 µg/g. The available textural and chemical data allow for the possibility of a metasomatic origin for the megacrysts (e.g. Hyndman, 1968). The presence of K-feldspar megacrysts in an intermediate member of a cogenetic sequence is not unusual (see Bateman and Wones, 1972) and may merely indicate that the Bungulla Porphyritic Adamellite crystallized under physicochemical conditions which differed from those operating in other members of the suite.

Iron-Titanium Oxides: In both intrusives and extrusives titano-magnetite and minor pyrite are usually the principal opaque phases. In almost all cases the original titanomagnetite contains exsolved fine and coarse lamallae or blebs of ilmenite. Lamellar ilmenite was not resolvable with the electron microprobe and attempts to obtain average titanomagnetite compositions by repeated scanning of single grains, failed to yield reproducable results. Optically uniform oxide grains or blebs formed by unmixing of original titanomagnetite have compositions close to the pure magnetite and ilmenite end-members and are unsuitable for geothermometric studies (cf. Buddington and Lindsley, 1964; Bowles, 1977).

(ii) Dundee Rhyodacite Suite

In Chapter 2 attention was drawn to the remarkable chemical uniformity of the ferromagnesian phases in the Dundee Rhyodacite, Tent Hill Volcanics and related ignimbrites. This uniformity is clearly demonstrated in Figures 3.17 to 3.20 and 3.22 to 3.24.

Mineral compositions are independent of whole rock chemistry (Figure 3.20C) and this is reflected in the 100 Mg/Mg+Fe ratio of the hosts which remains essentially constant with changing D.I. (Figure 3.21A). Although pyroxenes in the mafic aggegates are frequently mantled by magnesio-hornblende, there is no evidence of re-equilibration of the other mafic phases within the range of rock types analysed. (Hydrothermally altered samples are exceptions). This suggests that the clinopyroxene, hornblende and biotite phenocrysts were in equilibrium prior to eruption of the magma, and that the observed range of rock types resulted from sorting of the phenocrysts (and aggregates) during eruption and flow. It is believed

that chemical variation in the Tent Hill Volcanics largely reflects this sorting process. Because the residual liquids were impoverished in Fe, Mg, Ca and other ferromagnesian mineral components, and quenching was rapid, the mafic phases failed to re-equilibrate with the bulk chemistry of the newly formed rock systems.

The Dundee Rhyodacite itself may provide a reasonable indication of the bulk composition of at least the upper parts of the parent magma, as crystal sorting did not operate during its formation (cf. Flood et.al., 1980). The magma was probably homogenized by turbulent mixing because of the unique character of this eruption (see Chapter 4 for full discussion).

The pyroxenes forming mafic aggregates are more magnesian, slightly more aluminous and tend to be more frequently zoned than the phenocryst pyroxene (see Table 3.1 and Flood et al., 1977). The phenocrysts crystallized directly from the melt (Flood et al., 1977). However, the origin of the aggregate pyroxenes is more equivocal. Flood (1971) considered these aggregates to represent mafic residue carried up from the zone of partial melting and Flood et al. (1977) have considered the possibilities of a cumulate origin. With relation to the genesis of the Dundee Rhyodacite Suite magma these, and the original proposal of diorite-granite liquid hybridism (Shaw, 1964; Wilkinson et al., 1964), will be discussed in Chapter 6.

Pyroxene Thermometry: Calculated temperatures of equilibration of co-existing euhedral clinopyroxene and orthopyroxene in the Dundee Rhyodacite are listed below. Because of the limited number of orthopyroxene analyses collected in this study, the data of Flood et al. (1977) are considered to yield the most reliable equilibration temperature.

	CLINOPYROXENE		ORTHOPYROXENE			
	Anal. No.	Mg	Anal.No.	Mg	Temperature °C	
Flood et al., 1977	1	64.7	4	59.1	847*	877#
	13	64.2	13	52.6	830*	870#
This Study -	13	64.2	13	67.6	857*	852#
	13	64.2	13 (av)	60.2	839*	858#

* After Wood and Banno, 1973

\# After Wells, 1977

TABLE 3.1. PYROXENE DATA FOR DUNDEE RHYODACITE AND COMAGMATIC VOLCANICS

DUNDEE RHYODACITE

	PHENOCRYSTS									AGGREGATES				XENOLITHS		ORTHOPYROXENES	
Analysis No.	150A	150A	16	12	13	15	15	1#	2#	16	16	13	13	79	80	13	13
	core	rim				core	rim					core	rim				
SiO_2	52.17	52.19	51.96	52.38	51.83	51.96	52.26	52.65	52.07	53.35	51.47	52.36	51.63	51.81	51.94	50.84	52.94
Al_2O_3	0.83	0.84	0.88	0.80	0.91	1.24	0.92	0.90	1.44	1.66	2.89	2.18	1.80	0.88	0.93	0.91	1.39
TiO_2						0 22				0.24	0.40	0.40	0.26		0.12	0.15	0.33
Fe_2O	1.62	1.69	1.62	0.21	1.86	1.48	1.14	0.04	0.52	0.18	1.73	0.90	2.08	1.82	2.12	0.97	0.99
FeO	10.82	10.59	10.76	11.70	10.64	10.72	11.04	11.86	12.08	6.21	5.70	6.94	8.28	10.68	9.70	26.99	18.95
MnO	0.78	0.69	0.82	0.66	0.73	0.56	0.91	0.74	0.65	0.15	0.16	0.16	0.62	0.80	0.80	1.73	0.41
MgO	12.60	12.48	12.43	12.73	12.38	12.73	12.33	12.21	11.76	17.30	15.60	16.01	13.26	12.50	12.67	17.34	23.21
CaO	21.46	21.61	21.26	21.54	21.75	21.31	21.66	21.13	21.11	20.94	21.33	20.63	21.79	21.46	21.59	1.02	2.26
Na_2O	0.18	0.26	0.25		0.17	0.23	0.18	0.33	0.33		0.20	0.20	0.33	0.17	0.35		
K_2O																	
TOTAL	100.46	100.35	99.98	100.02	100.28	100.45	100.44	99.86	99.96	100.03	99.48	99.78	100.05	100.11	100.22	99.95	100.48
STRUCTURAL FORMULAE (6 oxygens)																	
Si	1.965	1.967	1.966	1.979	1.958	1.954	1.970	1.991	1.972	1.955	1.909	1.936	1.935	1.960	1.957	1.961	1.947
Al	0.037	0.037	0.039	0.036	0.041	0.055	0.041	0.040	0.064	0.072	0.126	0.095	0.080	0.039	0.041	0.041	0.060
Al^4	0.035	0.033	0.034	0.021	0.041	0.046	0.031	0.009	0.028	0.045	0.092	0.064	0.065	0.039	0.041	0.039	0.053
Al^6	0.002	0.004	0.006	0.015		0.009	0.010	0.031	0.037	0.027	0.035	0.031	0.015			0.002	0.007
Ti						0.006				0.007	0.011	0.011	0.007		0.003	0.004	0.009
Fe^{3+}	0.046	0.048	0.046	0.006	0.053	0.042	0.032	0.001	0.015	0.005	0.048	0.025	0.059	0.052	0.060	0.028	0.028
Fe^{2+}	0.341	0.334	0.341	0.370	0.336	0.337	0.348	0.375	0.383	0.190	0.177	0.215	0.260	0.338	0.306	0.871	0.583
Mn	0.025	0.022	0.026	0.021	0.023	0.018	0.029	0.024	0.021	0.005	0.005	0.005	0.020	0.026	0.026	0.057	0.013
Mg	0.708	0.701	0.701	0.717	0.697	0.714	0.693	0.688	0.664	0.945	0.862	0.882	0.741	0.705	0.712	0.997	1.272
Ca	0.866	0.873	0.862	0.872	0.880	0.858	0.875	0.856	0.857	0.822	0.847	0.817	0.875	0.870	0.872	0.042	0.089
Na	0.013	0.019	0.018		0.013	0.017	0.013	0.024	0.024		0.014	0.014	0.024	0.013	0.026		
K																	
TOTAL (X+Y)+Z	4.001	4.001	4.000	4.001	4.001	4.001	4.001	3.999	4.001	4.001	4.000	4.000	4.001	4.003	4.003	4.001	4.001
100.Mg/Mg+Fe	64.6	64.7	64.5	65.6	64.2	65.3	64.6	64.7	62.6	82.9	79.3	78.6	70.0	64.8	66.4	52.6	67.6

	TENT HILL VOLCANICS											RELATED VOLCANICS						
	PHENOCRYSTS						AGGREGATES					PHENOCRYSTS					AGGREGATES	
Analysis No.	1	3	5	5	6	10	2	1	8	8	6	178A	178A	21	21	31	25	25
			core	rim					core	rim		core	rim				core	rim
SiO_2	51.83	51.50	52.40	52.02	52.32	51.75	52.57	52.27	51.59	51.43	52.66	52.65	52.20	52.01	51.74	59.72	52.38	52.30
Al_2O_3	0.99	1.23	0.82	0.92	0.78	0.96	1.04	1.62	1.55	2.39	0.82	0.63	0.70	0.77	0.82	1.07	1.30	0.81
TiO	0.17	0.25					0.14	0.17	0.28	0.55				0.11			0.15	
Fe_2O_3	1.14	1.57	0.71	1.07	0.27	1.72	0.35	0.86	1.13	1.26	1.76	0.01	0.22	0.99	2.08	1.12	1.45	1.07
FeO	10.99	11.95	11.28	11.20	11.68	10.56	9.62	9.07	10.84	9.06	8.33	12.54	12.10	10.88	10.46	11.09	9.25	11.10
MnO	1.03	0.43	0.70	0.88	0.74	0.82	0.41	0.49	0.35	0.34	0.43	0.71	0.80	0.62	0.90	0.85	0.38	0.66
MgO	12.11	12.22	12.41	12.40	12.34	12.36	13.98	13.73	13.11	14.19	12.81	12.53	12.47	12.80	12.00	12.28	13.70	12.55
CaO	21.09	20.79	21.54	21.27	21.26	21.39	21.74	21.67	20.71	20.72	22.80	21.36	21.34	21.91	21.64	20.98	21.63	21.40
Na_2O	0.33	0.22	0.21	0.17	0.20	0.23		0.19	0.19	0.17	0.47				0.31	0.25	0.22	0.22
K_2O							0.07									0.08		
TOTAL	99.67	100.16	100.07	99.94	99.59	99.79	99.93	100.07	99.75	100.11	100.08	100.43	99.80	100.09	99.95	99.64	100.46	100.11
STRUCTURAL FORMULAE (6 oxygens)																		
Si	1.969	1.951	1.979	1.970	1.986	9.162	1.969	1.954	1.948	1.920	1.974	1.986	1.981	1.965	1.963	1.971	1.955	1.974
Al	0.044	0.055	0.037	0.041	0.035	0.043	0.046	0.071	0.069	0.105	0.035	0.028	0.031	0.034	0.037	0.048	0.057	0.036
Al^4	0.032	0.049	0.021	0.030	0.014	0.038	0.031	0.046	0.052	0.080	0.026	0.014	0.019	0.034	0.037	0.029	0.045	0.026
Al^6	0.013	0.006	0.016	0.011	0.021	0.005	0.015	0.025	0.017	0.025	0.010	0.014	0.012			0.019	0.012	0.011
Ti	0.005	0.007					0.004	0.005	0.008	0.015				0.003			0.004	
Fe^{3+}	0.033	0.045	0.020	0.031	0.008	0.049	0.010	0.024	0.032	0.036	0.050	<0.001	0.006	0.028	0.060	0.032	0.041	0.030
Fe^{2+}	0.349	0.379	0.356	0.355	0.371	0.335	0.302	0.284	0.342	0.283	0.261	0.396	0.384	0.344	0.332	0.352	0.289	0.350
Mn	0.033	0.014	0.022	0.028	0.024	0.027	0.013	0.016	0.011	0.011	0.014	0.023	0.026	0.020	0.029	0.027	0.012	0.021
Mg	0.686	0.690	0.699	0.700	0.698	0.699	0.781	0.765	0.738	0.790	0.716	0.705	0.706	0.721	0.679	0.695	0.762	0.706
Ca	0.858	0.844	0.872	0.863	0.865	0.869	0.873	0.868	0.838	0.829	0.916	0.863	0.867	0.887	0.880	0.853	0.865	0.866
Na	0.024	0.016	0.015	0.013	0.015	0.017		0.014	0.014	0.012	0.034				0.023	0.018	0.016	0.016
K							0.003									0.004		
TOTAL (X+Y)+Z	4.002	4.001	4.000	4.001	4.002	4.001	4.001	4.001	4.000	4.001	4.001	4.001	4.001	4.002	4.003	4.000	4.001	4.000
100.Mg/Mg+Fe	64.3	62.0	65.0	64.5	64.8	64.5	71.5	71.3	66.3	71.3	69.7	64.0	64.4	66.0	63.4	64.6	69.8	65.0

from Flood *et al.*, 1977

(iii) Granitoids and Emmaville Volcanics

The division of the Emmaville Volcanics and granitoids into two fields (Figures 3.20A and 3.20B respectively) has been attributed to the differences in ferromagnesian parageneses. However only the silicic granitoids (and probably rhyolites) with D.I. >80 show the expected increase in Fe component in their mafic phases with increasing D.I. Fe biotite and ferro-hornblende coexist only in rocks with very minor ferromagnesian contents. Fe in hornblende and biotites in the more mafic granitoids does not vary predictably with changing D.I. Similarly, the mg of hornblende and biotite generally do not correlate with the mg of their host rocks (not figured). Ewart (1971a) noted a similar lack of correlation between biotite and parent rock Mg number in volcanics of the Central Volcanic Region, New Zealand. The relative modal abundance of ferromagnesians in the granitoids and Emmaville Volcanics does, however, vary in a predictable manner so that whole-rock mg correlates with D.I. (Figure 3.21). The extensive overlap of the leucogranitoid and rhyolite fields (Figure 3.21D) again emphasizes the chemical similarity of these rocks.

Although the composition of hornblende is somewhat variable, the mg of the mafic phases in the xenoliths and granitoid host rocks are similar (linked by tie lines in Figure 3.20B). Hornblende and biotite in the xenoliths are in apparent equilibrium with the bulk chemistry of the host rocks. The relationship between xenoliths and host rocks will be discussed in Chapter 6 with reference to the origin of the magmas.

(B) TRACE ELEMENT CHEMISTRY

No attempt was made to monitor compositional variations in minerals as a means of investigating trace element partitioning during evolution of the magmas. In general the rocks are not amenable to such an investigation. Minor chloritization of the primary ferromagnesian phases, the presence of accessory mineral inclusions, and the difficulty of separating only those phases known to have crystallized from the melt are the major limiting factors. Mineral trace element data for samples of Dundee Rhyodacite, Tent Hill Volcanics, Mole River Diorite and three adamellites are presented in Table 3.2. In general, mineral trace element contents can be correlated with whole-rock trace element and modal data. Where there is a discrepancy in the "mineral balence"* (Lyakhovich, 1978) the influence of accessory

---

* The mineral balence is the relative amount of an element that is included in the common rock-forming minerals.

minerals is indicated. For example the comparatively high abundance of Ce, Nd, Y and Zr in hornblendes from adamellite 433B and Dundee Rhyodacite 397 is attributed to the presence of apatite and rare zircon inclusions (Deer et al., 1966; Lambert and Holland, 1974; Condie, 1978).

Adamellites: The Bungulla Porphyritic Adamellite 370 and undifferentiated adamellite 433B may be compared with the seriate-textured adamellite 446B of the porphyry group. Sample 446 is distinguished by relatively high Ba and low Rb (K-feldspar and biotite). The hornblende is Zn depleted, but biotite is enriched in Zn. The Zn contents of the ferromagnesians may not necessarily reflect the amount of Zn in the crystal lattices. Azzaria (1962) has shown that a considerable percentage of the trace base metals in ferromagnesians of granites is in a readily leachable form, implying that the metals are not wholly bound in the lattice but may be present as tiny sulfide inclusions (see also Taylor, 1966). The abundance of trace base metals in hornblende and biotite may therefore be influenced by the presence of co-precipitating sulfide phases.

The Bungulla Porphyritic Adamellite and its xenolith are relatively depleted in Ba (biotite and K-feldspar) and enriched in Rb (K-feldspar, and possibly biotite). The low Ba content suggests the magma was formed by small degrees of partial melting, Ba-bearing biotite was an important immobile residual of partial melting, or that Ba-rich, early crystallizing K-feldspar was effectively removed from the system (see Chapter 6).

Mole River Diorite: As indicated by the complex zoning of plagioclase in the Mole River Diorite, the magma has undergone a higher temperature (and pressure) crystallization episode where calcic plagioclase and hornblende were stable, and a lower pressure-temperature episode involving precipitation of more sodic plagioclase, K-feldspar, biotite and minor amphibole. Compared to the adamellites, biotite and hornblende are enriched in Cr, V and Ni and depleted in alkali metals, Zn and Nb. Like Ta, Nb partitions into iron-titanium oxides (Schock, 1979) and the presence of titanomagnetite as inclusions may influence the Nb concentrations of the ferromagnesians.

Both the highly calcic (av.) plagioclase and late-stage K-feldspar have low Sr, reflecting the Sr content of the whole rock. Textural relations indicate that K-feldspar joined plagioclase on the liquids during the latter stages of crystallization of the diorite. Although the entry of Sr into plagioclase will be perturbed at the onset of K-feldspar crystallization (Taylor, 1966; Brooks, 1968; Long, 1978), the thin

Figure 3.17 Biotite compositions classified according to the scheme of Foster, (1960). Compositions are expressed in terms of cation percent calculated on the basis of 22 oxygens with R^{3+} = total Al + Fe + Ti assigned to octahedral lattice sites. Where electron microprobe analyses were used, Fe^{3+} was calculated using values obtained for fully analysed biotites from rocks of similar composition as a guide. The following factors were used to calculate Fe^{3+} in biotites for the range of rock types represented on the diagram.

rhyolites (>70% SiO_2)	FeO x 0.10
all other volcanics	FeO x 0.063
leucogranites	FeO x 0.10
all other granitoids	FeO x 0.134
xenoliths in granitoids	FeO x 0.02

Biotites which plot outside the stipulated compositional fields were assigned a low Fe^{3+} content.

A Classification of Biotites

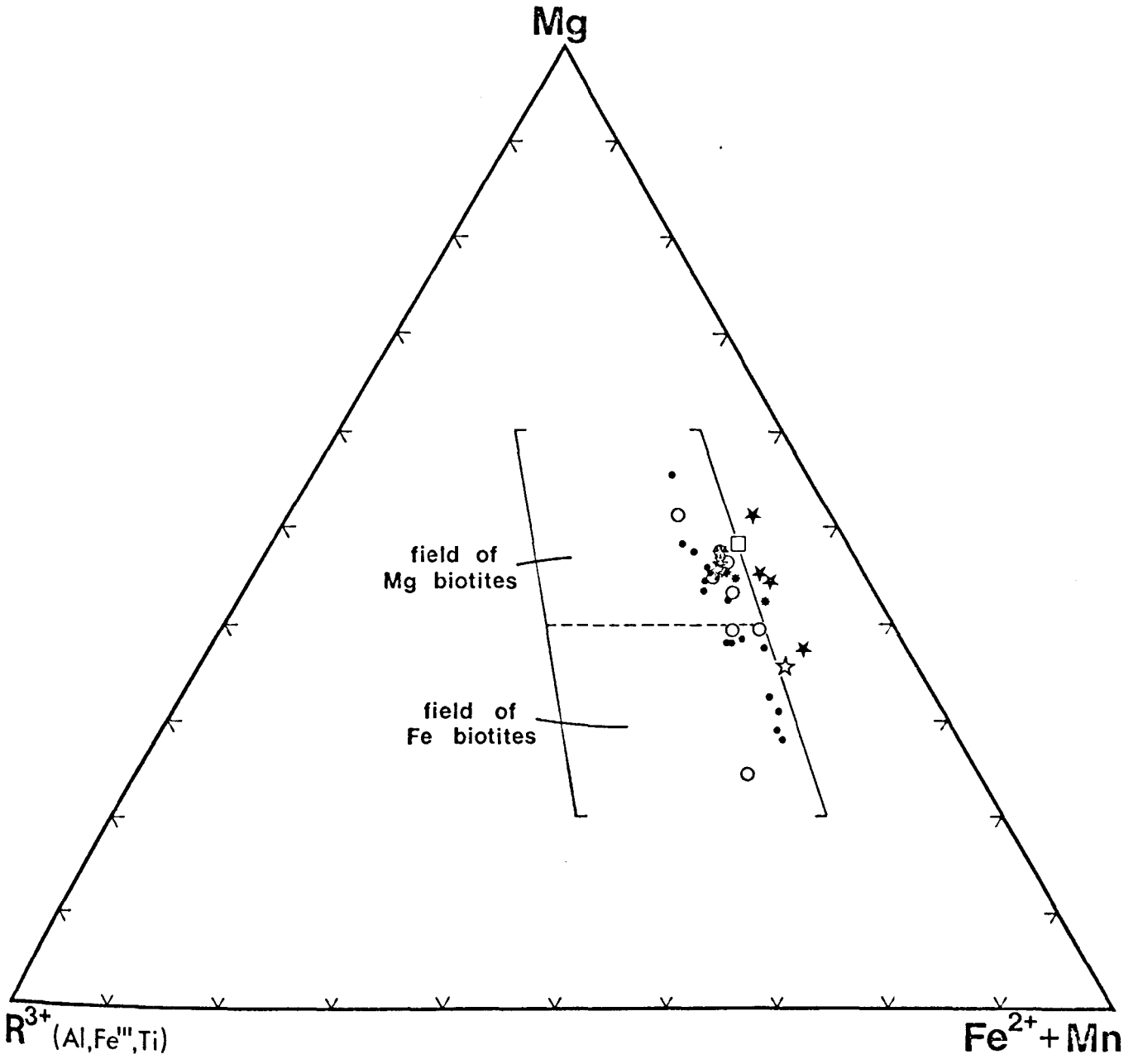

		Nº rocks
*	Dundee Rhyodacite	3
☆	Dundee Rhyodacite xenoliths	2
*	Tent Hill Volcanics	5
O	Emmaville Volcanics	8
•	Granitoids	16
★	Granitoid xenoliths	4
□	Mole River Diorite	1

(nomenclature after Foster, 1960)

Figure 3.18 Amphibole classification, broadly following the scheme proposed by Leake, 1968.

Minerals were analysed using an electron microprobe, with total iron content expressed as FeO. For this reason $Mg = MgO/MgO + FeO^{total} + MnO$ was used instead of the recommended Nigglis' mg. Failure to account for Fe^{3+} in calculation of structural formulae has also affected the value obtained for the amount of Si in the unit cell. As plotted, the data points are therefore laterally displaced by a small amount from their true positions. However, the diagram illustrates the broad range of amphibole composition within each division of the classification.

Si in the unit cell

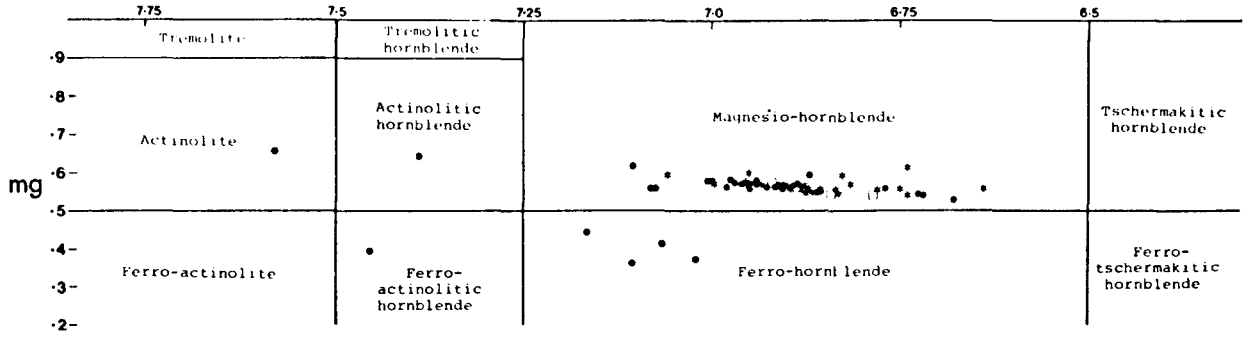

Σ Ca + Na + K < 2.50 Ti < 0.5

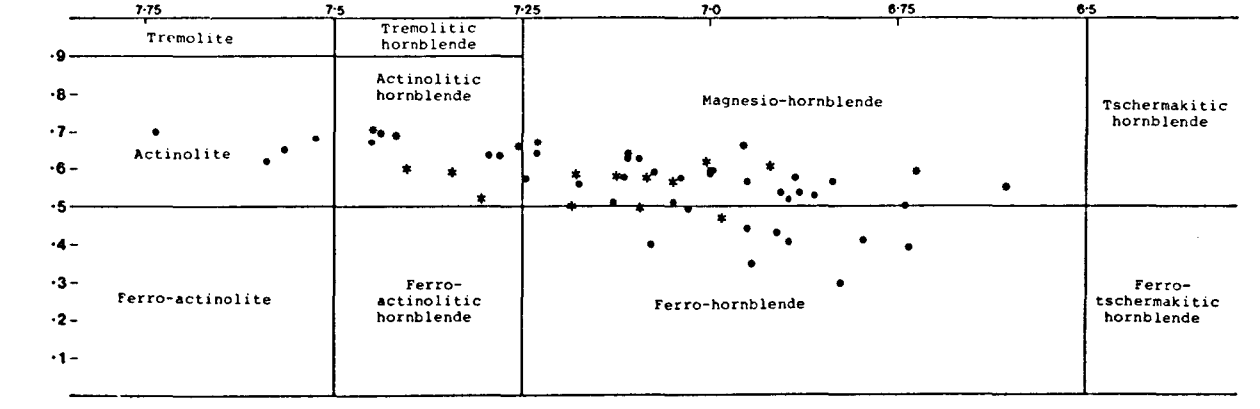

Σ Ca + Na + K < 2.50 Ti < 0.5

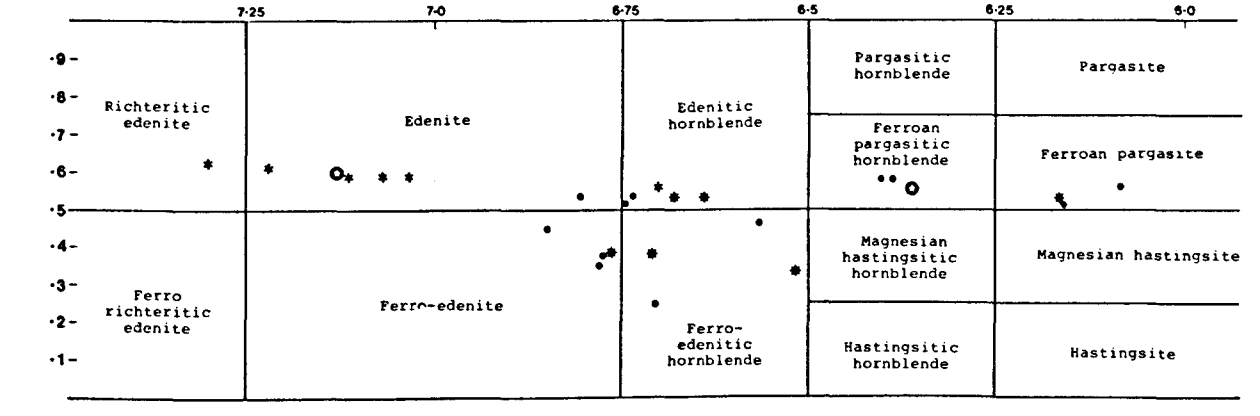

Σ Ca + Na + K > 2.50 Ti < 0.5

DIAGRAM	HOST ROCK	NO. OF ANALYSES	NO. OF ROCKS	SYMBOL
A	EMMAVILLE VOLCANICS	16	7	•
	DUNDEE RHYODACITE	18	5	•
	TENT HILL VOLCANICS	30	8	*
	DUNDEE RHYODACITE XENOLITH	4	1	□
B	GRANITOIDS	42	11	•
	GRANITOID XENOLITHS	12	3	*
	MOLE RIVER DIORITE	9	1	•
C	GRANITOIDS	12	5	•
	GRANITOID XENOLITHS	6	2	*
	EMMAVILLE VOLCANICS	6	2	•
	TENT HILL VOLCANICS	2	2	O

AMPHIBOLE CLASSIFICATION after Leake, 1968

fig. 3.19 PYROXENE CLASSIFICATION

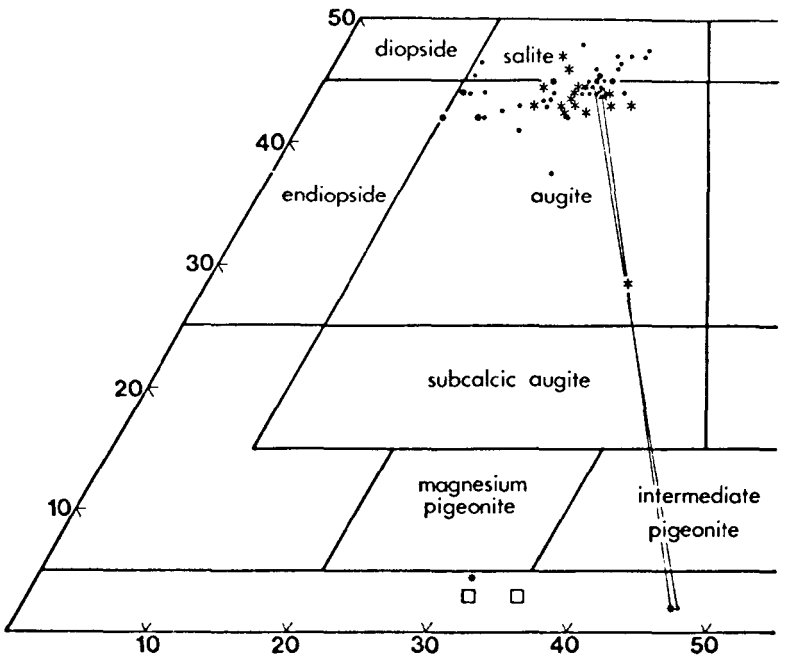

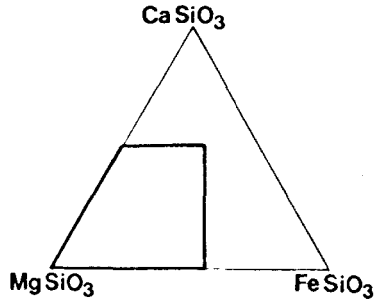

- Emmaville Volcanics
- Dundee Rhyodacite
- Tent Hill Volcanics
- Shannonvale Granodiorite
- Dundee Rhyodacite xenoliths

points plotted represent range of 103 individual analyses

tie lines link coexisting orthopyroxene and clinopyroxene

ATOMIC PROPORTIONS

EMMAVILLE VOLCANICS																
Mg	31.0*	39.5*	44.0	36.0*	39.0	51.0	33.0*	36.0*	35.0	33.0	43.0	36.0*	45.0	44.0	42.5	43.0
Fe	22.0*	17.5*	10.5	19.5*	17.0	47.0	20.0*	19.5*	17.0	20.5	10.5	20.0*	11.0	12.0	20.0	16.0
Ca	47.0*	43.0*	45.5	44.5*	44.0	2.0	47.0*	44.5*	48.0	46.5	46.5	44.0*	44.0	44.0	37.5	41.0

TENT HILL VOLCANICS													
Mg	39.5	36.0*	35.5	39.5	39.0	41.5	36.5	36.0*	34.0	38.0*	41.0	36.0*	35.5*
Fe	16.0	20.0*	20.0	16.0	18.5	30.0	19.5	20.0*	23.0	19.0*	16.0	19.5*	20.0*
Ca	44.5	44.0*	44.5	44.5	42.5	28.5	44.0	44.0*	43.0	43.0*	43.0	44.5*	44.5*

	DUNDEE RHYODACITE									DUNDEE xenoliths		SHANNONVALE GRANODIORITE	
Mg	36.0*	48.0	36.5*	36.0*	45.5	36.0*	51.5	64.5	36.0*	35.5*	36.0*	62.0	65.5
Fe	20.0*	10.0	19.0*	19.5*	12.5	20.0*	46.5	31.0	20.0*	20.5*	19.5*	35.0	31.5
Ca	44.0*	42.0	44.5*	44.5*	42.0	44.0*	2.0	4.5	44.0*	44.0*	44.5*	3.0	3.0

Data tabulated was selected to indicate the range of pyroxenes plotted and to highlight the uniformity of pyroxene compositions not adequately represented on the diagram. Asterisk denotes a typical analysis from an individual rock specimen.

Figure 3.20 Mg number of ferromagnesian minerals plotted against differentiation index of the host rock. Data points represent individual analyses.

A Emmaville Volcanics

B Intrusive rocks excluding Mole Granite and the Stanthorpe and Ruby Creek Adamellites

C Dundee Rhyodacite and Tent Hill Volcanics

Solid line in diagram B separates the "leucoadamellite" and "adamellite" fields. Similarly the Emmaville Volcanics are divisible into two fields.

Samples 18, 155 and 176 in diagram A are volcanics comagmatic with the Dundee Rhyodacite. Tie lines link xenolith and host rock.

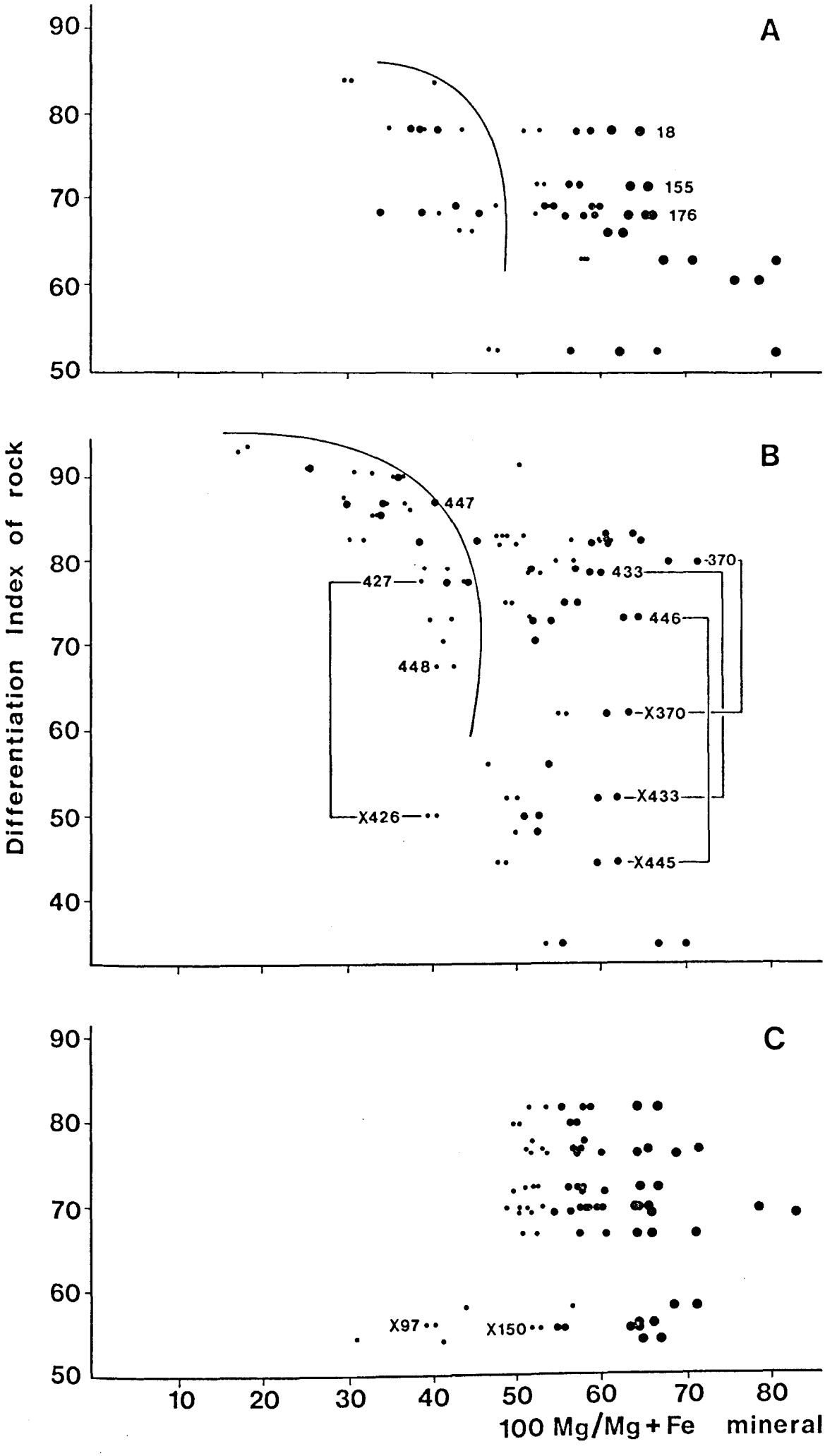
A
B
C
Differentiation Index of rock
90
80
70
60
50
40
18
155
176
447
427
448
433
370
446
X370
X433
X426
X445
X97
X150
10
20
30
40
50
60
70
80
100 Mg/Mg + Fe mineral
• biotite
• hornblende
• clinopyroxene

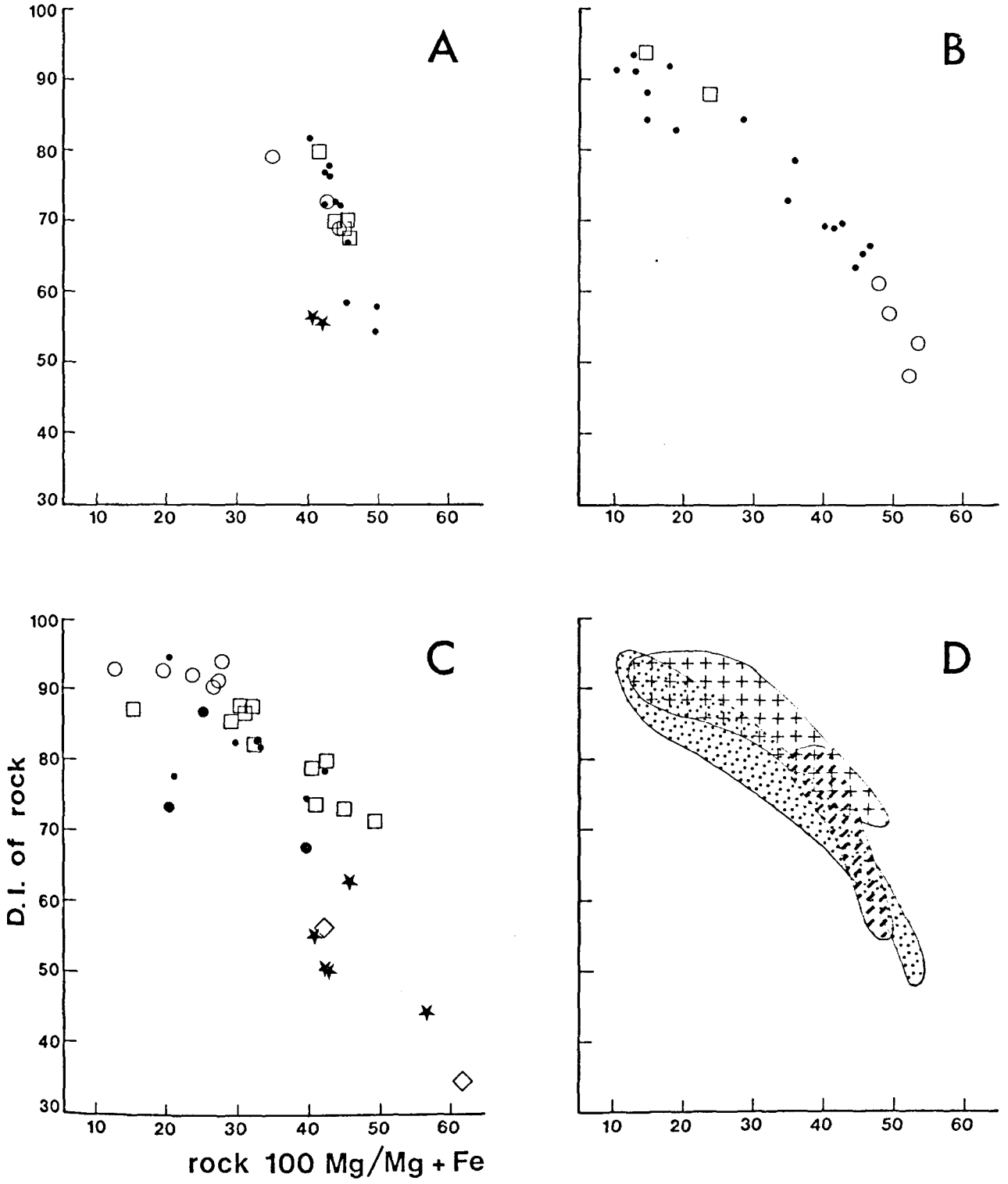

Fig. 3.21. Plots of D.I. vs. 100 Mg/Mg+Fe (atom %) for volcanic and intrusive rocks.

A Dundee Rhyodacite and related volcanics

square - Dundee Rhyodacite
dot - Tent Hill Volcanics
open circle - related ignimbrites
closed star - xenoliths in Dundee Rhyodacite

B Emmaville Volcanics

dot - rhyolites, rhyodacites and dacites
open circle - andesites
open square - "intrusive rhyolites"

C Intrusive rocks

small dot - undifferentiated granitoids and porphyries
large dot - adamellites from the Mole River. Nos. 446, 447 and 448
open circle - leucogranitoids
open square - adamellites
diamond - diorites
closed star - mafic xenoliths

D Summary of data from diagrams A, B and C

dots - Emmaville Volcanics
crosses - adamellites and leucogranitoids
dashed - Dundee Rhyodacite Suite

Figure 3.22 Biotites from Permian volcanics and intrusive rocks in the Tenterfield region, plotted in terms of Al, Mg and Fe + Mn (atomic %).

A Volcanics			No. of Rocks
small dot	-	Dundee Rhyodacite	6
large dot	-	Dundee Rhyodacite mafic xenoliths	2
open circle	-	Tent Hill Volcanics	10

B Volcanics			
dot	-	Emmaville Volcanics	9
open square	-	Volcanics comagmatic with the Dundee Rhyodacite	4

C Intrusive Rocks			
dot	-	granitoids	25
open square	-	xenoliths	4

Lower diagram shows fields of biotite composition for volcanic and intrusive rocks, summarizing data from diagrams A, B, and C.

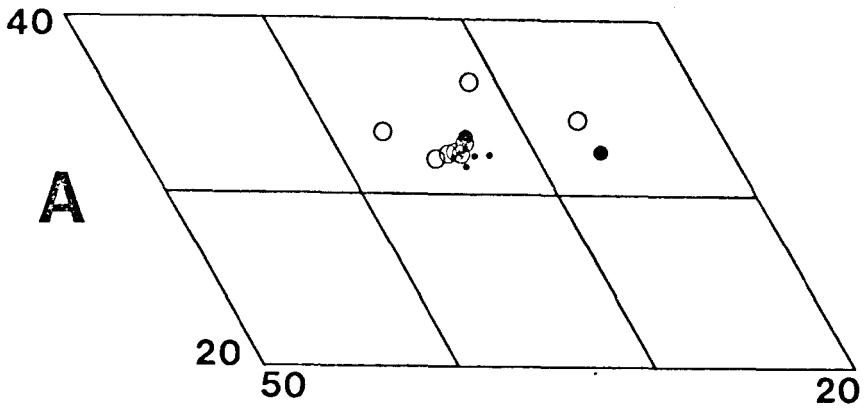

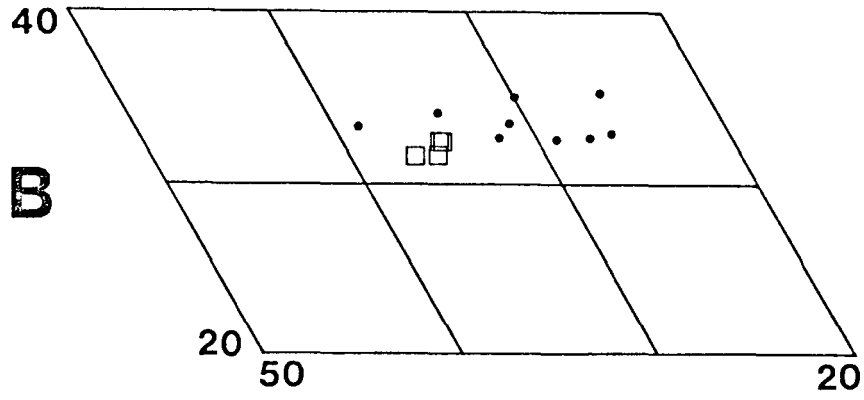

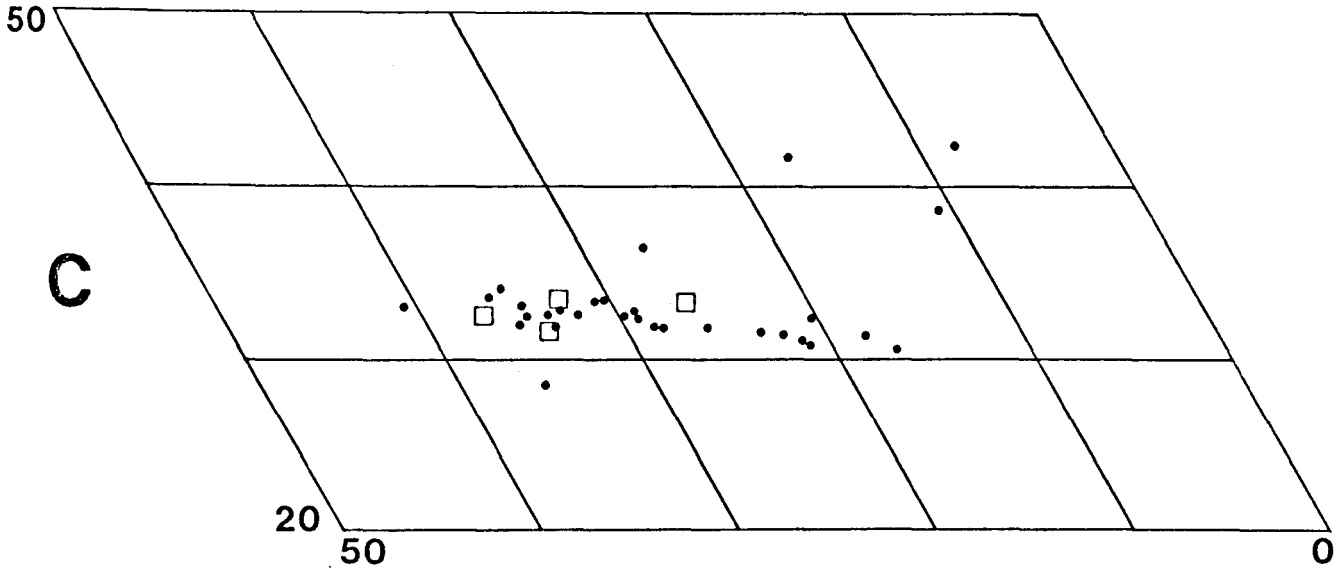

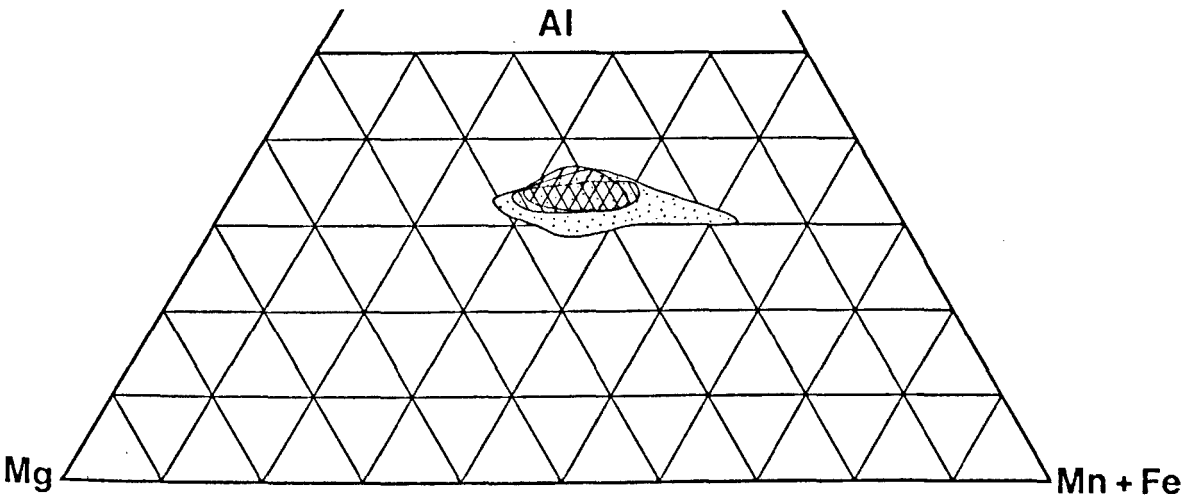

BIOTITES

Figure 3.23 Variation of Ca + Na + K with Si in the half-unit cell of amphiboles in volcanic and intrusive rocks from the Tenterfield region. Nomenclature for fields 1 to 9, for the pure magnesium end members of the calciferous and subcalciferous amphiboles (Leake, 1968, Fig.1), has been modified to incorporate the appropriate iron-rich end members (refer Fig. 3.18).

A Volcanic Rocks

open square - Tent Hill Volcanics

open circle - Dundee Rhyodacite

dot - Emmaville Volcanics

B Intrusive Rocks

dot - granitoids

open square - xenoliths

C Summary of data from diagrams A and B

The four compositional fields shown are:-

small dot - granitoids

large dot - Tent Hill Volcanics and Dundee Rhyodacite

random dashes - Emmaville Volcanics

circles - "average" Dundee Rhyodacite, Tent Hill Volcanics and comagmatic volcanics

Nomenclature

1. Richterite
2. *Richteritic endenite*
3. *Endenite* and *ferro-endenite*
4. *Endenite hornblende* and *ferro-endenitic hornblende*
5. Pargasitic hornblende and *ferroan pargastic hornblende*
6. Tschermakitic hornblende
7. *Magnesio-hornblende* and *ferro-hornblende*
8. Tremolitic hornblende, *actinolitic hornblende* and *ferro-actinolitic hornblende*
9. Tremolite and *actinolite*

Amphibole types represented on the diagrams are in *italics*. Structural formulae were calculated from electron microprobe analyses with total iron expressed as FeO.

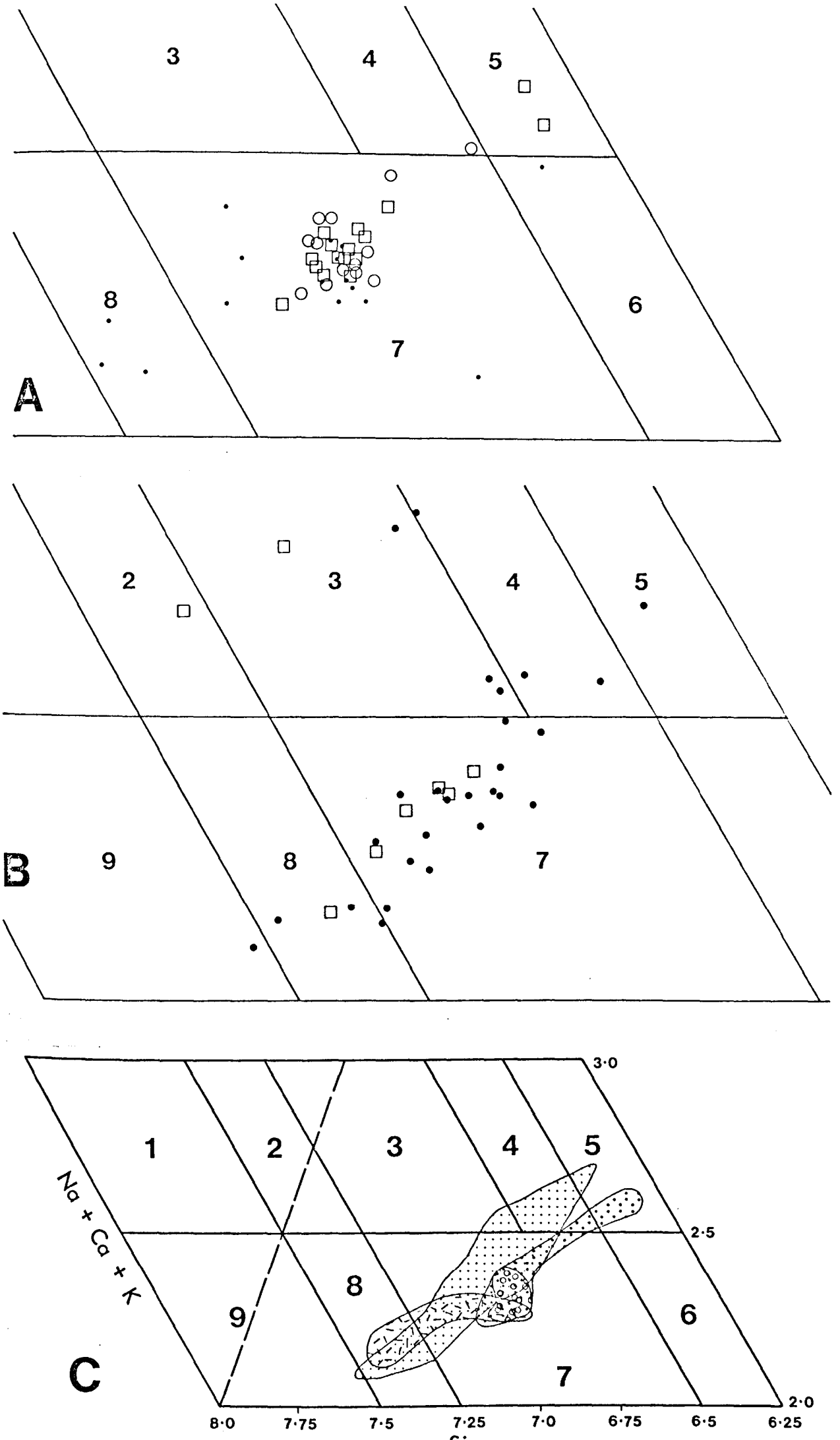
3
4
5
8
6
7
A
2
3
4
5
9
8
7
B
1
2
3
4
5
3·0
2·5
2·0
Na + Ca + K
9
8
6
7
C
8·0
7·75
7·5
7·25
7·0
6·75
6·5
6·25
Si

Figure 3.24 Calcic amphiboles from Permian volcanic and intrusive rocks in the Tenterfield region, plotted in terms of Ca, Mg, and Fe + Mn (atomic %).

A Volcanics			No. of Rocks
dot	-	Dundee Rhyodacite	5 plus mafic xenolith
open square	-	Tent Hill Volcanics	9

B Volcanics				
dot	-	Emmaville Volcanics	4	total 9
open square	-	Volcanics comagmatic with the Dundee Rhyodacite	5	

C Intrusives			
dot	-	granitoids	15
open square	-	xenoliths	4

Lower diagram shows fields of amphibole composition for volcanic and intrusive rocks, summarizing data from diagrams A, B, and C. Smallest field incorporates amphiboles from volcanics comagmatic with the Dundee Rhyodacite.

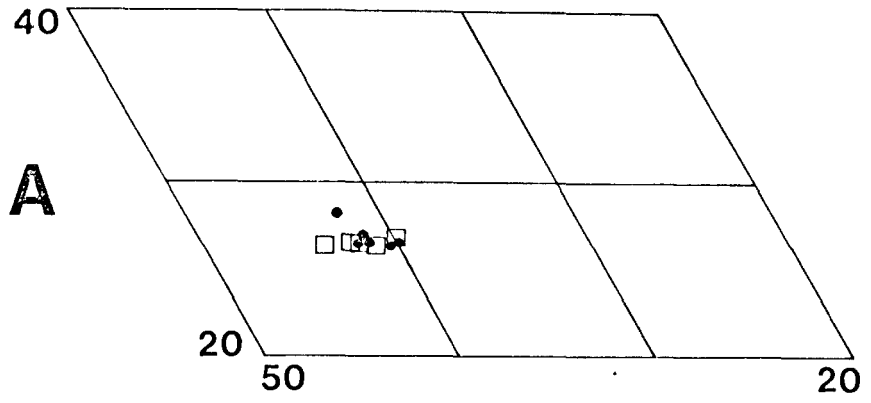

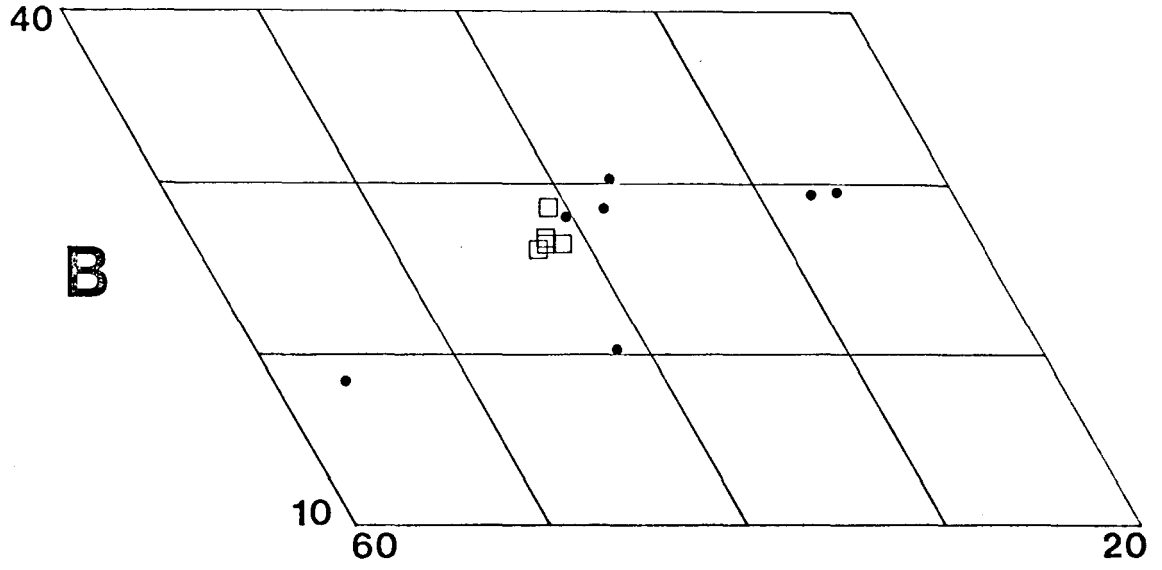

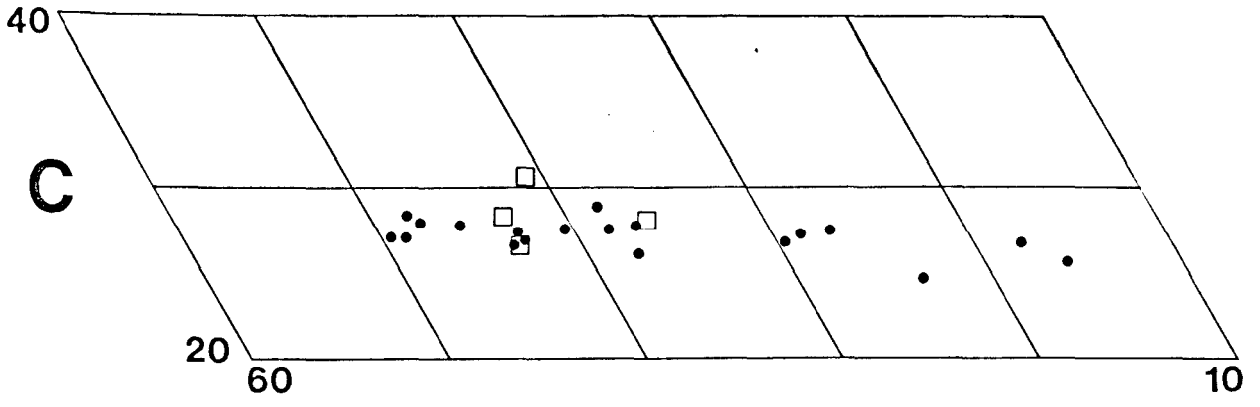

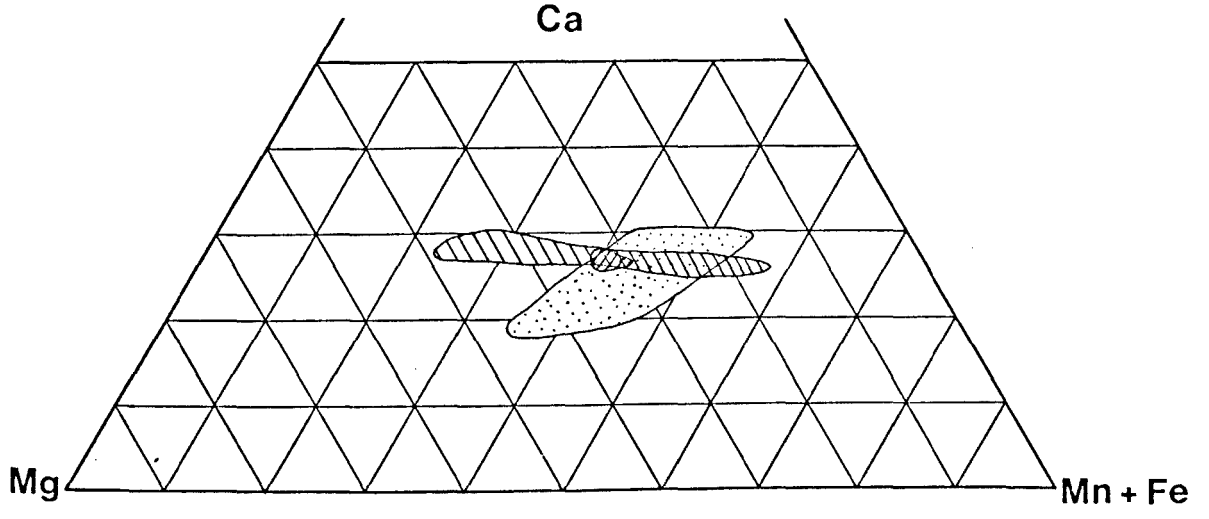

AMPHIBOLES

Table 3.2 MINERAL TRACE ELEMENT DATA (µg/g)

Field No.	Analysis No.	Mineral	Ni	Ce	Nd	Ba	V	Cr	Cu	Zn	Li	Rb	Y	Sr	Zr	Nb	Pb
397									60	190	9						
256	8	Clino-Pryoxene	99	52	49	103	299	487	24	133	28	23	78	47	86	7	30
445c	78		81	76	53	74	304	318	10	185	10	7	68	23	48	26	4
X370A	85		44	76	63	45	348	8	10	293	23	28	70	41	62	15	8
397			104	203	218	125	324	62	16	240	12	16	369	57	98	65	5
370	69		62	40	14	47	209	38	14	322	19	11	24	14	9	14	3
446B	51	Hornblende	55	69	67	87	218	12	9	197	20	11	114	19	148	24	5
433B	58		97	227	226	75	309	61	10	337	6	8	366	29	118	68	18
397				20	15	2562	419	91	16	348	140	615	72	5	37	64	9
256	8		112	12	16	5885	978	188	35	258	102	388	55	61	96	38	14
445c	78		144	4	6	872	624	307	18	292	162	262	35	11	8	7	3
446B	51		112	(2)	4	3192	408	12	16	332	201	413	40	6	65	22	12
433B	53	Biotite	100	6	-	1695	542	60	12	50	185	906	80	4	33	29	6
370	69		126	12	-	700	506	31	10	53	365	911	78	3	108	39	6
256	8		11	15	4	414	-	7	8	16	1	-	-	1301	-	-	14
370	69		15			62		8	7	9	9	-	-	578	24	-	15
X370A	85		8	26	5	41		8	18	15	6	45	7	555	107	-	28
397			7	18	3	391		7	4	10	5	-	-	826	18	(2)	23
446B	51		32	15	4	273		9	8	10	4	-	3	664	35	3	13
445c	78		7	14	3	54		8	8	9	4	-	5	111		-	3
433B	53	Plagioclase	11		6	203		10	10	17	2	-	3	587	29	-	19
446B	51		19			4092	6	13	7	7	6	178	15	231	-	-	18
445c	78		-			4460		8	6	8	1	155	13	204	-	-	15
433B	53		24			2103		8	8	20	2	379	30	253	17	-	36
X370A	85		28			879		9	4	9	5	611	52	308	-	-	58
370	69	K-Feldspar	28	-	-	793	-	8	5	8	5	537	44	309	-	-	51

397 Dundee Rhyodacite
256 Tent Hill Volcanic
445c Mole River Diorite
370 Bungulla Porphyritic Adamellite
X370A Bungulla Porphyritic Adamellite - xenolith
446B, 433B Undifferentiated adamellites

blank not determined
- below detection limit
(2) at lower level of detection

outer zones of more intermediate plagioclase are likely to be relatively enriched in Sr, as the partition coefficient of Sr is strongly dependent on T and P_{H_2O}, and Sr partitioning favours plagioclase of this composition (Brooks, 1968; Drake and Weill, 1975; Banno and Yamasaki, 1979).

Dundee Rhyodacite: Because they contain numerous accessory mineral inclusions, the hornblende of Tent Hill Volcanic 256, and most of the clinopyroxene separated from Dundee Rhyodacite 397, were rejected for analysis. Similarly the presence of accessory minerals and phenocryst fragments prevented effective separation of the felsic components of the siliceous groundmass in the Dundee Rhyodacite.

Compared to the Dundee Rhyodacite, the plagioclase and biotite of the Tent Hill Volcanics are relatively enriched in trace elements which enter these minerals at an early stage. Plagioclase from sample 256 (av. > An_{42}) contains more Sr than plagioclase in the Dundee Rhyodcaite (av. An_{37}). The biotite is enriched in Ba, V, Cr and Cu and relatively depleted in Li, Rb, Zn and Y. The data suggest that biotite and plagioclase in the Tent Hill Volcanic crystallized earlier than their counterparts in the Dundee Rhyodacite. An exhaustive mineral trace element study is required to fully investigate the possibility that the Dundee Rhyodacite was derived from a slightly more evolved magma than the Tent Hill Volcanics.

MAFIC XENOLITHS

(A) Xenoliths in the Dundee Rhyodacite

Two clinopyroxene-bearing microporphyritic xenoliths in Dundee Rhyodacite from north of Tent Hill were analysed. Compositional variation in these xenoliths is due to variation in the amount of microcrystalline groundmass present; the relative proportions of phenocryst phases are almost constant. Mafic mineral compositions are shown in Figure 3.20C. The hornblende in xenolith X97A has been made over to biotite, and compared to X150A, this xenolith has suffered more extensive deuteric alteration. Figure 3.2 shows that this alteration was essentially isochemical.

Plagioclase phenocrysts have a highly calcic core (up to An_{81}) which may represent refractory restite carried up from the zone of partial melting. Plagioclase in mafic aggregates of the host has been interpreted by Flood (1971) and Flood et al. (1977) as probable restite but it is significantly less calcic (< An_{53}). Although much of the core plagioclase in the xenoliths may be restite, the xenoliths are not samples

of depleted parent rock from the melting zone. All the ferromagnesian phenocrysts have crystallized from the melt, and like the felsic groundmass phases, are identical to those in the host. Because the xenoliths represent unusual mixtures of crystals and melt, the compositions of the phenocrysts bear no relation to the whole-rock chemistry, and the xenoliths do not plot on the Dundee Rhyodacite Suite trend for a number of major and trace elements (Figures 3.2 and 3.9).

(B) Mafic Xenoliths in Adamellites

Xenoliths analysed include tonalites X445A, X426A and B, quartz diorite X433A and microgranodiorite X370A. Major and trace element characteristics of the xenoliths are shown in Figures 3.2 and 3.10 respectively. For many elements the xenoliths plot on the low silica extension of the trend defining the major granitoid suite. However the quartz diorite and microgranodiorite are distinguished by relatively low Ca, Sr and Cr and high Rb, Zr and Zn. The quartz diorite contains abundant biotite rich in Ba.

All xenoliths except microgranodiorite X370A contain magmatic magnesio-hornblende and deuteric actinolitic hornblende. The more siliceous amphibole is present largely as a replacement of clinopyroxene but in X370A the pyroxene is mantled by primary magnesio-hornblende.

The available whole-rock and mineral data provide no clear indication of the origin of the xenoliths. The three most reasonable alternatives are that the xenoliths represent:

(a) re-equilibrated refractory residua from the melting zone,

(b) partly re-equilibrated, high pressure-temperature cumulate material,

or

(c) fragments of country rock that were incorporated into the magma above the zone of partial melting.

CHAPTER 4

THE VOLCANO-PLUTONIC ASSOCIATION

INTRODUCTION

VOLCANISM AND CALDERA DEVELOPMENT

(a) Recognition of Calderas

(b) Caldera Formation

FORMATION OF THE DUNDEE RHYODACITE AND RELATED VOLCANICS

GRANITOID INTRUSIONS

GRANITIC PORPHYRIES

THE VOLCANO-PLUTONIC SUITE: DISCUSSION

(a) Role of Faulting

(b) Properties of the Magma and Magma Emplacement

GRAVITY DATA

CHAPTER 4

THE VOLCANO-PLUTONIC ASSOCIATION

INTRODUCTION

Partly because of the relatively limited scope of previous investigations in the Emmaville-Tenterfield region, and partly due to misinterpretation of the Dundee Rhyodacite as an intrusive rock, the close relationship between the volcanic and subvolcanic rocks in the area has more or less remained unrecognized. The term "volcano-plutonic formation or association" has been assigned to regions where comagmatic volcanic and subvolcanic rocks are intimately associated both in space and in time (Ustiyev, 1965, 1970; Kochhar, 1972). In the major volcano-plutonic associations of the world, volcanism and plutonism are linked through caldera formation (Ustiyev, 1969). This also appears to be the case in the New England Geosyncline in northern New South Wales. The recognition of cauldron structures and very high-level plutonism in the Emmaville-Tenterfield area has permitted not only a more thorough unravelling of the magmatic history of the region, but also a fuller understanding of the metallogenesis.

There is abundant evidence of subvolcanic granitoid emplacement in the Emmaville region. South and west of Emmaville, a large number of small granitoid masses intrude the Emmaville Volcanics. Some of these intrusions may be quite large plutons in the process of being unroofed. North of Deepwater, the Bolivia Range, Pye's Creek, Mount Jonblee and other leucoadamellites have intruded the volcanic pile and are now comparatively well exposed. Small inliers of Stanthorpe Adamellite are exposed northwest of Wallangarra, suggesting that the entire sequence of Wallangarra Volcanics is underlain by this adamellite pluton. Near Tenterfield, several masses of the Dundee Rhyodacite have been intruded by magmas of adamellite and leucoadamellite composition.

The fracture-fill metalliferous veining and widespread low-grade contact metamorphism in the volcanics south of Dundee and north of Deepwater provide indirect evidence for the presence of acid plutons close to the present erosion surface. The Glen Eden, Bakers claim and Bullock Mountain molybdenite deposits south and west of Dundee (Weber et al., 1978) and the Emmaville cassiterite stockwork deposits, are examples of high-level granite-derived orebodies within Emmaville Volcanic country rocks.

In this chapter the volcano-plutonic association will be discussed with reference to the relationship of the pyroclastics to caldera formation, the subsequent engulfment of some cauldron blocks by acid magmas, and intrusion of granitoids to high crustal levels within the caldera outflow-facies volcanics.

VOLCANISM AND CALDERA DEVELOPMENT

(a) Recognition of Calderas

While mapping the Tenterfield region Shaw (1964) noted three prominent ring structures, each spatially associated with individual masses of "Dundee Adamellite Porphyrite". Recognition of the volcanic nature of this rock type (Flood et al., 1977; this study) has led to a re-interpretation of the "ring fault dyke rocks" and their relationship to the Emmaville Volcanics and Dundee Rhyodacite. It is now proposed that the Tenterfield, Brassington and Dundee masses of the Dundee Rhyodacite fill cauldron subsidence regions. The caldera margins remain partly defined by acid dyke rocks which are considered to occupy formerly active ring faults. Similar conclusions cannot be made with respect to the Bolivia and Timbarra masses because the original boundaries of these masses have been extensively modified by granitic intrusions or regional faulting. Flood et al. (1977, p.301) interpreted the localized hydrothermal alteration along the western margins of the Dundee mass (first reported by Vernon, 1959, p.102), and the "subvertical foliation about the Dundee mass", to be consistent with a cauldron-fill mode of occurrence. The sporadic hydrothermal alteration of contact rocks has been verified in this study (see Ch.2) but no "subvertical foliation" has been observed; the foliation is commonly sub-horizontal, dipping gently towards the caldera centre.

The interpretation that the Brassington and Tenterfield masses of the Dundee Rhyodacite delineate individual calderas has not been proposed formerly. In fact Flood et al. (loc.cit.), impressed by the compositional uniformity of the Dundee Rhyodacite, assumed that all masses once comprised a single "ignimbritic flow" (p.301). This interpretation is not well supported by the patterns of contact metamorphism produced by the subsequent high-level granitoids. Contact metamorphism of the Dundee, Bolivia and Brassington masses is confined to a narrow aureole ($\lesssim$ 100m), which suggests high-angle contacts with the granitoids. This contrasts with granitoid-Emmaville Volcanic contacts which typically dip at very low angles, shown by broad zones of contact metamorphism in the Volcanics. High-angle ring faults

may therefore have been a partial control on granitoid emplacement; intrusion was channelled away from subsidence areas so that Dundee Rhyodacite masses were virtually unaffected, while the volcanics outside cauldron structures were domed and extensively metamorphosed. This implies that the Bolivia mass, although completely surrounded by intruded adamellites, is also bounded by high-angle faults which, even if not directly related to caldera formation, at least influenced the geometry of the intrusive contacts.

Together with the recrystallized ring porphyries, the Mackenzie Adamellite and Nonnington Leucoadamellite form a composite intrusive mass uniquely elliptical in plan. It seems plausible that these granitoids have intruded a formerly active volcanic centre by complete displacement of the cauldron block. The ring porphyries at the northern margin are the only remnants of the earlier cauldron structure. This conclusion has also been made by Cuddy (quoted in Jones, 1976) following a study of the fracture pattern of the complex. The Mount Mackenzie intrusive centre may therefore represent a limiting case of intrusion into a cauldron block, where "assimilation", or erosion following doming has removed all traces of a prior volcanic history.

As pointed out by Oftedahl (1978), the ignimbrite-cauldron association is so close in southwestern U.S.A. that the presence of thick ignimbrites alone is evidence for a cauldron (e.g. Smith and Bailey, 1968; Smith et al., 1961; Lipman, 1975). In eastern Australia this association is recognized in the Palaeozoic volcanic province of central Victoria (e.g. McLaughlin, 1976; Birch, 1978) and in the Georgetown region, northern Queensland (e.g. Branch, 1966; Bailey, 1977). The cauldrons near Tenterfield were therefore recognized mainly on the basis of associated structures and rock types. Ustiyev (1970) noted that high-level intrusion of acid magmas and caldera-related volcanism mark the final stage of igneous activity in many of the world's large geosynclines. Cauldron formation therefore also appears to coincide with the stage of development of the New England Batholith s.l. during Late Permian times.

(b) Caldera Formation

The Emmaville Volcanics represent the first cycle of acid magmatism in this part of the New England Geosyncline. They outcrop for hundreds of square kilometres south and west of Emmaville and they almost certainly extended northwards into southern Queensland in Late Permian times. To date no source for these massive outpourings (i.e. volcanic vents) has been found and in this respect the Emmaville Volcanics are therefore similar to acid ignimbrites associated with

cauldrons in many areas elsewhere (e.g. western San Juan Mountains District, Colorado - Lipman et al., 1973; Lipman, 1975).

It is envisaged that the volcanic cycle commenced when a dominantly liquid and quite fluid magma rose to high levels in the sedimentary basement. The mechanism of emplacement of this magma in conjectural, but emplacement was unlikely to have been by simple stoping because of the lack of a high density contrast between intruding magma and silicic basement sediments. Extensive assimilation of sedimentary rocks can be excluded on the basis of isotope geochemistry (O'Neil et al., 1977; Shaw, 1964), and the relatively low temperatures of acid magmas (e.g. Winkler, 1976, Winkler et al., 1975). The melts probably rose to high levels along pre-existing zones of weakness in the crust, i.e. emplacement during a period of crustal tension (Shaw, 1964; Myers, 1975; Ustiyev, 1965; Sides, 1981).

A build-up of pressure in the high-level chambers, possibly as a consequence of magma degassing, may have domed the thin crust and initiated tensile fracturing in the roof rocks. According to Roberts (1970), ring faults so formed may be occupied by magma, forming dykes that dip steeply inwards at the surface. Under conditions of relatively low magma pressures, tension above the chamber can be relieved by an arcuate fracture ". . .exactly the case with the ring dyke which forms only a segment of a circle" (Stillman, 1970, p.44). Ring dykes associated with the Dundee and Tenterfield Calderas appear to be of this type. A magma that is tapped by a ring fault can become fluidized due to pressure-induced or retrograde boiling, thereby initiating either explosive (Plinian) or ignimbritic eruption at the surface, depending largely on the prevailing gas content of the fluidized magma (Harris et al., 1970; Phillips, 1974; Roberts, 1970; Reynolds, 1954; Tazieff, 1970; Wilson, 1977).

By the process just described, the eruption of vast volumes of ash-flow rhyolite which formed the Emmaville (and Wallangarra) Volcanics may have occurred in the calderas now recognized near Emmaville and Tenterfield. The depletion of underlying magma chambers triggered cauldron subsidence of the typical Glencoe type (McCall, 1963; Roberts, 1974; Williams, 1941).

The virtual absence of ash-fall material in the region and the large diameter of the cauldrons preclude explosion mechanisms of caldera formation (Steinberg, 1974). It should be noted that any radial fracturing of surrounding country rocks (which, if present, would indicate upwelling in response to high magma pressures (Phillips, 1974)), has been buried by volcanics or obliterated by subsequent granitoid intrusions. Relatively low gas pressures in the magma chambers are therefore indicated by the development of ring dykes, and the (non-explosive) products of

eruption. Furthermore, extremely volatile-rich magmas, even of relatively low density rhyolitic composition, are unlikely to have risen passively to the levels indicated in the Tenterfield region (Harris, 1977; Cann, 1970).

The duration of the volcanic activity giving rise to the Emmaville and Wallangarra Volcanics is not known but may have lasted for many millions of years. Subsidence in all calderas may have been already well advanced during the waning periods of rhyolitic volcanism.

Massive outpourings of fluidized hornblende-biotite rhyodacitic magma marked the second and final phase of Permian volcanism in the region. The ignimbritic Dundee Rhyodacite probably was erupted from a central vent or through pre-existing ring fractures reactivated in response to magma resurgence. Field studies suggest that volcanic activity was associated with pre-existing calderas at several localities and that these calderas were filled with the products of eruption. This differs from the interpretation made by Flood et al. (1977). They considered the Dundee Rhyodacite once formed a continuous, thick ash-flow sheet that was subsequently rifted apart by the intrusion of younger plutons to form eight discrete masses. An alternative model more consistent with the unusual textural features and present distribution of the Dundee Rhyodacite masses is discussed in the following section.

FORMATION OF THE DUNDEE RHYODACITE AND RELATED VOLCANICS

From the petrographic descriptions presented in Chapter 2 it is clear that although many features of the Dundee Rhyodacite support an ash-flow origin, the typical microgranular groundmass textures are not those normally associated with ignimbrites. Somewhat unusual conditions are required to supplant the pyroclastic textures of typical ignimbrites, and the validity of any model of formtion of the Dundee Rhyodacite largely depends on the satisfactory provision of such requirements.

The Wyberba and Sunnyside masses are obvious flow sheets with vestigial eutaxitic textures, but the true nature of the remaining masses is conjectural because any original volcanic textures have not been preserved. For this reason it would not be valid to immediately infer a volcanic origin for the other masses, although the Wyberba and Sunnyside masses were certainly derived from magmas equivalent to those which formed the other masses. The bulk of the Dundee mass has

a microgranular groundmass texture virtually identical to that found in the other masses (excluding Wyberba and Sunnyside), hence it is assumed that they all shared a common cooling history. Consequently, conclusions relevant to the origin of the Dundee mass should apply to the other masses. The Dundee was studied in more detail because, unlike the other masses, its margins are not fault bounded or intruded by later plutons.

The Dundee mass lacks those features diagnostic of an intrusive origin. The foliation, observed up to 1km from the contact zone, may have been induced by flow in the upper regions of an intrusive plug or shallow sill, but the gradual transition to ignimbrites near the margins of the mass is not consistent with this hypothesis.

However, the form of the Dundee mass can be explained by two broadly similar mechanisms. One is that the Dundee mass is a pseudo-pluton (as described by Rutten, 1969) with ignimbritic margins. In this model the mass represents the crystallized product of a fluidized magma that welled out of a large vent only to collapse within the confines of the vent rim. In regions of earlier cauldron subsidence the margins of such a pseudo-pluton would be defined by the caldera rim. Evidence of flow would be localized at the margins where the magma thinned on encountering the obstacle of the caldera rim. Any magma that overflowed or breached the rim would crystallize to form a true ignimbrite (cf. the Wyberba and Sunnyside masses) but the main body of magma within the caldera could be expected to defluidize and crystallize in a manner analogous to a high-level intrusive pluton. Because eruption of the Dundee Rhyodacite magma from an active ring fracture is not a requirement of the model, extrusion of the Tent Hill Volcanics (which now occupy such a ring fracture), may have occurred either before or after the caldera was filled. However for purposes of comparison with the ash-flow sheet hypothesis (discussed below) the Tent Hill Volcanics are shown to have erupted before the Dundee Rhyodacite in Figure 4.1.

The size of the initial vent is impossible to ascertain. If the 300+ km^2 area of the Dundee mass represents the size of the original vent, the pseudo-pluton could be extremely thick, presumably grading at depth into a more coarsely-textured granitoid. However, regional gravity anomaly data suggest that the Dundee mass is relatively thin (see p.86). For this reason eruption of rhyodacite magma from a small vent (or vents) within a subsided cauldron block is much preferred.

A modification of the pseudo-pluton model is that the major volume of the Dundee mass represents a lava flow which grades into ignimbrite at the margins. Logic dictates that the ignimbrite preserved at the margins was a precursor to

Figure 4.1: Models of formation of the Dundee Rhyodacite.

The diagrams are schematic northeast-southwest cross-sections through the Dundee caldera showing the stages of development of the Dundee Rhyodacite and Tent Hill Volcanics. The high-level granitoid shown in stage 4 represents an idealized subvolcanic pluton which dates to the first major intrusive episode. The doming of roof rocks considered to accompany such intrusions is not shown but is explained in the text. For purposes of comparison, the Tent Hill Volcanics are shown as predating the Dundee Rhyodacite in the pseudo-pluton model, but this interpretation is not favoured (*see* text).

DUNDEE RHYODACITE — MODELS OF FORMATION

IGNIMBRITE SHEET

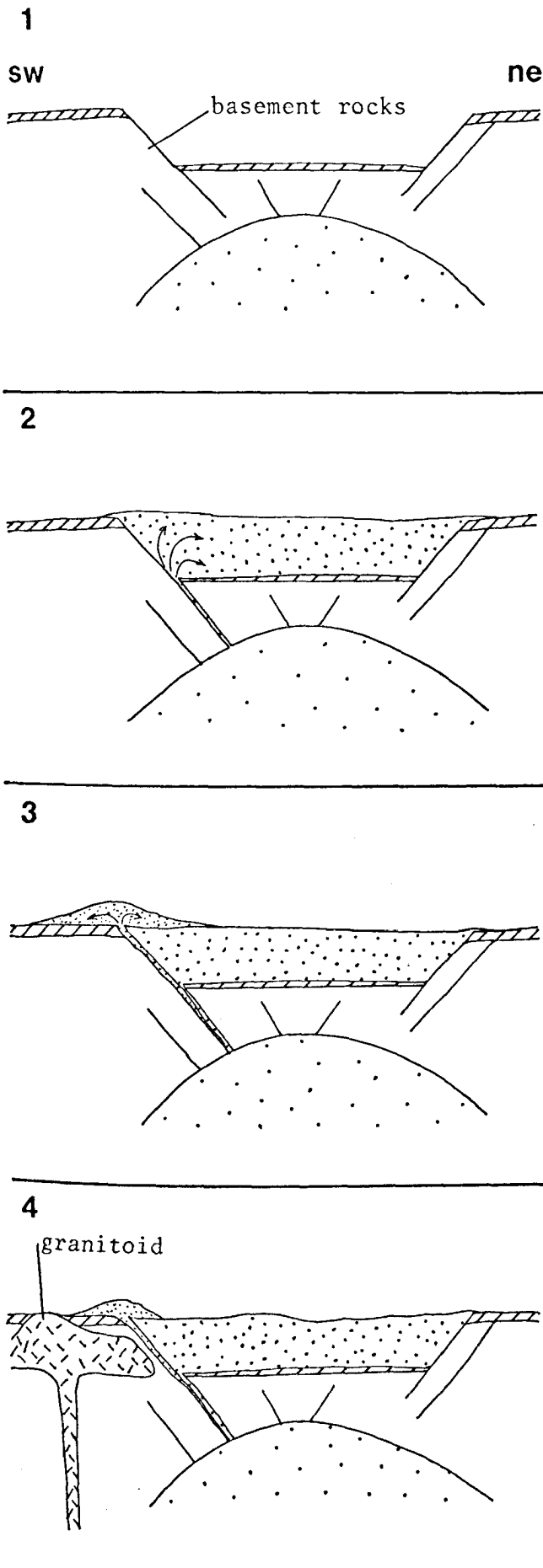

PSEUDO — PLUTON

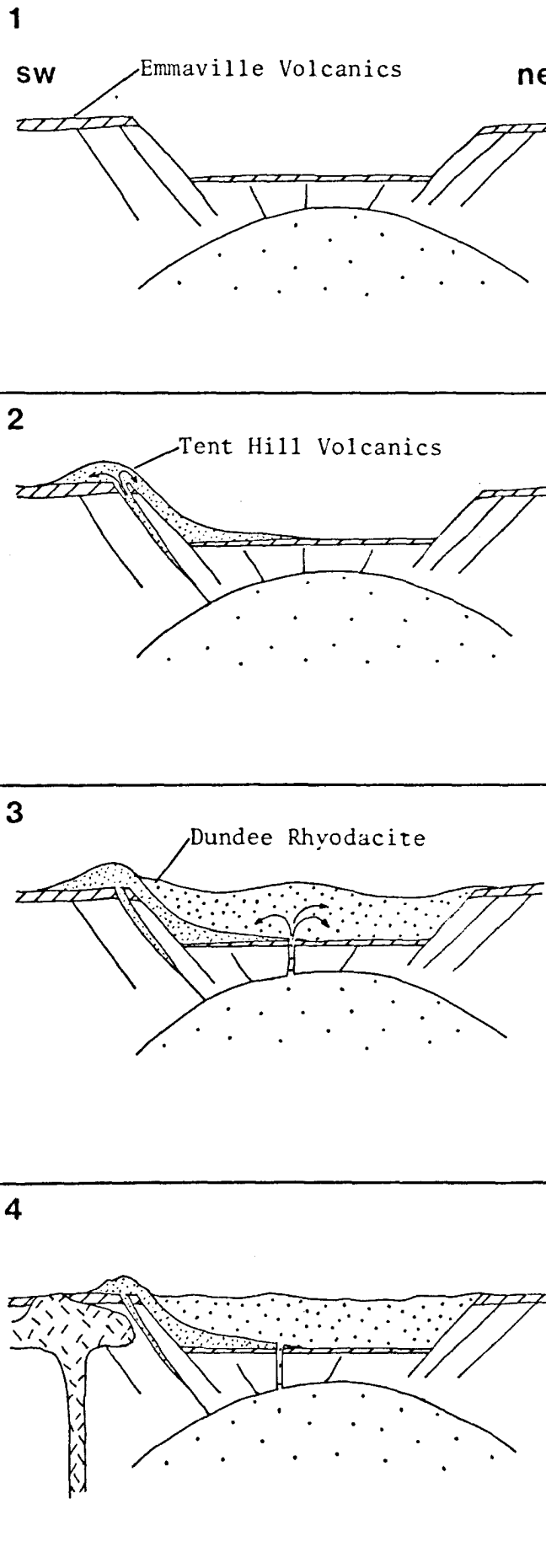

eruption of the lava from a central vent or vents. The lava would thus represent a volatile-poor rhyodacite magma no longer capable of fluidization necessary for eruption as an ignimbrite. However the absence of flow banding and foliation throughout most of the Dundee mass is perhaps the strongest criticism of this model.

Another, perhaps more standard, explanation of the features of the Dundee mass is that it represents a massive, recrystallized cauldron-fill ignimbrite sheet (Fig. 4.1). If eruption occurred from central vents, all the features of a pseudo-pluton described above would be relevant to this ignimbrite sheet model. However, if eruption was triggered from an arcuate ring fracture, the model requires that the Tent Hill Volcanics must post-date the formation of the Dundee Rhyodacite. The Tent Hill Volcanics are the last products of the eruptive episode which produced the Dundee Rhyodacite ignimbrite sheet. In this model the Tent Hill Volcanics fill the ring fracture that tapped the Dundee Rhyodacite source magma. The similar composition of the Tent Hill Volcanics and the Dundee Rhyodacite lends support to this model, and contact relations with the Dundee Rhyodacite are not contradictory. Assuming that the Rhyodacite was rapidly extruded over the floor of an existing caldera to form a thick sheet, the preservation of flow foliation and eutaxitic textures only at the margins would appear entirely reasonable.

Mineralogical and chemical data (Chapters 2 and 3) suggest that the Tent Hill Volcanics represent a magma less evolved that the Dundee Rhyodacite, and although field relations are equivocal, these data are consistent with a younger age for the Tent Hill Volcanics. The Volcanics may represent magma compositions at a level deeper than the one tapped to produce the Dundee Rhyodacite. Alternatively they may represent a less evolved magma that had migrated upwards following evacuation of the upper part of the magma chamber. Although further supportive evidence is lacking in this case, the existence of primary compositional zonation in high-level magma chambers has been reported in a number of studies on caldera-related pyroclastic volcanism. Products of successive eruptions are interpreted to represent progressively deeper tappings of the compositionally zoned magma chamber, e.g. Smith and Bailey, 1966; Sparks et al., 1973; Hildreth, 1979; Bailey et al., 1976; Byers et al., 1976; Lipman, 1967, 1975; Crecraft et al., Smith, 1979; Blake, 1981.

The Tent Hill Volcanics grade outwards at the Rhyodacite contact from ignimbrites almost indistinguishable from border-facies Dundee Rhyodacite to ignimbritic dacites and lithic tuffs. The clastic material in some facies of the Tent Hill Volcanics is country rock volcanic fragmenta plucked from the walls of the vent and incorporated into the fluidized acid magma during its passage to the surface as a result of gas coring and piecemeal stoping, mechanisms that are well documented in

ignimbrite terrains elsewhere (e.g. Reynolds, 1954, 1969; Myers, 1975; Phillips, 1974). Quite commonly, magma resurgence opens new concentric fractures situated closer to the centre of the cauldron block (Roberts, 1974), but there is no evidence that this occurred in the Dundee or any of the other calderas in the Tenterfield region. In fact the Tent Hill Volcanics define the original ring fracture of the Dundee caldera which may well have been a vent for earlier rhyolitic volcanism.

The recrystallized acid volcanics, leucocratic intrusive porphyries and related dyke rocks that partly surround the Brassington and Tenterfield masses are compositionally dissimilar to the Tent Hill Volcanics and are not obviously related to the Dundee Rhyodacite. Many of these rocks may represent the crystallized remnants of the acid magmas which formed the Emmaville Volcanics, as they now fill arcuate ring fractures that were likely sites of rhyolitic volcanism. The acid dyke rocks also differ from the Tent Hill Volcanics in that, contrary to the ash-flow sheet model for the Dundee mass, these dyke rocks and the Rhyodacite apparently did not erupt from the same vent. (No accidental xenoliths of ring dyke material occur in Dundee Rhyodacite from the Brassington and Tenterfield masses). Because of these differences, the pseudo-pluton (or central vent-ignimbrite sheet) model is more consistent with the features of the Dundee Rhyodacite when all the masses with microgranular groundmass textures are treated as a whole.

The pseudo-pluton model also satisfies the conditions needed to produce the unusual mixture of volcanic and subvolcanic textures evident in the Dundee Rhyodacite. As pointed out by Flood et al. (1977), a high proportion of broken and brecciated phenocrysts is a common feature of ignimbrites (see also Lipman, 1967). Turner and Bowden (1979) imply that the presence of phenocryst fragmenta may be a useful criterion to distinguish ignimbrites (fluidized) from lavas (not fluidized). The fracturing or breakage of brittle phenocrysts and the shredding of biotite may be attributed to the turbulent conditions which prevailed during eruption and high-velocity flow of the fluidized magma.

The presence of strongly welded analogues of the Dundee Rhyodacite which overlie Emmaville Volcanics at the margins of the Dundee mass (see Chapters 2 and 3) suggests that the caldera was not only filled but had in fact overflowed at some localities. Similarly, most of the magma was retained in the calderas near Tenterfield but in some cases the caldera rim was breached, or flow was otherwise directed outwards, to overlie the Emmaville and Wallangarra Volcanics (e.g. the Wyberba-Sunnyside ash-flow sheet). By comparison with known calderas of size comparable to those in the Emmaville and Tenterfield regions, the levels of subsidence of the cauldron blocks and hence the thickness of the Rhyodacite filling

the calderas can be estimated (see later). The opportunity for rapid accumulation and confinement of great volumes of fluidized rhyodacite magma are important concepts in the pseudo-pluton model. The abnormal thickness of the cooling units prevented rapid heat loss, resulting in subsolidus recrystallization of the quenched groundmass, the development of a microgranular texture, and the obliteration of pristine pyroclastic features.

Ash-flows are renowned for their extreme mobility (Miller and Smith, 1977; Francis and Baker, 1977) and commonly enormous volumes (Smith, 1960), so it is possible that the Dundee Rhyodacite was deposited as a single ash flow (Flood et al., 1977), presumably extending from the Dundee caldera northwards towards Tenterfield. However it has been emphasized that this hypothesis is not compatible with the observed patterns of metamorphism. Furthermore, simple rifting of the sheet by high-level plutons does not adequately explain the present distribution of the masses, some of which are widely separated. The single flow sheet hypothesis also denies the possibility of a genetic relationship between the Rhyodacite and the existence of cauldrons, and places undue emphasis on the importance of only one particular volcanic centre. In addition, no thinning, welding zonation or significant large-scale modal and compositional variation is detectable in the Dundee Rhyodacite. These are features which characterize extensive ignimbrite sheets in other parts of the world (Smith, 1960a).

The nature of large ignimbrite-forming eruptions has been described by Sparks et al., 1978; Sparks and Wilson, 1976 and Wilson et al., 1978, who favour gravitational collapse of an explosive eruption column to promote the high mobility of ash flows. This mechanism of ignimbrite formation may not be directly applicable to the Dundee Rhyodacite which lacks the associated ash-fall (Sparks and Walker, 1977) or co-ignimbrite lag-fall deposits (Wright and Walker, 1977). High magma mobility is not a requirement for formation of the Dundee Rhyodacite and it is envisaged that the rhyodacite eruption was a (relatively non-explosive) violent frothing of magma from central vents in the cauldron blocks. This more passive style of eruption is similar to that described by Ross and Smith (1961). In terms of the current model advocated by Sparks and Wilson (1976), unusually low particle velocities would be required to limit the height of the eruption column.

Because of the compositional and textural uniformity of the Rhyodacite throughout the region, it presumably formed in one catastrophic event of a magnitude comparable to any documented to date (cf. the Bishop Tuff in California; Bailey, 1976). It appears therefore that ash-flow eruption of Rhyodacite may have occurred simultaneously from a number of centres, some of which are still preserved

as recognizable cauldrons. Such a widespread distribution of volcanic centres implies one large, high-level magma chamber below much of the region, or several individual chambers containing an identical magma. It is intriguing to contemplate the mechanism which triggered eruption at all centres simultaneously, but the structural data necessary to identify this tectonic event were not collected in this study.

The concept of large volumes of acid magma being underlain by and in contact with a periodically replenished "underplated" basaltic magma which acts as a source of heat to maintain fusion (Smith, 1979; Rice, 1981; c.f. Huppert and Turner, 1981) and sometimes initiates explosive acid volcanism (Sparks et al., 1977; Sigurdsson and Sparks, 1981; Rice, 1981) is apparently not applicable in the Tenterfield region as basaltic or basalt-rhyodacite mixed magma ejecta are absent.

It is perhaps surprising that cauldron subsidence apparently did not accompany formation of the Dundee Rhyodacite, because the eruption must have involved evacuation of hundreds of cubic kilometres of magma from high-level chambers. However, by analogy with similar thick ash-flows, extrusion may have been completed in only a few minutes (Ross and Smith, 1961; Wilson et al., 1978). It is not reasonable to assume that subsidence could keep pace with this rate of magma chamber depletion and it has been proposed that the Rhyodacite must have flowed into pre-existing calderas. Crustal movements to restore equilibrium probably commenced soon afterwards and the upward rise of new magmas to lower-pressure zones possibly occurred during this period of re-adjustment.

Subsequent to their recognition of the ignimbritic nature of the Dundee Rhyodacite (Flood et al., 1977), these authors have recently interpreted the Rhyodacite as the crystal-rich fraction of a massive ash-flow eruption devoid of the vitric fraction thought to represent at least 36 wt.% of the original magma (Flood et al., 1980). For many reasons already outlined, there is little evidence to support such a concept. The complimentary ash-fall tuffs representing the fugitive vitric fraction required by Flood et al., here conservatively estimated to be in excess of 100 km^3, are notably absent and clearly are not represented by the ash-flow Tent Hill or Emmaville Volcanics because of compositional and age constraints respectively. The very uniformity of the Dundee Rhyodacite in terms of both texture and geochemistry suggests that original magma compositions were essentially maintained by the Rhyodacite during and after eruption, consistent with observations noted by Smith (1979) that ash-flow tuffs of major eruptions represent ". . . 'instant' sample(s) of a magmatic system." (Smith, 1979, p.25).

GRANITOID INTRUSIONS

Two major episodes of granitoid emplacement, indicated by isotopic and relative ages of the plutons, are now recognized in the Emmaville-Tenterfield area. The first episode involved granitoids of the New England Batholith s.s. which intruded the volcanic terrain about 238 Ma, concluding with emplacement of the 236 Ma Mole Granite. Granitoids emplaced during the second episode, which belong to Korsch's (1977) Stanthorpe Plutonic Suite, are the younger Stanthorpe and Ruby Creek Adamellites, dated at 222 Ma (Evernden and Richards, 1962).

In a review of volcano-plutonic formations, Ustiyev (1970) generalized that where post-orogenic magmatism is in the form of extensive pyroclastic acid volcanism (usually associated with cauldron formation), the effusive rocks are characteristically accompanied by ". . . synchronous but mostly somewhat later, granitoid intrusives." The Emmaville-Tenterfield region appears to fit this model well.

One of the most obvious and characteristic features of volcano-plutonic formations is the very high level of emplacement of the intrusives. For example, granitic plutons that have intruded comagmatic volcanic rocks have been documented in Sudan (Neary et al., 1976), Nigeria (Turner and Bowden, 1979), U.S.A. (Hamilton and Myers, 1967), U.S.S.R. (Ustiyev, 1970), India (Kochhar, 1972) and South Australia (Turner, 1975). In the Georgetown Inlier, northern Queensland, adamellites were intruded hundreds of metres into the volcanic pile, to crystallize under a cover estimated to be less than 200m (Branch, 1966, 1967). Oftedahl (1959) has reported plutons in the Oslo region that also cooled under a thin roof - only 200 to 500m of volcanics. Although there is considerable evidence, both direct and indirect, for comparable high-level subvolcanic intrusion in the Emmaville-Tenterfield area (see introductory section of this chapter), the actual level of emplacement of the plutons cannot be estimated accurately because the original thickness of the Emmaville Volcanic pile is unknown.

Two features of the Dundee Rhyodacite are particularly relevant to this discussion:

(a) as the last volcanic to be erupted in the Permian, it was exposed at the surface during the intrusive episodes,

and

(b) because it was erupted as a single event (albeit possibly from vents in different calderas), and apparently assumed the form of a simple cooling unit (Smith, 1960a), by analogy with reported ash-flows the Rhyodacite is unlikely to have been more than 600m thick (Smith, 1960; Fiske et al., 1977).*

This would be an absolute maximum limit of the thickness of the Wyberba-Sunnyside ignimbrite outflow sheet, but it may not be relevant to masses confined to cauldron structures. The thickness of sheets (or pseudo-plutons) filling subsidence regions is largely limited by the depth of subsidence. A maximum subsidence in the order of 1000m is consistent with the size of the proposed calderas in the Emmaville and Tenterfield regions (Ross and Smith, 1961; Birch, 1978). This means that for any granitoid to have intruded the Dundee Rhyodacite and be now exposed, the minimum depth of emplacement (or maximum depth of erosion) since the Late Permian was of the order of 1000m. The Billyrimba Leucoadamellite and Cottesbrook Adamellite serve as examples of this high-level of emplacement as both have intruded the Brassington Cauldron block.

Less information is available concerning levels of erosion outside the regions of cauldron subsidence. Although probably no more than 1000m has been eroded from subsidence areas, there is no reason to expect that this was typical of the entire region. In fact the exposure of granitoids at topographically higher levels than the Dundee Rhyodacite strongly suggests that levels of intrusion may have been significantly higher outside the calderas. As already noted, granite intrusion was partly controlled by ring faults. This is well illustrated by the Bungulla Porphyritic Adamellite which squeezed up between the Tenterfield and Brassington Calderas, metamorphosing the ring dykes. High-level emplacement may have been facilitated by doming of the volcanic roof rocks outside the caldera margins, without affecting the cauldron blocks (defined by ring fractures). In the absence of evidence for stoping or rifting (cf. Flood et al., 1977), doming is proposed as the major mechanism for highest level emplacement.

The Mole Granite warrants special comment, as it presents an example of the style of emplacement which may be typical of the smaller acid plutons in the area. Kleeman et al. (in prep.) consider the Mole Granite to be a thin, discoidal mass which formed when a low viscosity acid melt rose to within 2-4km of the surface and

---

* Recent mapping in New Mexico, U.S.A., suggets that 1.5 km may be a more realistic upper limit for the thickness of single flow sheets which fill very large calderas (W.E. Elston, pers. comm.).

spread out along the unconformable contact between Early Permian sediments and overlying Late Permian sediments and Gibraltar Ignimbrite (Vickery, 1972).

This model closely resembles the "floored sheet" hypothesis of formation of the Boulder Batholith, Montana (Hamilton and Myers, 1967, 1974). Access of the Mole Granite magma to upper crustal levels was via a narrow conduit(s), terminating at the unconformity, where the magma spread laterally under conditions of isostatic equilibrium to form the characteristic mushroom-shaped pluton.

Although there is some doubt that the Mole Granite terminated its emplacement at a mappable unconformity, it is possible that crystallization of the magma proceeded under conditions of isostatic equilibrium (cf. Badham et al., 1976) before P_{total}-P_{H_2O} equilibrium was attained. If so, the Q-An-Ab-Or tetrahedron (Figure 4.2) cannot be used to indicate the load pressure (and hence depth of emplacement) at which the Mole Granite crystallized.* Eadington and Nashar (1978) speculated that the topazites in the apical parts of the Mole pluton crystallized at (load) pressures of 1 to 2 kb, corresponding to a depth of perhaps 3 to 8 km. However this estimate is based on extrapolation of experimental data in the idealized system "granite-H_2O-HF" conducted at ∿1 kb (Glyuk and Anfilogov, 1974). The existence of a sedimentary roof pendant is indication that doming of the country rocks may have accompanied intrusion (cf. Hamilton and Myers, 1967), and like the granitoids near Tenterfield, the Mole Granite outcrops at a predominantly higher level than the Rhyodacite in the Dundee caldera. The suggested maximum thickness of the Dundee Rhyodacite again argues in favour of very shallow emplacement of the Mole Granite, with attendant doming of its roof.

In his discussion of emplacement of the northern part of the New England Batholith (s.l.), Shaw (1964) proposed that high-angle faulting controlled the upward

---

* A standard interpretation of the data presented in Figure 4.2 would be that most of the granitoids (e.g. not only the Mole Granite) crystallized at P_{H_2O} = 1 kb.

However, using isobaric lines determined by von Platen & Holler (1966) and Winkler (1976), the average granitoid in the area crystallized at >2 kb P_{H_2O}. (The data for the volcanics are equivocal and no comment will be made here.)
The "granite triangle" and "feldspar triangle" should be used only as a general indication of the proximity of plotted rock compositions to the compositions of accepted granite minima. The diagrams should not be interpreted to indicate water pressures in melts immediately prior to crystallization because of the many simplifications inherent in the experimentally determined isobaric lines, and the fundamental assumption that the melt components represent a system in compositional equilibrium (see Johannes, 1980).

Figure 4.2: Leucocratic intrusive and volcanic rocks plotted on the Q-Ab-Or ("granite triangle") and the An-Ab-Or ("feldspar triangle").

c-d and A-B are projections of the $P_{load} = P_{H_2O} = 1$ kb low temperature melting quaternary cotectic surface determined by James and Hamilton, 1969. Rocks plotted have D.I. >90.

1 Contact metamorphosed and metasomatized Emmaville Volcanics.

2 Wallangarra Volcanics.

3 Acid ring dyke rocks.

4 Emmaville Volcanics.

5 Nonnington Leucoadamellite.

6 Clive Adamellite.

7 Bolivia Range Leucoadamellite.

8 Ruby Creek Adamellite.

9 Mole Granite.

0 Stanthorpe Adamellite.

Data sources: Juniper, 1974; Thomson, 1976, Flinter *et al.*, 1972; this study.

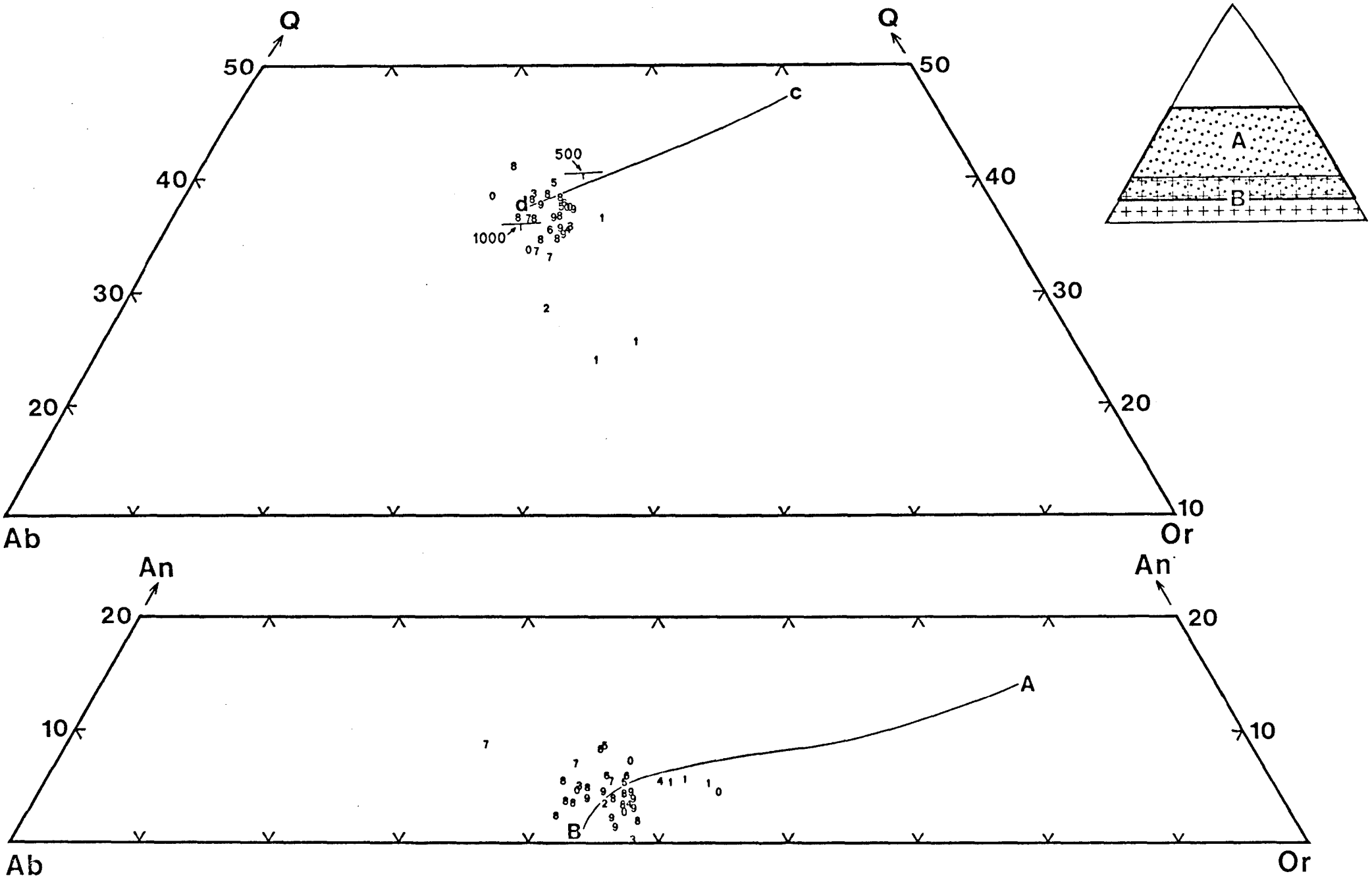
Q
50
40
30
20
10
Ab
Or
c
d
500
1000
Q
50
40
30
20
10
An
Ab
Or
A
B
A
B

movement of magma, and that the volume occupied by each intrusion was made available by the "gentle wedging action of magma compensated by transcurrent movement along high-angle faults" (pp. 337 - 338). It is difficult to assess the possible contribution to emplacement by faulting but the massive, unstructured form of plutons, the absence of a tectonically induced foliation, and (in some cases) the truncation of boundaries by faults, suggests that faulting mostly post-dated the main intrusive episode. (Korsch et al. (1978) argued that a 17 km dextral displacement on the Demon Fault was completed between the first and second episodes.) Furthermore, Shaw's proposal does not account for the vertical displacement of overburden when providing room for the intruding magma.

Clearly the many parameters that control the rate of ascent, level of emplacement and spacing geometries of granitic magmas, including the thickness, density and viscosity of the country rocks, the temperature, crystallinity and composition of the magma and the size of the resultant pluton, as well as regional structural criteria, must be considered in any assessment of magmatic intrusion (Hyndman et al., 1980; Rickard and Ward, 1981; Hyndman, 1981).

In conclusion, the preferred model is that granitoids intruded to moderately high levels along fractures during a period of mild crustal tension (Shaw, 1964) and were finally emplaced by doming of roof rocks within or just below the Permian volcanic pile. The erosion of probably only a few hundreds of metres of original country rock has now exposed large volumes of granitoid outside the regions of cauldron subsidence. Studies of terrestial sediments both east and west of the New England region, indicate that "major unroofing of the New England Batholith" was probably completed by Middle Triassic time (Bourke et al., 1977, p.38). Certainly the Mole Granite was substantially unroofed by the Cenozoic because alluvial "deep lead" cassiterite deposits derived from the Granite are currently being exploited beneath Tertiary basalt near Emmaville.

GRANITIC PORPHYRIES*

In volcano-plutonic associations the occurrence of granitic porphyries with volcanic and subvolcanic rocks has been frequently noted (e.g. Ustiyev, 1965; Kochhar, 1972). Two feldspar-quartz porphyries outcrop extensively in the region

---

* The term refers to those porphyritic rocks with microgranular groundmass textures and differentiation indices of > 80. Compositionally, most granitic porphyries in the area are adamellites.

north and west of Tenterfield, and more sporadically west and southwest of Mount Mackenzie. These rocks are texturally and mineralogically similar to the ring dyke porphyries of the Brassington Caldera and the Mount Mackenzie intrusive complex. Irrespective of their ultimate origin, granite porphyries in volcanic regimes are characteristically restricted to high crustal levels. A short discussion of the possible origins of such porphyries is presented here because they appear to represent a link between volcanism and subvolcanic intrusion.

Granitic porphyries can generally be divided into two types:

(a) Rocks with microgranular groundmass textures produced by autometamorphism or contact metamorphism.

(b) The finely crystalline products of a rapidly quenched magma.

The two types may be indistinguishable on any basis other than field relations (Fyfe, 1970), which explains why correct identification is difficult when such rocks are poorly exposed.

The most common metavolcanic type of porphyry, which forms at the contact between shallow intrusive and extrusive rocks (Fyfe, 1970; Branch et al., 1960; Branch, 1966, 1967; Ustiyev, 1965) is probably represented north and west of Tenterfield. The intrusive magma which bakes the overlying volcanics is itself chilled at the margins (type b porphry), and if (as is usually the case in volcano-plutonic formations) the intrusion was comagmatic with the volcanics, the contact becomes a broad, diffuse zone of relatively homogeneous granitic porphyry.

Acid volcanic rocks which form microgranular textures by autometamorphism are restricted to the central regions of very thick (>180m) ash flows (Smith, 1960). Ignimbrites of the required thickness are usually only found in cauldron subsidence areas. The Dundee Rhyodacite is the only known likely example of this type of porphyry in the New England Batholith s.l., but others are known in Central Victoria (McLaughlin, 1976; Birch, 1978). The porphyritic Lake Mountain Biotite Rhyodacite which partly fills the Cerberean Caldera in central Victoria, has a groundmass composition very similar to the low-temperature ternary minimum-melt composition of the Dundee Rhyodacite groundmass. Furthermore the estimated thickness of the Biotite Rhyodacite (Birch, 1978) is roughly comparable to that of the Dundee Rhyodacite, so it is hardly surprising that the groundmass textures are very similar (Plate 2). Very coarse textures (0.5mm) have been reported in the groundmasses of alkaline ignimbrite sheets from the Ningi-Burra Complex, Nigeria (Turner and

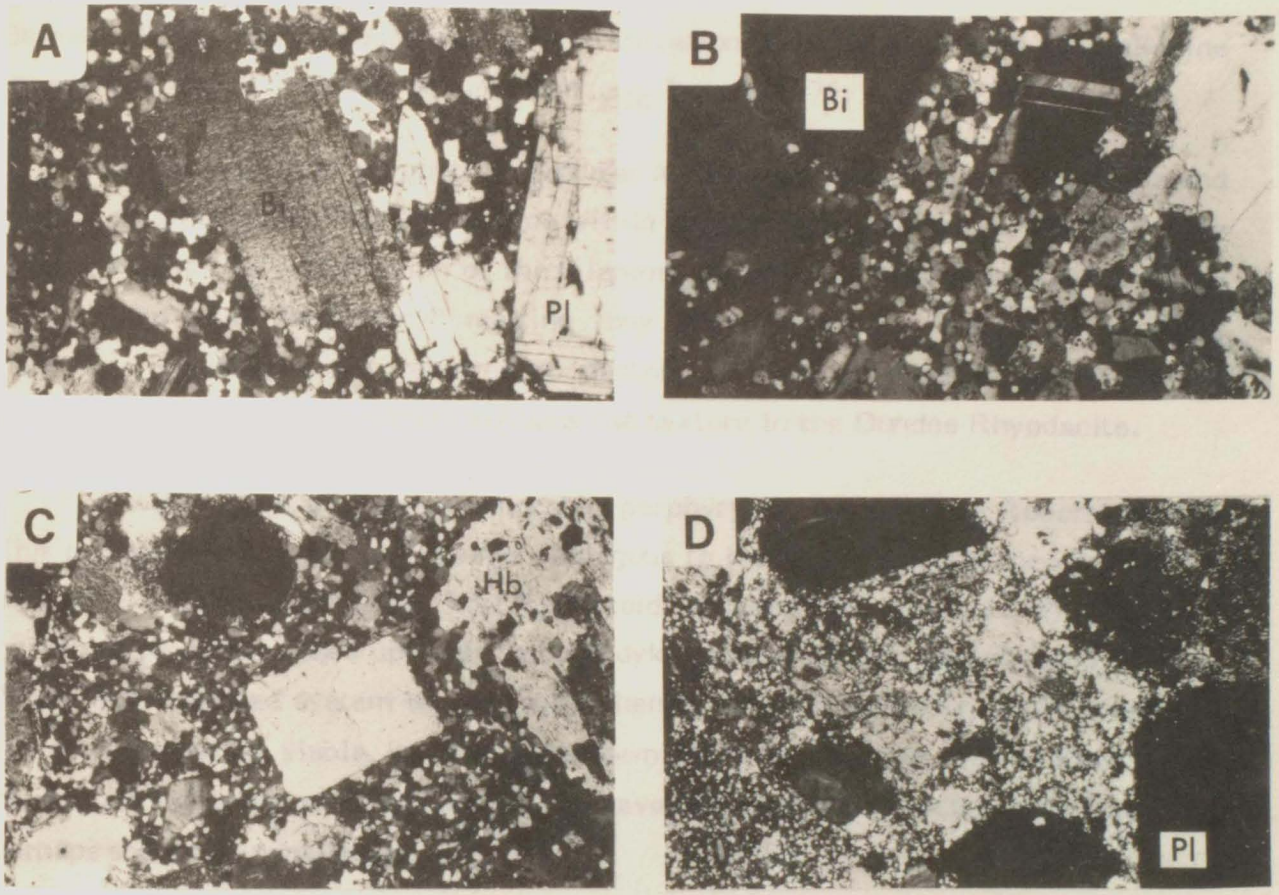

Plate 2. Recrystallized Volcanics - Comparison of textures.

A Quartz-biotite-hypersthene rhyodacite from the Violet Town Volcanics, Strathbogie Complex, north of the Cerberean Cauldron in Central Victoria. Sample taken from road cut at Yarraweeng, 15.5 km southeast of Violet Town.

B Quartz-biotite-hypersthene rhyodacite from the Cerberean Cauldron, Central Victoria. Sample taken from location 17 of McAndrew and Marsden (1968, p. 101, 110).

C Dundee Rhyodacite from the Timbarra mass - unusually coarse-grained sample.

D Dundee Rhyodacite from the Dundee mass - typical specimen.

C and **D** show the range in grain size of the microgranular recrystallized groundmass characteristic of Dundee Rhyodacite from cauldron structures. The Victorian examples have much coarser groundmass textures. See text for fuller discussion.

Magnification x 18
Illumination - cross polarized ordinary light.

Bowden, 1979), and "granophyric" recrystallization of some Australian calc-alkaline rhyolitic ignimbrites is well documented (e.g. Turner, 1975; Branch, 1966).

The formation of porphyritic textures in "pseudo-plutons" during degassing and cooling of an original fluidized magma within a crater vent (Rutten, 1969), is broadly similar to the recrystallization of thick ignimbrite sheets. Rutten believes that due to retained heat "secondary" melting may occur after the magma is erupted; however remelting is not required to destroy original pyroclastic textures. The pseudo-pluton model adequately explains the texture in the Dundee Rhyodacite.

Another type of autometamorphic porphyry is described by Roberts (1966). This porphyry is formed in a manner analogous to the ignimbrite and rheo-ignimbrite examples. Roberts describes how "granitoid textures" are produced by continued perecolation of hot gases upwards through dyke rocks originally consolidated from an "entrained fluidized system of gas, solid phenocrysts and, probably, liquid droplets." If such a process is viable, its role in the formation of porphyries such as those in the Mackenzie intrusive complex (which may have occupied a once-active ring fracture), perhaps should be considered.

The "intrusive rhyolites" which occur as vertical pipe-like bodies in the volcanics of the Webbs Consols Mine area, are acid porphyries showing clear signs of crystallization from a quenched melt. The rapid nucleation and limited grain growth which produced the characteristic groundmass textures were the result of rapid expansion and release of volatile components of the magma during its emplacement in the volcanic pile. Depending on the initial water content of the melt, rapid expansion can induce a pressure quench that causes undercooling of the liquid sufficient to produce immediate crystallization (Fenn, 1977; Jahns & Burnham, 1969; Whitney, 1975a). The same theory applies to the formation of aplites which occur at the contacts of some leucoadamellites near Bolivia and Tenterfield (refer Chapter 2). Granophyric textures are commonly developed at the margins of epizonal granitic plutons that have intruded volcanic country rocks (e.g. Branch, 1966). The close association of granophyric granite with recrystallized volcanic rocks at Webbs Consols Mine is analogous to that described by Harker (1904) in rocks from the Isle of Skye. Observing gradual transitions from granophyric to spherulitic devitrification textures, Harker concluded that the granophyric textures were developed in rocks that were originally glassy. This conclusion has been confirmed by experimental studies (Luth, in Schweickert, 1976) and observations of recrystallized volcanic rocks (e.g. Smith, 1960a). That such textures can result from devitrification of non-volcanic pressure-quenched liquids has been proposed by Schweickert (1976). However, there is little evidence to suggest that melts of

granitic composition commonly quench to a glass in an intrusive environment, and true pressure quench-derived granitic porphyries exhibit microgranular, not granophyric, textures. It is therefore likely that the granophyre at Webbs Consols represents the eroded remnant of a thick ignimbrite sheet, or the more coarsley recrystallized portion of a series of thinner sheets intruded by the Webbs Consols host adamellite.

From the above discussion it is suggested that although most granitic porphyries cannot be classified on the basis of origin, those in the study area fit the model of subvolcanic intrusion presented earlier in this chapter. The porphyries north and west of Tenterfield may represent the metamorphosed basal layers of Late Permian acid volcanics, or, more likely, are the chilled roof rocks of granitic plutons close to the present erosion surface.

THE VOLCANO-PLUTONIC SUITE: DISCUSSION

The volcano-plutonic rock suite in the Tenterfield region belongs to the "post orogenic" stage of geosyncline development according to the classification scheme of Ustiyev (1970). Ustiyev (1969) was careful to note the coherence of magmatism and metallogeny - for example the tin-tungsten and polymetallic mineralization associated with subvolcanic granitic intrusions in the Sorychev Complex (Verkhoyansk-Chukotka Belt) may be compared with the mineralization in the Emmaville region. By way of contrast, caldera-related polymetallic mineralization of the San Juan volcanic field, Colorado, differs markedly from the ores near Emmaville. In fact the differences in style can be related to the degree of caldera development which is much more advanced in the San Juan region (Lipman et al., 1973) than at Tenterfield. This will be discussed later in connection with cauldron resurgence phenomena which characterize many calderas in Colorado (Smith & Bailey, 1968; Lipman, 1975).

(a) Role of Faulting

According to the accepted ideas of caldera formation by crustal subsidence, the active ring faults (and less important radial fractures) initially form during doming of the crust in response to high "magma pressures". Of greater significance is the relation of high-level magmatism to faulting on a regional scale. Although most realize the importance of the relationship, few authors offer a detailed treatment of the problem.

For example, Ustiyev (1969) proposes "alternating compression and tension" during the magmatic episode, but gives no indication of the magnitude of faulting, or its bearing on emplacement of magmas in the crust. Similarly, Oftedahl (1978) and Segalstad (1975) state that normal faulting accompanies volcanism in the Oslo Rift, and infer that volcanism and caldera formation were focussed by the en-echelon fault system related to graben formation. Neither author is prepared to speculate on the causes of faulting or, in the manner of Shaw (1964), on how compensating fault movements might create room for the intruding magmas. McLaughlin (1976) faces the problem more directly and proposes that magma emplacement was controlled by bedrock regional structural trends, which in turn influenced the structural symmetry of the Acheron and Cerberean Cauldrons in central Victoria.

A more complete account of faulting in the Georgetown Inlier offered by Branch (1966, 1967) may be relevant to processes which operated in the Tenterfield area. In the Georgetown Inlier regional doming was produced by the accumulation of magma in an enormous chamber at the zone of melting in the lower crust. This doming supposedly re-activated major basement faults in the block, which became volcanic conduits when they tapped the huge magma chamber. High-level magmas were emplaced by "underground cauldron subsidence" and also by rise along "subvolcanic conduits" (Branch, 1967). The existence of a "regional" magma chamber at the zone of melting may be criticized in terms of the Taylor instability models described by Fyfe (1973), but the other ideas on magma emplacement proposed by Branch (loc.cit.) are of interest to this study.

Rise of magma along "subvolcanic conduits" is part of the model of formation of the Mole Granite pluton described by Kleeman et al. (in prep.), and it is the mechanism most favoured to explain the levels of intrusion of many plutons in the Tenterfield area. A "volcanic conduit" may be a reactivated basement fault or intersection of faults, or possibly a still-warm channel to the upper crust pioneered by an earlier magma rising as a diapir (Grant, in Fyfe, 1970).

(b) Properties of the Magma and Magma Emplacement

The massive, unstructured form of the Tenterfield granitoids, rarity of accidental xenoliths, and the absence of major cataclasis at the margins of plutons have been cited (Shaw, 1964; this thesis) as evidence that emplacement was essentially passive. This is surprising when comparison is made with other volcano-plutonic formations, where underground cauldron subsidence and piecemeal stoping (possibly aided by gas-coring mechanisms - Pitcher, 1974) as well as doming, may have been operative.

The capacity of a fluidized magma to intrude by stoping is now well known (Reynolds, 1954; Myers, 1975). The efficiency of the gas-coring mechanism is dependent on the prevailing pressure which determines volatile solubility and therefore the point at which the magma becomes fluidized. As noted by Pitcher (1974) it is the actual level at which a magma becomes fluidized which determines whether that magma can stope upwards by the gas-coring mechanism. In the Emmaville area, high-level magmas probably became fluidized only when they were tapped at the surface and ash-flow volcanics were erupted as a result. Pyroclastic eruption ceased when the volatile content of the magma remaining in the chamber dropped below the level required to sustain fluidization. This magma then rose slowly to subvolcanic levels until isostatic equilibrium was attained or crystallization reached an advanced stage. Any volatiles remaining in the melt were probably expelled at these low confining pressures, possibly contributing to the doming of the volcanic roof rocks.

The presence of rapakivi texture in the Bolivia Range Leucoadamellite may provide more evidence of high-level emplacement, according to a recently published interpretation for the origin of this texture. A pressure quench mechanism proposed by Cherry and Trembath (1978) most adequately explains the formation of rapakivi texture in rocks as siliceous as the Bolivia Range Leucoadamellite. Their studies show that polybaric crystallization under vapour-present conditions requires a pressure decrease of 0.5 - 1.0 kb in water-saturated, highly acid melts at low $P_{confining}$ values. Resorption of K-feldspar phenocrysts and subsequent crystallization of albite-rich mantles, ostensibly as a consequence of rapid decrease of $P^{melt}_{H_2O}$, is consistent with ramifications of the model of water dissolution in albite melts proposed by Burnham (1975).

There is no indication of the effects of massive hydrous degassing in either the Bolivia Range Leucoadamellite or its country rocks, which would appear to indicate effective loss of water from the system. This water may have formed hydrous minerals in hydrothermally metamorphosed roof rocks now removed by erosion, but the actual cause of the pressure quench remains unexplained. Perhaps more consistent is the hypothesis that the rocks overlying the high-level chamber were ruptured during the final stages of magma emplacement. Surface tapping of the magma reservoir would provide conditions for the pressure quench, as well as an avenue of escape for the fugitive volatiles.

Several features of the subvolcanics indicate that most crystallized from volatile-poor magmas. Shaw (1964) first noted minor development of miariolitic cavities in some granitoids, but the total absence of pegmatites (the Mole Granite

and Ruby Creek Adamellite are exceptional in this respect). This is typical of epizonal granites associated with ring complexes and rhyolitic volcanism (Buddington, 1959). A second consequence of "dry" magmas was that the doming effect of intrusion was enhanced. Doming is thought to occur above viscous types of magma, as these are less able to rise by stoping mechanisms (Oftedahl, 1978). Perhaps surprisingly there is no evidence of cauldron block resurgent doming, but this may be because of the thickness and structural coherence of the subsided blocks (see Smith & Bailey, 1968) rather than the absence of magmas suited to produce doming.

Smith and Bailey (loc.cit.) also noted that ore deposits are more commonly associated with resurgent cauldrons than with other cauldron types. This is certainly true of the San Juan Volcanic Province where one third of the calderas have associated mineralization (Steven and Eaton, 1975) and most are of the resurgent type (Lipman et al., 1973). By comparison caldera-related mineralization is not developed in the Tenterfield area and no cauldron is of the resurgent type. The link between mineralization and resurgent cauldrons will be discussed in Chapter 5.

GRAVITY DATA

A " . . . Bouguer anomaly of -69 mgal round the Bolivia, Tenterfield and Wallangarra areas . . . " (Shaw, 1964, p.339) has not been verified in more recent studies (see Figure 4.3). Shaw assumed that the region was in isostatic equilibrium and computed the -69 mgal result to indicate a thickened crust extending 5.5 km below the Mohorovicic discontinuity.

Green and Kridoharto (1975) considered the Uralla-Kingston district (south of Armidale, New South Wales) to be in isostatic equilibrium on the basis of the Airy model, because the regional gravity anomaly in this area is -60 mgl. In the vicinity of Emmaville, where the elevation is about the same as Uralla, regional gravity anomalies can vary by as much as 20 mgal within 40 km (refer Figure 4.3), from -55.3 mgal southwest of Tenterfield to -30 mgal near Deepwater. In terms of the Airy model the crust here is denser than normal and not in isostatic equilibrium. That the regional gravity contours are strongly influenced by subsurface plutons is also indicated.

Higher gravity over the southwest portion of the area is consistent with the surface geology which shows that high-level plutonism is comparatively poorly developed. The lack of a significant density contrast between country rocks and the intracaldera volcanics explains why cauldron subsidence regions are not defined by

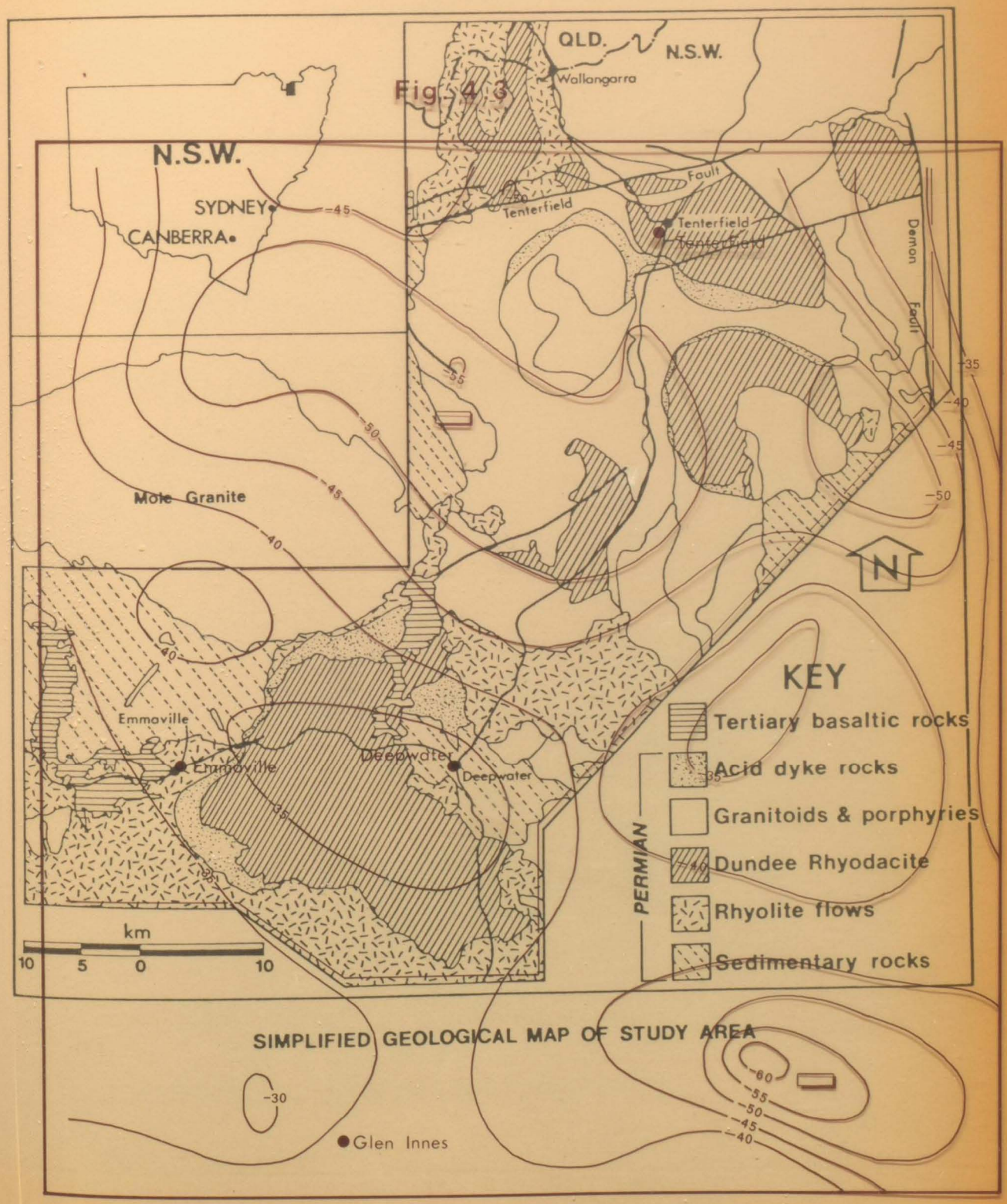

1970 **Bouguer Anomalies** BMR Grafton sheet

Fig. 4.3

1970 **Bouguer Anomalies** Grafton sheet B M R

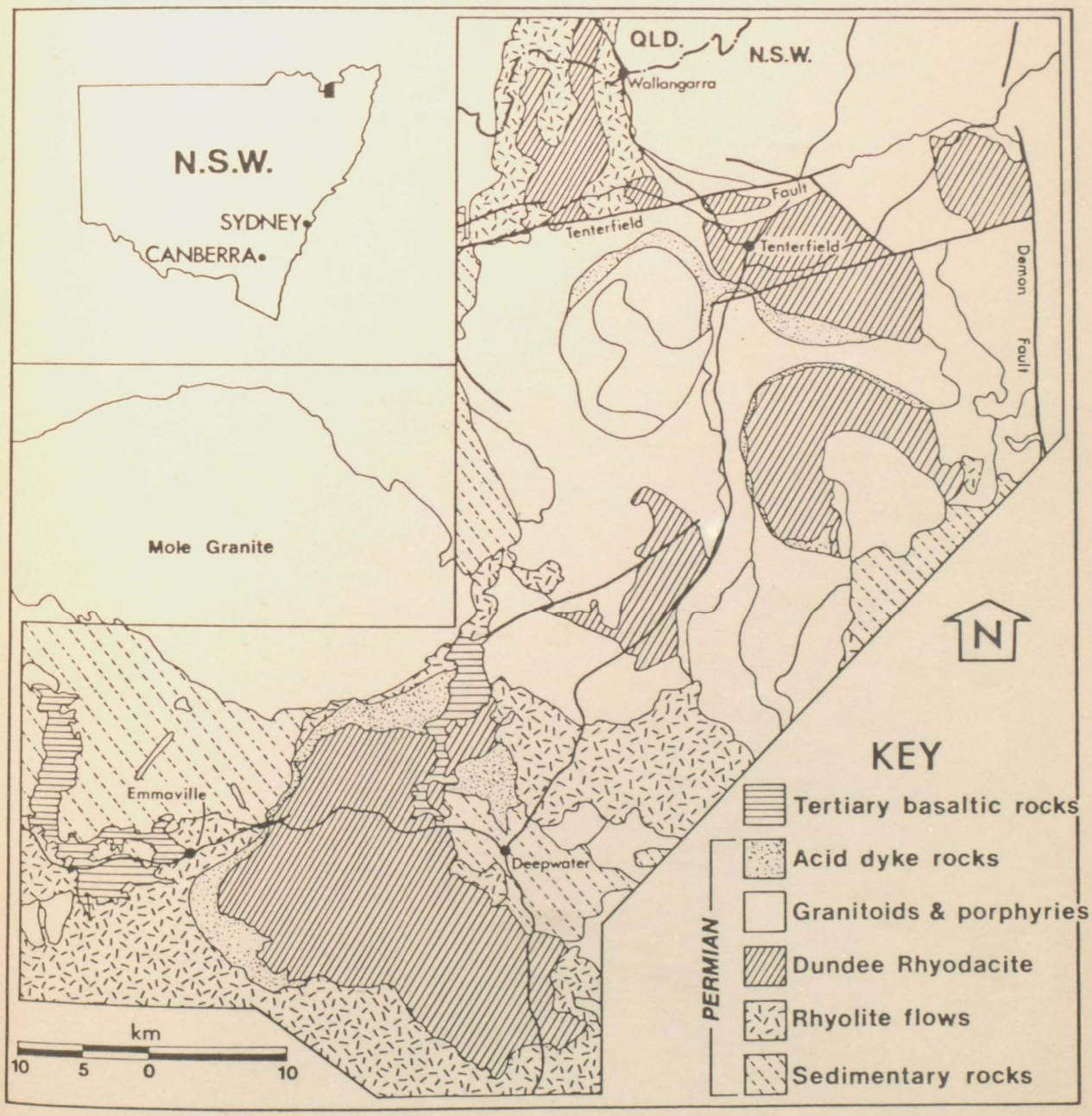

SIMPLIFIED GEOLOGICAL MAP OF STUDY AREA

the regional gravity contours. Perhaps for the same reasons, the larger calderas in Hokkaido, Japan (i.e. those greater than 20 km in diameter) are associated with very poorly defined gravity anomalies (Yokoyama, 1965).